Regulation of the mammalian mitochondrial unfolded protein response

I n a u g u r a l - D i s s e r t a t i o n

zur

Erlangung des Doktorgrades

der Mathematisch-Naturwissenschaftlichen Fakultät

der Universität zu Köln

vorgelegt von

Dominic Seiferling

aus Heidelberg

Köln 2015

Berichterstatter: **Prof. Dr. Aleksandra Trifunovic**

                                  Prof. Dr. Elena I. Rugarli

Tag der mündlichen Prüfung: 18.01.2016

To my family, friends and Lisi

Table of contents

List of figures

List of tables

Abbreviations

3'	three prime end of DNA sequence
^{35}S-met	radioactive methionine isotope
5'	five prime end of DNA sequence
A	adenosine
ADP	adenosine diphosphate
AMA	antimycin A
AmpR	ampicillin resistance gene
APS	ammonium persulfate
ATF	activating transcription factor
ATFS-1	activating transcription factor associated with stress
ATP	adenosine triphosphate
BN	blue native
bp	base pairs
BSA	bovine serum albumine
C	cytosine
C/EBP	CCAAT-enhancer-binding protein
CAM	chloramphenicol
CAT	chloramphenicol acetyltransferase
CCD	charge-coupled device
cDNA	complementary DNA
CHOP	C/EBP-homologous protein
Ci	Curie
Ckmm	muscle creatinine kinase
CLPP	caseinolytic mitochondrial matrix peptidase proteolytic subunit
CMV	promoters for cytomegalovirus
COX	cytochrome c oxidase
Cre	bacteriophage P1 derived site-specific recombinase
CTRL	control
Cyt	cytochrome
Da	Dalton

DAB	diaminobenzidine tetrahydrochloride
DAPI	4,6-diamidino-2-phenylindole
DARS2	mitochondrial aspartyl-tRNA synthetase
DKO	double knockout
DMSO	dimethyl sulfoxide
DNA	desoxyribonucleic acid
DNase	deoxyribonuclease
dNTP	desoxyribonucleotide-triphosphate
DOX	doxycycline
DPE	downstream promoter element
dsRNA	double stranded ribonucleic acid
DTT	dithiothreitol
dTTP	deoxythymidine triphosphate
E-box	enhancer box
ECL	enhanced chemoluminiscence
EDTA	ethylendiamine tetraacetate
eGFP	enhanced green fluorescent protein
eIF2α	α subunit of the eukaryotic initiation factor 2
ER	endoplasmatic reticulum
ETC	electron transport chain
EtOH	ethanol
FADH$_2$	flavin adenine dinucleotide hydrate
FBS	fetal bovine serum
FCCP	carbonylcyanide p-trifluoromethoxyphenylhydrazone
FGF21	fibroblast growth factor 21
Flp	flippase
Frt	flippase recognition target
g	gram
G	guanine
GTP	Deoxyguanosine triphosphate
H$_2$O	water
HCl	hydrochloric acid

HEPES	N-2-hydroxyethylpiperazine-N-2-ethansulfonic acid
HPRT	hypoxanthine-guanine phosphoribosyltransferase
HSE	heat shock element
HSP60	60 kDa heat shock protein, mitochondrial
HSR	heat shock response
i.e.	*id est*
IMM	inner mitochondrial membrane
IMS	inter membrane space
ISR	integrated stress response
k	kilo
KanR	kanamycin resistance gene
kb	kilo bases
KCl	potassium chloride
KO	knockout
l	liter
L	loxP flanked
lacZ	gene encoding β-galactosidase
LB	lysogeny broth
LC-MS	liquid chromatography–mass spectrometry
LUC	luciferase
m	milli
M	molar
MEF	mouse embryonic fibroblasts
MgCl$_2$	magnesium chloride
MIA	mitochondrial intermembrane space import and assembly protein
MIB	mitoisolation buffer
min	minute
mRNA	messenger RNA
mtARS	mitochondrial aminoacyl-tRNA synthetase
mtDNA	mitochondrial DNA
mtEFG	mitochondrial elogantion factor G
mtHSP70	heat shock 70 kDa protein, mitochondrial

mtIF	mitochondrial initiation factor
MTS	mitochondrial targeted sequence
MURE	mitochondrial unfolded protein response element
n	nano
NaCl	sodium chloride
NADH	β-Nicotinamide adenine dinucleotide, reduced
NaF	sodium fluoride
NAH_2PO_4	monosodium phosphate
$NaHCO_3$	sodium bicarbonate
NaOH	sodium hydroxide
nDNA	nuclear DNA
NeoR	neomycin resistance gene
NLS	nuclear localization signal
NTB	nitrotetrazolium blue
OD	optical density
OMM	outer mitochondrial membrane
ORF	open reading frame
OXPHOS	oxidative phosphorylation
p	pico
PAGE	polyacrylamide gel electrophoresis
PAM	presequence translocase-associated motor
PBS	phosphate buffered saline
PCR	polymerase chain reaction
PFA	paraformaldehyde
P_i	phosphates
PKR	protein kinase R
PQ	paraquat
PuroR	puromycin resistance gene
PVDF	polyvinylidene fluoride
qPCR	quantitative polymerase chain reaction
RNA	ribonucleic acid
RNAi	RNA interference

RNase	ribonuclease
ROS	reactiove oxygen species
ROT	rotenone
rpm	revolutions per minute
rRNA	ribosomal RNA
SAM	sorting and assembly machinery
SDH	succinate dehydrogenase
SDHA	succinate dehydrogenase
SDS	sodiumdodecylsulfate
S.E.M.	standard error of the mean
siRNA	small interfering RNA
T	transgene
TBE	tris-borate-EDTA buffer
TBS	tris buffered saline
TCA	tricarboxylic acid cycle
TEMED	tetramethylethylenediamine
TFAM	mitochondrial transcription factor A
TIM	translocase of the inner membrane
TOM	translocase of the outer membrane
Tris	2-amino-2-(hydroxymethyl)-1,3-propandiole
tRNA	transfer RNA
TSS	transcription start sites
TWEEN	polyoxethylene-sorbitan-monolaureate
U	units
UPR^{ER}	ER unfolded protein response
UPR^{mt}	mitochondrial unfolded protein response
V	volt
v/v	volume per volume
w/v	weight per volume
WT	wild type
ΔOTC	truncated ornithine transcarbamylase
μ	micro

Abstract

The molecular mechanisms of the mammalian mitochondrial unfolded protein response (UPR^{mt}) are largely unknown. In this study, *in vitro* as well as *in vivo* models were used to assess the role of the mitochondrial chaperones and proteases as well as potential signalling factors in the context of the mammalian UPR^{mt}.

The mitochondrial chaperones HSP60 and mtHSP70 were found to be highly expressed under regular cell culture conditions in various cell types and not amenable to further induction by mutant mitochondrial proteins or toxins compromising mitochondrial function. It is argued that highly proliferative cells constantly express mitochondrial chaperones at high levels as they were found to orchestrate a broad cellular survival programme. The data in this study collectively demonstrate that HSP60 and mtHSP70 are not suitable as a readout for UPR^{mt} induction *in vitro*. Further, this study provides the first direct evidence that levels of the transcription factor ATF5 correlate with the expression of known UPR^{mt} markers *in vitro* and *in vivo* upon mitochondrial stress. In addition, it is shown that ATF5 is able to translocate to mitochondria *in vivo*, whereas it is found in the nucleus in stressed cells *in vitro*. Intriguingly, it was also found that the matrix protease LONP1 not only responds to mitochondrial unfolded protein stress, but also seems to regulate the mammalian UPR^{mt} signalling. Thus, the conclusion can be drawn that both ATF5 and LONP1 are implicated in the UPR^{mt} in mammals.

The matrix protease CLPP exerts a key role in the induction of the UPR^{mt} signalling in *C. elegans*. To better understand the role of CLPP in UPR^{mt} signalling *in vivo*, CLPP was depleted in hearts from DARS2-deficient animals that show a strong upregulation of UPR^{mt} signalling due to disrupted mitochondrial translation. Notably, it could be demonstrated that CLPP is not required, nor does it activate UPR^{mt} signalling *in vivo*. Surprisingly, the pathological changes and diminished respiration due to DARS2 deficiency can be mitigated by the loss of CLPP by partially rescuing mitochondrial translation. Therefore, evidence is provided that on the one hand questions our current understanding of the UPR^{mt} signalling in mammals, but on the other hand identifies CLPP as novel modulator of mitochondrial translation, which might be used for the development of new therapeutic approaches against translational defects in mitochondrial disease.

Zusammenfassung

Die molekularen Mechanismen der ungefalteten Proteinantwort in Mitochondrien (UPR^{mt}) sind in Säugetieren weitestgehend unerforscht. Um den UPR^{mt} Signalweg besser zu verstehen, wurde in dieser Studie, unter Zuhilfenahme von *in vitro* und in vivo Modellen, zum ersten Mal die Rolle mitochondrialer Chaperone und Proteasen sowie potenzieller Signalfaktoren näher charakterisiert.

Es konnte gezeigt werden, dass die mitochondrialen Chaperone HSP60 und mtHSP70 unter regulären Zellkulturbedingungen in mehreren Zelllinien äußerst hoch exprimiert werden. Weder die Expression mutierter mitochondrialer Proteine, noch die Behandlung mit verschiedenen Chemikalien konnten den Gehalt von HSP60 und mtHSP70 weiter erhöhen. Hieraus kann gefolgert werden, dass proliferierende Zellen eine kontinuierlich hoch regulierte mitochondriale Chaperon-Expression besitzen, was damit erklärt werden könnte, dass diese während der Aktivierung von zellulären Überlebensprogrammen eine wichtige Rolle spielen. Infolgedessen sind die mitochondrialen Chaperone HSP60 und mtHSP70 nicht geeignet um eine UPR^{mt} Aktivierung in Zellkultur zu bemessen. Ferner konnte diese Studie den ersten unmittelbaren Nachweis erbringen, dass während mitochondrialem Stress der zelluläre Gehalt des Transkriptionsfaktors ATF5 mit der Expression von bereits bekannten UPR^{mt} Markern sowohl *in vitro* als auch *in vivo* korreliert. Darüber hinaus kann sich ATF5 *in vivo* in die Mitochondrien verlagern, wohingegen es sich unter Stress *in vitro* im Zellkern befindet. Interessanterweise konnte außerdem gezeigt werden, dass die Matrixprotease LONP1 im Laufe von ungefaltetem Proteinstress aktiviert wird, als auch selbst einen potentiellen Regulator des UPR^{mt} Signalwegs in Säugern darstellt. Demnach kann geschlussfolgert werden, dass sowohl ATF5 als auch LONP1 eine Rolle in der UPR^{mt} von Säugetieren spielen.

Die Matrixprotease CLPP spielt eine entscheidende Rolle bei der Auslösung des UPR^{mt} Signalwegs in *C. elegans*. Um die Funktion von CLPP im UPR^{mt} Signalweg in Säugern näher zu charakterisieren, wurde CLPP in DARS2-defizienten Mäusen deletiert. DARS2-defiziente Mäuse selbst weisen, bedingt durch einen starken mitochondrialen Translationsdefekt, eine massive Hochregulierung des UPR^{mt} Signalwegs auf. Bemerkenswerterweise konnte in dieser Studie gezeigt werden, dass CLPP weder für die

UPR^{mt} benötigt wird, noch als Aktivator der UPR^{mt} in Säugern fungiert. Darüber hinaus verbessert der Verlust von CLPP sowohl die ausgeprägte Pathologie als auch die verminderte Zellatmungsleistung von DARS2-defizienten Tieren. Der mildere Phänotyp hat seine Ursache dabei in einer partiell verbesserten Translation in doppel-defizienten Tieren. Diese Ergebnisse stellen zwar das momentane Verständnis des UPR^{mt} Signalwegs in Säugern in Frage, allerdings identifizieren sie auch gleichermaßen eine gänzlich neue Rolle für CLPP in der Modulation der mitochondrialen Translation. Dies wiederum eröffnet neue Wege für die Entwicklung von Therapien zur Verbesserung von translationalen Defekten in mitochondrialen Krankheiten.

1 Introduction

Roughly 2 billion years ago, the ambient oxygen level dramatically increased in the earth's atmosphere (Kurland and Andersson, 2000). Most likely, this environmental trauma marked a turning point in the evolution of life. Organisms were forced to adapt to the new environment and the fittest survived by natural selection. It is believed that at the time a so-called symbiogenesis (Greek: syn "together"; bios "living"; genesis "origin or birth") took place, where a α-proteobacterium invaded a single cell organism, this time not for the sake of killing, but rather to start a long lasting cooperation. This phenomenon is known as "endosymbiotic theory" that suggests how eukaryotic cells originated from prokaryotes (Margulis, 1970). Mitochondria are thought to be derived from such ancestral bacterial endosymbionts, introducing an oxidative respiratory system into the host cell (Gray et al., 1999).

1.1   Mitochondrial structure and function

Mitochondria (Greek: *mitos* "thread"; chondros "granules") were first discovered in the 19th century, as small structures found in the cytosol of almost every eukaryote (Ernster and Schatz, 1981). Mitochondria are enclosed by two single membranes, the outer (OMM) and inner mitochondrial membrane (IMM) that create two distinct compartments within the

organelle, the intermembrane space (IMS) and the matrix (Alberts et al., 1983). Mitochondria are dynamic organelles that form a network among the cell comprising approx. 20% of its volume (McBride et al., 2006). Mitochondria contain their own circular DNA (mtDNA) in the matrix that comprises a great similarity to the genome of the bacterium *Rickettsia prowazekii* (Andersson et al., 1998). During the course of evolution the symbiont genome has been strongly reduced in size and genes were transferred to the host nucleus through a process called *endosymbiotic gene transfer* (Timmis et al., 2004). Mitochondria harbour their own separate replication, transcription and protein-synthesis machinery that maintains and produces polypetides encoded by the mtDNA. The mitochondrial proteome comprises roughly 1500 proteins of which 99% are nuclear-encoded mitochondrial proteins that need to be actively imported into mitochondria, sorted to the right compartment, properly folded and assembled to complexes (Neupert and Herrmann, 2007). The dual origin of the mitochondrial proteome gave rise to a highly complex process that coordinates respiratory complexes to be assembled in the correct time and right stoichiometric (Kurland and Andersson, 2000).

The hallmark ability of mitochondria is the use of oxygen to efficiently produce ATP, the cell's major energy source, via oxidative phosphorylation (OXPHOS). This process enables the generation of roughly 15 times more ATP from glucose compared to glycolysis under anaerobic conditions. Energy can be derived from the breakdown of carbohydrates via glycolysis and tricarboxylic acid (TCA) cycle, fatty acid oxidation, pyrimidine biosynthesis or choline and amino acid oxidation that all fuel the OXPHOS machinery. Mitochondria are not only the "powerhouses of the cell", but also carry out various other processes such as iron-sulfur (Fe-S) cluster biogenesis, programmed cell death (apoptosis), steroid synthesis, calcium homeostasis and reactive oxygen species (ROS) formation (Lill and Muhlenhoff, 2008; Miller, 2013; Nunnari and Suomalainen, 2012).

During oxidative phosphorylation electrons are passed along a series of complexes that is called the electron transport chain (ETC) (Hatefi, 1985). The ETC is embedded in a specialized invaginated region of the IMM, termed cristae, that greatly increase the surface area, allowing a greater capacity for ATP generation. The ETC consists of four respiratory enzyme complexes (complex I - NADH:ubiquinone oxidoreductase; complex II - Succinate

dehydrogenase; complex III - Ubiquinol cytochrome-c reductase; and complex IV - cytochrome c oxidase) that are organized in a specific order within the IMM that enables a flux of electrons between complexes. In the beginning, the electrons are donated via redox reactions from NADH (via complex I) or $FADH_2$ (via complex II) into the electron transport chain and terminally accepted by oxygen (via complex IV). The flow of electrons through these complexes releases energy in three steps that is transiently stored as an electrochemical proton gradient across the IMM. The resulting chemiosmosis drives the ATP synthase (F_1F_0 ATPase or Complex V) that produces ATP from ADP and phosphate. This utilizes the potential energy of the concentration gradient formed by the amount of protons that flow back through the ATP synthase into the matrix. Reduced oxygen, generated through acceptance of electrons via complex IV, is terminally joined to protons coming though complex V to build up H_2O. The electrochemical gradient is a crucial attribute of mitochondria that drives also other important processes, such as organelle biogenesis via protein import and calcium buffering (Neupert and Brunner, 2002; Williams et al., 2013). Reduced membrane potential is accounting for mitochondrial dysfunction that in turn activates stress pathways (Martindale and Holbrook, 2002; Zamzami et al., 1995).

1.2   Mitochondrial genetics and disease

Mitochondria possess their own genome, termed mtDNA, that is a small, circular, double-stranded DNA molecule of approx. 16 kb in size. mtDNA harbours genes for 13 proteins that are essential core components of the mitochondrial respiratory complexes I, III, IV and V. This vital information allows mitochondria together with nuclear-encoded OXPHOS subunits to build up the respiratory chain that is essential for mitochondrial activity. In addition, 2 ribosomal and 22 transfer RNAs essential for mitochondrial translation are also encoded by mtDNA. All together, mtDNA contains 37 genes in vertebrates that encompass nearly 93% of its total sequence, which makes the genetic information very dense throughout the whole molecule (Wallace, 2007). The residual 7% are non-coding sequences that harbour regulatory elements, such as the D-loop region (approx. 1000 bp) comprising the heavy and light strand promoter (HSP and LSP,

respectively) and the origin of replication for the heavy strand (O_H), whereas the origin for replication for the light strand (O_L) is located in a distant position relative to the D-loop.

Single polycistronic transcripts are made from these promoters that were further processed to generate mature rRNAs, tRNAs, and mRNAs. These transcripts also serve as primers for the replication of one of the strands. Mammalian mtDNA replication is divided into two phases (i) the leading-strand synthesis and (ii) the lagging-strand synthesis (Clayton, 2003). First, the leading-strand synthesis starts at O_H and runs unidirectionally copying roughly two-third of the mtDNA. As a result, the origin of replication of the lagging-strand (O_L) gets exposed as single strand, allowing through a specific secondary structure the initiation of the lagging-strand synthesis. Eventually, both strands are joined together after completed synthesis and ligation generating a closed circular mtDNA molecule.

Mitochondrial DNA is organized in nucleoid structures that have roughly 100 nm in diameter and contain 1-2 copies of mtDNA in average (Kukat et al., 2011). It has been proposed that nucleoids are complex structures, containing a core, where replication and transcription takes place as well as peripheral layers that harbour mitochondrial translation and OXPHOS complex assembly (Bogenhagen et al., 2008). In contrast to nuclear DNA, the mtDNA is present in multiple copies that range from a few in sperm to greater then 100000 in mature oocytes (DeLuca and O'Farrell, 2012; Wai et al., 2010). Interestingly, a third of the total DNA content in oocytes is mtDNA. Unlike nuclear DNA that is carefully copied chromosome-by-chromosome, mtDNA is replicated and turned over at random, to a rate independent of the cell cycle (Bogenhagen and Clayton, 1977).

In vertebrates, mtDNA is almost completely maternally inherited, whereas the paternal mtDNA is degraded after fertilization and never transmitted to the offspring (Al Rawi et al., 2011). Due to the fact that children inherit their entire mtDNA from their mothers, mtDNA mutations and therefore mtDNA disorders, are transmitted maternally. Mitochondria contain between 2 to 10 mtDNA molecules that might vary in sequence therefore causing a mixed pool of mtDNAs within the cell, termed heteroplasmy (Larsson, 2010). In mtDNA diseases, some of the mtDNAs are wild type, while some carry mutations. The load of mutations determines the manifestation as well as the outcome of a

possible mitochondrial disease (Tuppen et al., 2010). Since mitochondria are randomly distributed during cell division, leading to an incidental sort among daughter cells, it is important for the cell that the proportion of mitochondria carrying wild type and mutant mtDNA does not exceed a certain threshold (Stewart and Chinnery, 2015). Once a certain threshold is exceeded it is very likely that cells develop a mitochondrial dysfunction. In contrast, homoplasmy describes a cell that has only identical mtDNA copies, however, copies might be all normal or all mutated.

Mutations in mtDNA can cause defects in OXPHOS that might lead to mitochondrial disorders (Holt et al., 1988; McFarland et al., 2004; Wallace et al., 1988). Over the years more than 250 pathogenic mtDNA mutations have been described that cause a broad clinical spectrum of mitochondrial disorders (Tuppen et al., 2010). Further, it has been shown that not only mtDNA mutations, but also a decrease in the mtDNA copy number can trigger mitochondrial malfunction (Clay Montier et al., 2009). In addition to mitochondrial disorders, mtDNA mutations are connected with various other pathologies such as cancer, diabetes, cardiovascular disorders, neurodegeneration, as well as age-associated mitochondrial dysfunction (Wallace, 2005). During ageing is has been observed that a mosaic distribution of cells develop mitochondrial respiratory chain dysfunction due to accumulation of point mutations or deletions in their mtDNA (Larsson, 2010).

In the past two decades this pattern was not only found in many human tissues, but also in mouse models with enhanced rates of mtDNA mutations (Trifunovic et al., 2004) or deletions (Tyynismaa et al., 2005) that also displayed hallmarks of ageing. The proposed source of mutations in mtDNA occurring during ageing was mainly accounted to the mitochondrial free radical theory of ageing that argues that ageing results from the damage generated by reactive oxygen species (ROS) (Beckman and Ames, 1998; Harman, 1956). It was believed that ROS are only toxic molecules that exclusively cause oxidative stress, directly damaging sensitive and biologically significant targets. However, ROS generation was also interpreted as beneficial event since it is also believed that they are involved in cell signalling by acting as redox signals through a process known as mitohormesis, and their detrimental consequences are possibly just side effects of compromised signalling (Yun and Finkel, 2014). In contrast to the mitochondrial free radical theory of ageing, low

levels of ROS promote health and ultimately extend lifespan (Ristow and Schmeisser, 2014).

1.3 Mitochondrial translation

Mitochondria possess their own protein synthesis machinery that allows the generation of the 13 OXPHOS subunits encoded by the mtDNA. Although this process was discovered as early as 1958 (McLean et al., 1958), the exact mechanisms as well as all the components contributing to mitochondrial translation are still not completely known. The main obstacle in order to decipher this process is the lack of a proper *in vitro* translation system that allows correct initiation and synthesis of mtDNA-encoded proteins. It should be noted that mitochondrial translation resembles its prokaryotic counterpart more closely than its eukaryotic. However, it still presents specific characteristics that are present in neither case. Firstly, the mitochondrial genetic code exhibits several distinct differences from the universal code (Osawa et al., 1992). For instance, UAG serves as stop codon. Furthermore, UGA is used as codon for tryptophan rather than a stop codon. In addition, AUA encodes for methionine instead of isoleucine. Secondly, mitochondrial mRNAs contain very few 5'untranslated nucleotides and no cap structure (Grohmann et al., 1978; Montoya et al., 1981). Thirdly, the decoding system in mitochondria is simplified using only 22 tRNAs instead of 31 suggested by Crick's wobble hypothesis (Barrell et al., 1980). Fourthly, mammalian mitochondria only use a single tRNA^{Met} for initiation as well as elongation in contrast to the prokaryotic and eukaryotic cytoplasmic translation that need two specialized species (Mikelsaar, 1983).

1.3.1 The mitochondrial translational machinery

Mitochondrial translation requires roughly 150 different proteins that are involved in the protein synthesis of the 13 OXPHOS subunits. All components of the mitochondrial translational machinery, apart from 2 rRNAs and 22 tRNA, are encoded by the nucleus and therefore need to be imported from the cytosol. The basic mitochondrial translational machinery consists of: (i) several initiation, elongation and termination factors; (ii)

mitochondrial ribosomal proteins (MRPs) and assembly factors; (iii) aminoacyl-tRNA synthetases, tRNA-modifying enzymes and rRNA methylating enzymes.

The mammalian mitoribosome exhibits a sedimentation coefficient of 55S and comprises large subunit (39S) and a small subunit (28S), containing a 16S rRNA and a 28S rRNA, respectively (Amunts et al., 2015; Greber et al., 2015). The bacterial 5S rRNA is replaced by structural similar tRNA in mammals, such as tRNA^{Val} (human) or tRNA^{Phe} (porcine) (Brown et al., 2014; Greber et al., 2014). In contrast to bacteria, mammalian mitoribosomes have shorter rRNAs and the overall rRNA content is much lower. Nevertheless, mitoribosomes compensate the reduction in rRNA levels with a correspondingly higher protein content (Amunts et al., 2015; Greber et al., 2015). Overall the mitoribosome contains 80 ribosomal proteins, of which 36 are specific to mitochondria (Amunts et al., 2015). Moreover, mitoribosomal proteins are roughly 60% larger than their corresponding bacterial counterparts (Brown et al., 2014). The higher protein mass leads to a strikingly different morphology compared to the bacterial 70S ribosome (Sharma et al., 2009; Yusupov et al., 2001). Numerous mitoribosomal proteins cover almost completely the surface, shielding the rRNA core from reactive oxygen species (Amunts et al., 2015). Since all proteins translated in mitochondria are hydrophobic, integral membrane proteins, mitoribosomes are permanently tethered to the IMM via the 39S subunit (Amunts et al., 2015).

Mammalian mitochondria contain 22 tRNAs corresponding to each amino acid apart from serine and leucine that possess two tRNAs each. Mitochondrial tRNAs have distict features that separate them from their canonical counterparts. In general, mitochondrial tRNAs are shorter and often miss key nucleotides that are important for the L-shaped tertiary structure of bacterial and eukaryotic cytoplasmic tRNAs. It has been also observed that mitochondrial tRNAs lack conserved tertiary interactions, particulary long-range interactions of D- and T-arms, which result in a weaker three-dimensional structure (Helm et al., 1999; Steinberg et al., 1994; Zagryadskaya et al., 2004). Although direct structural evidence is missing, cryo-EM revealed that tRNAs bound to the P-site basically reconstitutes the L-shape with a breach elbow region (Sharma et al., 2003). The structure of this tRNA roughly resembles the one of canonical tRNAs, however, some regions remain strikingly different.

Although, many of the core components necessary for mitochondrial translation have been discovered, it is very likely that many more factors play a role, directly or indirectly, in mitochondrial translation, which still remain to be identified
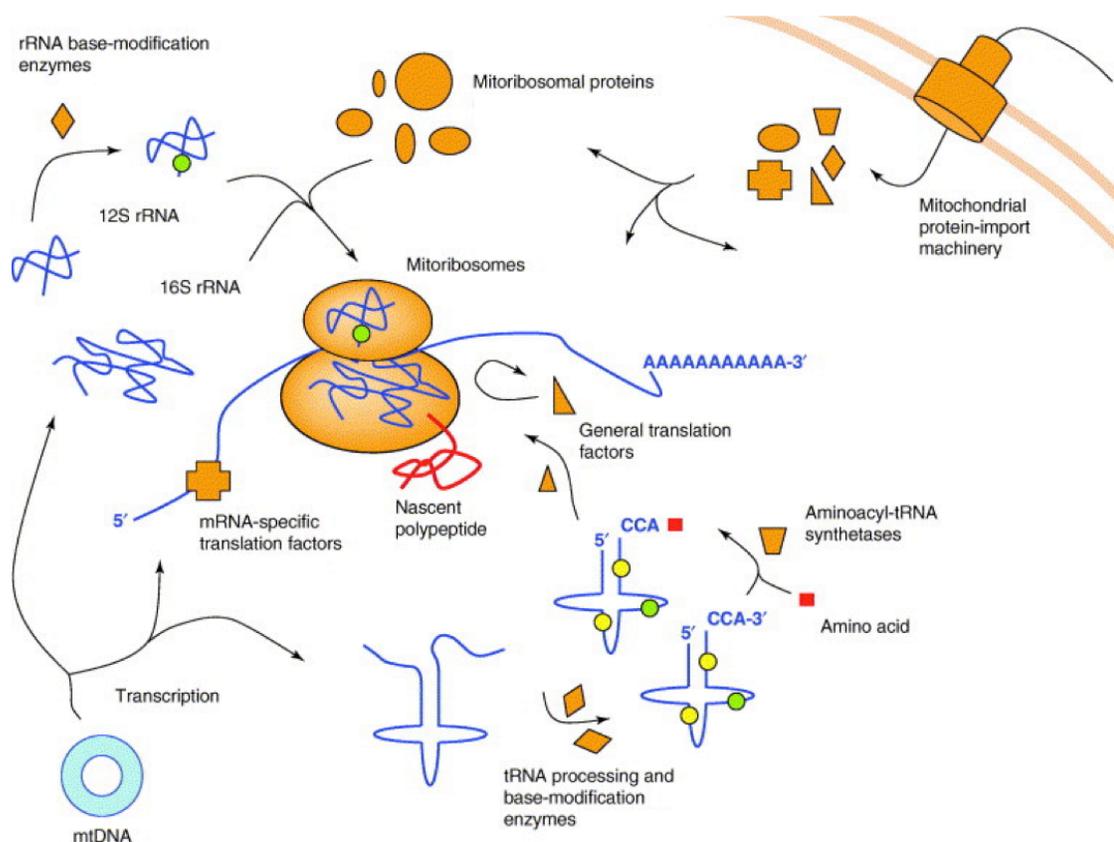
Figure 1.1: The mitochondrial translational machinery.
Nuclear-encoded mitoribosomal proteins are imported into mitochondria and combined with mitochondrial-encoded rRNA to assemble the functional mitoribosome. mtDNA-encoded mRNAs get translated by these mitoribosomes with the help of tRNAs also encoded by the mtDNA. All other enzymes required for the mitochondrial translational machinery are nuclear-encoded and get imported from the cytosol (e.g. aminoacyl-tRNA synthetases). Orange icons depict nuclear-encoded protein, whereas blue lines represent mtDNA-encoded transcription products. Reprinted with modifications from (Jacobs and Turnbull, 2005).

1.3.2 The mitochondrial translation process

Mitochondrial translation is split into three main phases: initiation, elongation, termination as well as a final ribosome recycling step that all require specific sets of supporting factors (Christian and Spremulli, 2012). Our knowledge about the basic

mechanism of mitochondrial protein synthesis is derived from studies in bacteria and some studies in mitochondria. Nevertheless, the exact mechanism how the protein synthesis starts is poorly understood to date. Mitochondrial mRNAs miss important features that regularly facilitate ribosome binding or guide the ribosome to the start codon, such as a Shine-Dalgarno sequence or a 7-methylguanlyate cap structure, which are found in prokaryotes or in the eukaryotic cytoplasm, respectively (Temperley et al., 2010). It is believed that the 28S subunit contains a special mRNA entry gate that detects the unstructured 5'sequences of mitotochondrial mRNAs leading to the initiation of translation (Jones et al., 2008; Sharma et al., 2003).

The current model proposes that the mitochondrial initiation factor mtIF3 catalyses the dissociation of the mitoribosome into the small and the large subunit, that allows a sequence-independent binding of the mRNA to the 28S small subunit, while preventing premature binding of the 39S large subunit (Christian and Spremulli, 2009; Koc and Spremulli, 2002). Moreover, mtIF3 induced complex formation is also thought to correctly position the start codon to the peptidyl (P) site of the mitoribosome, creating access for fMet-tRNA^{Met}. Subsequently, a second initiation factor mtIF2 mediates binding of fMet-tRNA^{Met} to the 28S small subunit that is considerably enhanced by GTP (Liao and Spremulli, 1990; Ma and Spremulli, 1996). Recombining both the large and the small mitoribosome subunits leads to dissociation of mtIF3 (Haque et al., 2008). In addition, the 39S large subunit promotes GTP hydrolysis on mtIF2, enabling the release from the complex and the completion of the initiation phase.

As a next step, the elongation phase is carried out by mitochondrial specific elongation factors such as mtEFTu, mtEFTs, and mtEFG (Smits et al., 2010). First, the elongation factor mtEFTu associates with GTP and an aminoacylated tRNA to form a ternary complex. In this step, mtEFTu protects the tRNA from hydrolysis as well as transports it to the acceptor (A) site of the 28S small subunit facilitating the codon-anticodon recognition. During this step GTP is hydrolyzed on mtEFTu that triggers the release of mtEFTu-GDP, which is subsequently recycled by mtEFTs to active mtEFTu-GTP. After the release, the aminoacyl-tRNA translocates into the peptidyl (P) site of the mitoribosome, enabling the peptide bond formation, thereby adding one amino acid to the growing peptide. The elongation factor mtEFG1 catalyses the translocation step that moves

the tRNA from P to exit (E) site of the mitoribosome, whereby the mRNA is advanced by one codon. It is not clear by now, whether the mitoribosome contains an actual E site, since the bovine mitoribosomal E site deviates markedly from corresponding bacterial and eukaryotic cytosolic sites. This might also suggests that the E site is either very weak or even absent in the mitoribosome (Mears et al., 2002; Mears et al., 2006). Finally, the tRNA dissociates from the mitoribosome, enabling the re-start of a new elongation cycle. To date not all factors implicated in the elongation process are known, as well as the functional role of mtEFG2 is still missing.

Once a stop codon (UAA, UAG, AGA or AGG) enters the A site, the termination phase initiates (Chrzanowska-Lightowlers et al., 2011). The stop codon gets recognized by the mitochondrial release factor (mtRF1 or mtRF1a), which causes the polypeptide that is connected to the final tRNA in the P site to be released. Subsequently, the nascent polypeptide dissociates from the tRNA through hydrolyzation of the connecting ester bond, which is catalysed by GTP. Once the newly synthetized protein has been released, the mitochondrial ribosome recycling factors (mtRRF and possibly mtEFG2) facilitate the dissociation of mitoribosomal subunits, tRNA and mRNA, enabling their recycling for a new round of protein synthesis (Bertram et al., 2001; Marintchev and Wagner, 2004).

1.3.3 Aminoacyl-tRNA synthetases and mitochondrial disorders

Aminoacylation of mitochondrial tRNAs is catalysed by mitochondrial aminoacyl-tRNA synthetases (mtARSs) that are key enzymes for the translation of the genetic information. Therefore, the fidelity of translation depends on the accurate recognition of amino acids and tRNA by these enzymes. mtARSs catalyse the ligation of a specific amino acid to their cognate tRNA, using the same two-step reaction as cytosolic tRNAs, where they form an intermediate aminoacyl-adenylate through activation with ATP followed by the transfer of the aminoacyl group to the tRNA (Ibba and Soll, 2000).

Mitochondrial translation uses 20 different ARSs that are all encoded in the nucleus, thus being translated in the cytosol and imported into mitochondria. Three mtARSs (GARS, KARS, and QARS) also act in the cytosol, making them essential for both

mitochondrial and cytoplasmic translation (Antonellis and Green, 2008). It should be noted that mtARSs seem to have a reduced catalytic efficiency for tRNA aminoacetylation by contrast to prokaryotic and cytosolic homologues, as demonstrated for various mtARSs (Bonnefond et al., 2005; Bullard et al., 2000; Sanni et al., 1991). The glutaminyl-tRNA synthetase is absent in mitochondria as well as many bacteria. However, an indirect transamidation pathway generates glutaminyl-tRNA^{Gln}, where tRNA^{Gln} first gets charged by EARS2 (aminoacylates both tRNA$^{Glu/Gln}$) with glutamate and converted to glutaminyl-tRNA^{Gln} by tRNA-dependent aminotransferases (Nagao et al., 2009). Thus, 19 different mtARS generate 20 charged tRNA, while 3 mtARS have double localization. Some mtARSs are capable to aminoacylate both mitochondrial as well as prokaryotic tRNAs, but prokaryotic ARSs fail to do so in mammalian mitochondria (Fender et al., 2006; Kumazawa et al., 1991). This illustrates the high sequence and structural relaxation of mt-tRNAs that is likely a result of the high divergence of mtDNA during evolution (Fender et al., 2012).

The general structure of ARSs comprises a catalytic domain, an anticodon binding domain, and sometimes an editing domain that removes mischarged amino acids, circumventing the incorporation of a wrong amino acid during translation (Beebe et al., 2008). Further, there are two distinct classes of AARSs with respect to their catalytic site: class I enzymes that are comprised of five parallel β-strands connected through α-helices and the two signature motifs; class II enzymes that mainly consist of a sheet of six antiparallel β-strands and three motifs of less-conserved sequences (Bonnefond et al., 2005). Interestingly, it has been shown that ARSs also have acquired additional functions during evolution. Cytosolic ARSs are associated with extracellular and intracellular events such as apoptosis, synthesis of rRNA, or tRNA export to the cytosol (Guo and Schimmel, 2013). Mitochondrial ARSs were also found having additional roles; for instance, the mitochondrial lysyl-tRNA synthetase in yeast has a role in both aminoacetylation and import of cytosolic tRNA^{Lys} into mitochondria (Smirnova et al., 2012).

Mutations in ARSs are found to cause mitochondrial protein synthesis deficiencies that have been associated with diverse clinical pathologies (Table 1.1) (Antonellis and Green, 2008). The clinical presentations are mainly characterized with an early onset and a transmission via autosomal recessive traits. Interestingly, the high tissue specificity of

mtARSs disorders is difficult to explain by their role in mitochondrial translation since all ARSs are ubiquitous enzymes working in the same pathway. However, it is possible that this very strict genotype-phenotype correlation found for most of the genes is due to still unknown functions of mitochondrial ARSs. It has been suggested that loss-of-function mutations might result in some residual enzymatic activity that cause alterations in different tissues during development (Konovalova and Tyynismaa, 2013). For instance, mutations in synthetases for glycine (GARS) and lysine (KARS) lead to peripheral neural pathologies, like autosomal dominant forms of Charcot–Marie–Tooth disease type 2D (CMT2D) and a dominant intermediate Charcot–Marie–Tooth disease (DI-CMT), respectively (Antonellis and Green, 2008). Since both GARS and KARS are acting not only in the cytosol but also in mitochondria the question of the primary cause for the disease is still matter of investigation. The first mitochondrial ARSs found to cause a disease was a mutation in DARS2 (aspartate-tRNA-synthetase) that leads to leukoencephalopathy with brain stem and spinal cord involvement and lactate elevation (LBSL) (Scheper et al., 2007). Since the first discovery of diseases caused by AARS2 mutations numerous other AARS2 pathologies have been described (Table 1.1).

Table 1.1: Pathologies associated with mutations in mtARS.

Gene	Clinical picture	Organ	Onset	Reference
DARS2	Cerebellar ataxia, spasticity, dorsal column dysfunction, cognitive impairment	Brain	Childhood/Adulthood	(Scheper et al., 2007)
RARS2	Encephalopathy with lethargia, hypotonia, epilepsy, and microcephaly	Brain	Perinatal	(Edvardson et al., 2007)
YARS2	Myopathy, lactic acidosis, and sideroblastic anemia (MLASA)	Muscle	Childhood	(Riley et al., 2010)
SARS2	Hyperuricemia, pulmonary hypertension, renal failure, and alkalosis (HUPRA)	Kidney	Perinatal	(Belostotsky et al., 2011)
AARS2	Hypertrophic cardiomyopathy, delayed motor development, cerebellar ataxia	Heart	Childhood	(Gotz et al., 2011)
MARS2	Autosomal recessive spastic ataxia	Brain	Childhood/Adulthood	(Bayat et al., 2012)
HARS2	Sensorineural hearing loss and ovarian dysgenesis (Perrault syndrome)	Cochlea, ovary	Childhood/Adulthood	(Pierce et al., 2011)
LARS2	Sensorineural hearing loss and ovarian dysgenesis (Perrault syndrome)	Cochlea, ovary	Childhood/Adulthood	(Pierce et al., 2013)

FARS2	Epileptic encephalopathy, liver disease, and lactic acidosis	Brain, muscle	Perinatal	(Elo et al., 2012)
EARS2	Global developmental delay or arrest, epilepsy, dystonia, spasticity, and high lactate	Brain	Early childhood	(Steenweg et al., 2012)
VARS2	Psychomotor delay, seizures, facial dysmorphism, lactic acidosis	Brain	Childhood	(Pierce et al., 2013)
TARS2	Psychomotor delay, hypotonia	Brain	Perinatal/early childhood	(Pierce et al., 2013)
GARS	Charcot-Marie-Tooth (CMT) disease 2D or distal hereditary motor neuropathy VA	Nerve	Childhood/Adulthood	(Seburn et al., 2006)
KARS	Autosomal recessive CMT (intermediate, B)	Nerve	Childhood/Adulthood	(Santos-Cortez et al., 2013)

1.4 Mitochondrial protein homeostasis

The life of proteins can be influenced by a broad variety of environmental changes, disease and ageing. A functional cellular machinery, which constantly monitors and supports protein folding and protein degradation, is essential to maintain a functional protein homeostasis. On the one hand, chaperones facilitate a functional protein-folding environment for newly synthetized as well as misfolded proteins; on the other hand proteases clear out the overload of irreversibly misfolded or misassembled proteins (Bukau et al., 2006; Sauer and Baker, 2011). Since the majority of the mitochondrial proteome (around 1500 proteins) is encoded in the nucleus and subsequently produced in the cytosol, a massive influx of proteins has to be timed and proteins have to be specifically distributed in each compartment exhibiting its right folding (Neupert and Herrmann, 2007). Thus, a major challenge in mitochondria occurs during import, where proteins have to be unfolded, cleaved, properly refolded and often assembled with proteins encoded by the mitochondrial DNA (mtDNA). In addition, transient stresses, such as infections or reactive oxygen species (ROS), or chronic stresses, such as diseases or age-related pathologies, perturb the protein homeostasis in mitochondria (Galluzzi et al., 2012).

1.4.1 Protein import

The majority of mitochondrial proteins are imported by the use of a cleavable amino-terminal presequence that is also known as mitochondrial targeting sequence (MTS) (Chacinska et al., 2009). The MTS forms positively charged amphipathic α-helices that interact with the translocase of the outer mitochondrial membrane (TOM complex) (Abe et al., 2000). After translocation through the TOM complex the preproteins are passed to the presequence translocase of the inner mitochondrial membrane (TIM23 complex). The membrane potential across the inner mitochondrial membrane (ΔΨ, negatively charged on the matrix side) drives the translocation of the positively charged preproteins into the matrix (Martin et al., 1991). Finally, the presequence-targeted protein is pulled inside the matrix via the concerted action of the presequence translocase-associated motor (PAM) together with the ATP-dependent heatshock protein 70 (mtHsp70) (Chacinska et al., 2005; Mapa et al., 2010). The MTS is generally cleaved by the mitochondrial processing peptidase (MPP).

Proteins targeted to the inner membrane contain a hydrophobic part c-terminal to the presequence that enables a lateral release within the TIM23 complex (Glick et al., 1992; Meier et al., 2005). Alternatively, designated innermembrane proteins can be fully or partially translocated into the matrix and then inserted into the IMM through the OXA export machinery, which also integrates mtDNA-encoded OXPHOS subunits (He and Fox, 1997; Hell et al., 1998; Ott and Herrmann, 2010). In contrast, complete hydrophobic inner membrane proteins do not contain a presequence and therefore use alternative import routes (Endres et al., 1999; Rehling et al., 2003). The so-called carrier pathway imports and sorts proteins containing an internal targeting sequence that mainly comprises members of the large metabolite carrier family (Brix et al., 1999). This pathway also makes use of the TOM complex, but then alternatively guides to the small TIM chaperones in the intermembrane space and the carrier translocase of the inner membrane (TIM22 complex) that make use of the membrane potential for insertion (Curran et al., 2002; Endres et al., 1999; Rehling et al., 2003).

Again another mitochondrial import pathway makes use of the mitochondrial intermembrane space import and assembly (MIA) machinery that is used by cysteine-rich

intermembrane space proteins (Banci et al., 2009; Chacinska et al., 2004). In principle, intermembrane space proteins enter mitochondria via the TOM complex in a reduced, unfolded confirmation. Subsequently, the central component of the MIA machinery Mia40 forms a transient disulfide bond with the incoming protein through its oxidoreductase function. The generated disulfide bond allows the intermembrane space protein to be stably folded and also prevents relocation to the cytosol. Finally, Mia40 gets reoxidized by the sulfhydryl oxidase Erv1 that facilitates its recycling for new rounds of precursor import and oxidation.
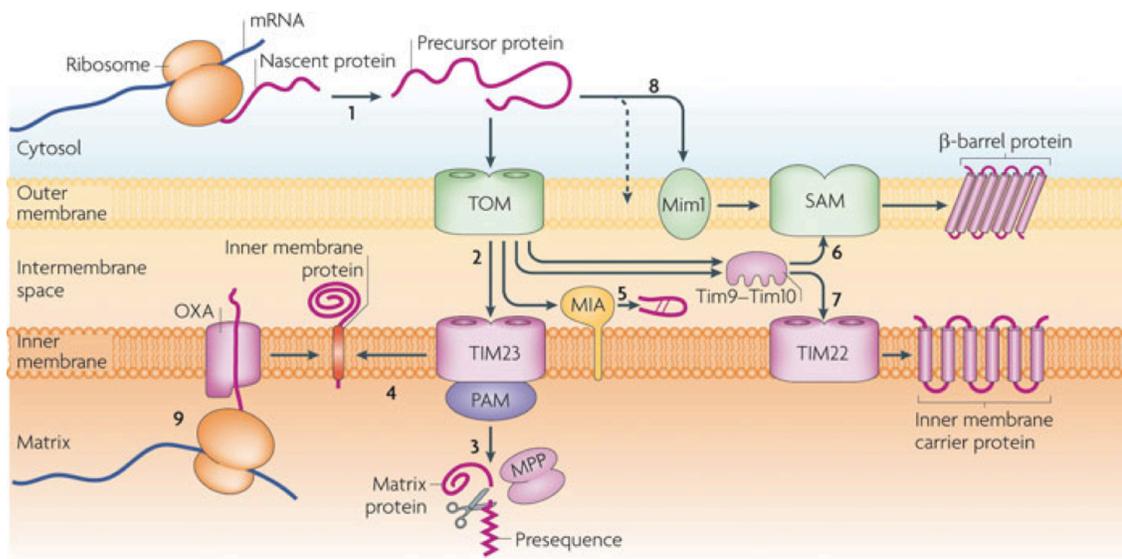
Figure 1.2: The mitochondrial import machinery.
The vast majority of the mitochondrial proteome is generated in the cytosol and imported via the translocase of the outer mitochondrial membrane (TOM) complex [1]. Subsequently, newly imported proteins get sorted via different pathways according to their final destination [2]. Matrix proteins follow the presequence pathway through the translocase of the inner membrane (TIM23) complex and the presequence translocase-associated motor (PAM). Presequences are removed from the mitochondrial processing peptidase (MPP) within the matrix [3]. Some inner membrane proteins are released from the TIM23 complex in lateral direction [4]. Intermembrane space proteins get imported and oxidized by the mitochondrial inter membrane space assembly (MIA) machinery [5]. Small TIM chaperones (TIM9-TIM10 chaperone complex) guide hydrophobic precursor proteins either to the OMM via the sorting and assembly (SAM) machinery [6] or to the IMM via the TIM22 complex (carrier pathway) [7]. Outer membrane proteins bypass the TOM channel and get inserted directly into the membrane using different pathways (e.g. mitochondrial import (MIM) complex [8]. Proteins synthesized within mitochondria are exported to the IMM by the oxidase assembly (OXA) machinery [9]. Reprinted with modifications from (Schmidt et al., 2010).

Outer mitochondrial membrane proteins are subdivided into two classes. One the one hand, β-barrel proteins enter mitochondria via the TOM complex, interact with small TIM chaperones (TIM9-TIM10 chaperone complex) of the intermembrane space, and are embedded into the outer membrane by the sorting and assembly machinery (SAM complex) (Kutik et al., 2008; Paschen et al., 2005). On the other hand, the class of α-helical outer membrane proteins have several suggested import routes, however, this process is not completely understood. It has been described that some α-helical proteins are imported via the mitochondrial import (MIM) complex (Becker et al., 2011; Dimmer et al., 2012). It is generally believed that most α-helical outer membrane proteins bypass the TOM channel using alternative entry pathways (Krumpe et al., 2012; Meineke et al., 2008; Otera et al., 2007).

1.4.2 Protein folding in the matrix

Mitochondria contain numerous chaperones and co-chaperones that facilitate folding and thereby stabilize the three-dimensional structures, preventing proteins from aggregation (Voos, 2013). Here, we focus on the mitochondrial chaperones mtHSP70 and HSP60 as they are key for the protein homeostasis in the mitochondrial matrix. These chaperones create a so-called mitochondrial folding network that is responsible not only for import and folding of matrix proteins, but also various other protein quality control reactions. Most aspects so far have been extensively studied in yeast, however, more and more data are also available from the mammalian system (Deocaris et al., 2006; Voos and Rottgers, 2002).

mtHsp70

The major mitochondrial Hsp70 (mammals: mtHsp70; yeast: Ssc1) is an essential protein that plays a role in the translocation of mitochondrial proteins into the matrix as well as facilitates folding of newly imported proteins to their native confirmation (Liu et al., 2001; Strub et al., 2000). These attributes have been described to be inevitable for cellular survival under all growth conditions (Craig et al., 1987).

The mtHsp70/Ssc1 associated protein import can be divided into two functional aspects: (i) the protein translocation through both the TOM and TIM complex and (ii) the complete protein unfolding as consequence of the small channel of the translocase complexes (Gambill et al., 1993; Voisine et al., 1999). The energy for both processes comes from the inner mitochondrial membrane potential ($\Delta\Psi$) as well as the ATP hydrolysis in the matrix. As the membrane potential is used to insert polypeptides into the translocase complexes, ATP hydrolysis is carried out by the ATPase domain of mtHsp70 enabling the movement and unfolding of the matrix-targeted proteins through the membrane pores. mtHsp70 is the only ATP-dependent protein in this process, which again highlights its importance during the import of matrix proteins (Moro et al., 2002).

The activity of mtHsp70 during matrix import is closely connected with constituents of the TIM23 translocase complex, such Tim44, Pam18 and Pam16, which influence the import-specific activity of mtHsp70 and are inevitable for an effective transport of polypetides into the matrix (Kronidou et al., 1994; Li et al., 2004; Rassow et al., 1994; Truscott et al., 2003). In addition, the nucleotide exchange factor Mge1 facilitates recycling of nucleotide-regulated substrate affinity states of mtHsp70 during preprotein translocation (Schneider et al., 1996).

Furthermore, the interaction of mtHsp70 with the channel might exert an active pulling force on the incoming preprotein chain that is needed to master conformational limitations during the unfolding reaction, however, a detailed molecular mechanism still remains elusive (Lim et al., 2001; Voisine et al., 1999). Once an unfolded preprotein enters the matrix, the folding process is initiated by mtHsp70 (Liu et al., 2001). In this regard, mtHsp70s closely resemble the chaperone function of cytosolic Hsp70s that fold nascent polypeptides during translation (Peisker et al., 2010). It is believed that mtHsp70 stabilizes nascent polypeptide chains in order to avoid irregular interactions of still unfolded segments. In this process the folding reaction per se is slowed down, which allows more proteins to be folded properly. The folding reaction is carried out in close cooperation with another major mitochondrial matrix chaperone, Hsp60. The specificity of mtHsp70 for either import or protein folding is determined by the interaction with different types of J-family co-chaperones (Horst et al., 1997). For instance, the protein Mdj1 (mitochondrial DnaJ homolog) is implicated in the folding reaction of mtHsp70 (Rowley et al., 1994;

Westermann et al., 1995). Additionally to its chaperone and translocation activity, mtHsp70 is also involved in the protein biosynthesis of OXPHOS subunits as well as their assembly to functional complexes in the inner membrane (Herrmann et al., 1994).

Another feature of mtHsp70 function is the ability to keep proteins soluble during protein degradation in order to prevent aggregation (Wagner et al., 1994). Interestingly, knockdown of hsp-6 (homolog of mammalian mtHsp70) in *Caenorhabditis elegans* (*C. elegans*) induced a premature ageing phenotype that highlights its importance in multicellular organisms (Kimura et al., 2007). In mammals, mtHsp70 has also been described to a play crucial role in various human pathologies, such as cancer and Parkinson's disease (Jin et al., 2006; Wadhwa et al., 2006). Nevertheless, a clear role for mtHsp70 in mammalian mitochondrial protein quality control and its effects on pathology still needs to be defined.

Hsp60

In the mitochondrial matrix, Hsp60 is the key component of the protein machinery that facilitates folding and assembly of newly imported preproteins (Martin, 1997). Like the whole Hsp60 protein family, mitochondrial Hsp60 forms a homo-oligomer of 14 subunits that is arranged in two rings of 7 subunits each that give rise to a "double doughnut" structure (Sigler et al., 1998; Xu et al., 1997). Both rings shape a large inner cavity that allows accommodation of unfolded proteins with a size up to 50 kDa. Substrates of Hsp60 not only interact with hydrophobic amino acid residues in the inner cavity, but also get protected inside from other components of the surrounding environment. Upon binding of ATP, the Hsp60 molecule undergoes a large conformational change that converts the inner cavity to be more hydrophilic, allowing the release of bound proteins and thus new rounds of folding (Walter, 2002). Hsp60 closely cooperates with a specific cochaperone, termed Hsp10, which forms a lid on top of Hsp60 to cover the opening of the central cavity (Fenton et al., 1996). Hsp10 is believed to coordinate the release of bound substrates by regulating both single Hsp60 monomer behaviour as well as the ATPase cycle (Martin et al., 1993).

The crucial role of Hsp60 in mitochondrial biogenesis was initially demonstrated using a yeast null mutant that was unviable due to its severe folding defects (Cheng et al., 1989). The same study also showed that conditional Hsp60 mutants tend to accumulate unfolded proteins in the matrix that could not be further assembled into functional enzyme complexes. Subsequent analyses demonstrated that newly imported preproteins physically interact with Hsp60 in the matrix, thereby significantly elevating the overall folding efficiency (Langer and Neupert, 1991; Ostermann et al., 1989; Reading et al., 1989). A yeast proteomics approach aiming at identifying potential Hsp60 substrates in mitochondria suggested that it is not generally required for all mitochondrial proteins (Dubaquie et al., 1998). Interestingly, some substrates can also fold without the Hsp10 cochaperone, while others do not even need the Hsp60/Hsp10 system in the first place. However, a subset of mitochondrial proteins has also been shown to be dependent on Hsp60 to acquire their native conformation (Rospert et al., 1996). Nascent polypeptide chains that arise from translocation always interact first with Hsp70 chaperones and then with Hsp60 chaperones in a subsequent step (Voos, 2013). This again illustrates the close cooperation of both major chaperone classes in the folding of mitochondrial matrix proteins.

Despite being mainly implicated in folding after import, Hsp60 is also suggested to play a role in general protein quality control reactions. Recent studies demonstrated that Hsp60 protects from protein aggregation of endogenous matrix proteins upon heat stress (Bender et al., 2011), which supports a more central role in maintaining protein homeostasis upon normal as well as stress conditions. In agreement with these observations, mammalian Hsp60 is upregulated upon oxidative stress as well as under conditions where protein folding is compromised (Mitsumoto et al., 2002; Yoneda et al., 2004; Zhao et al., 2002). Numerous studies demonstrated a neuropathological role for Hsp60; for instance, in patients with an autosomal dominant form of hereditary spastic paraplegia (Bross et al., 2007; Bross et al., 2008; Hansen et al., 2007; Hansen et al., 2002). Additionally, it has been described that Hsp60 interacts with mutant mitochondrial enzymes in patient cell lines, which is in line with its role in protein quality control reactions (Pedersen et al., 2003). Remarkably, patient cell lines that exhibit Hsp60 deficiencies displayed a decrease of matrix protease components, possibly linking different protein quality control networks intrinsically (Hansen et al., 2008).

1.4.3 Protein degradation

Mitochondrial protein homeostasis not only relies on molecular chaperones, but also on a selective proteolysis of terminally damaged, misfolded, and non-assembled proteins that cannot be rescued anymore. Under regular conditions, mitochondrial proteins are continuously recycled by proteases to guarantee a constant functionality of the mitochondrial proteome (Augustin et al., 2005). Moreover, during mitochondrial protein transport, sorting, maturation, and assembly an overload of improperly targeted, unassembled, or damaged proteins might occur that also needs to be degraded by proteases (Anand et al., 2013; Fischer et al., 2012). Various endogenous stress conditions, such as ROS-induced protein damage and ageing also increase the load of non-functional proteins that bear a serious threat to cellular homeostasis (Stadtman and Berlett, 1998). Mitochondrial proteases are highly conserved proteins that serve as a first line of defence against proteotoxic stress (Baker et al., 2011). Apart from various mitochondrial peptidases, that are not further discussed here, there are three classes of chambered mitochondrial proteases: the soluble protease families Lon and ClpP, as well as the FtsH/membrane AAA protease family.

Lon

The Lon protease family was initially found and extensively studied in bacteria and was shown to be conserved among virtually all eukaryotes (Desautels and Goldberg, 1982; Gottesman, 1996; Van Dyck et al., 1994). Lon family members form homo-oligomeric ring-shaped protein complexes that belong to the AAA+ protein family. Lon proteases comprise three functional domains, the catalytic protease domain, the ATP-binding domain and a substrate binding N-terminal domain (Cha et al., 2010). In prokaryotes, Lon was described as one of the key proteases that degrade damaged proteins (Desautels and Goldberg, 1982; Goldberg and Waxman, 1985).

Functional studies in *Saccharomyces cerevisiae* (*S. cerevisiae*) showed that Pim1 (homologue of mammalian Lon) is essential for the degradation of denatured or oxidatively damaged proteins (Bota and Davies, 2002; Suzuki et al., 1994). The importance for Pim1 has been demonstrated by the consequences of a deletion, which resulted in a respiratory

deficient phenotype due to mtDNA defects (Suzuki et al., 1994; Van Dyck et al., 1994). In human cells, LON was found to be involved in protein quality control, removal of oxidized proteins as well as in the regulation of respiration (Voos, 2013). However, it has not been fully characterized by now. Lon tightly cooperates with matrix chaperones, which retain proteins unfolded prior to proteolysis (Bender et al., 2011; Wagner et al., 1994).

To date, most of the Lon substrates found could not be systematically categorized by a specific motif. However, there is evidence that proteins with complex structures and organisations, such as iron/sulfur cluster containing proteins, are more prone for Lon degradation. For instance, mammalian LON has been described to degrade ACO2 (aconitase 2, mitochondrial), an iron/sulfur cluster protein, the steroidogenic acute regulatory protein (StAR), as well as the mitochondrial transcription factor A (TFAM) (Bota and Davies, 2002; Granot et al., 2007; Matsushima et al., 2010). It was reported that LON levels decline in an age-dependent manner as observed in aged mice, which is accompanied by ROS-induced protein damage and enhanced mitochondrial dysfunction (Bota et al., 2005; Bota et al., 2002). In line with these observations it was shown that lifespan of the fungus *Podospora anserina* could be significantly increased by overexpression of Lon (Luce and Osiewacz, 2009). In general, Lon was found to be upregulated in response to various cellular or environmental stresses. For instance, both oxidative stress and heat stress induce Pim1 in yeast (Bender et al., 2011; Van Dyck et al., 1994). Similarly, the mammalian Lon protease responds to oxidative and heat stress, as well as serum starvation, ER stress and hypoxia (Fukuda et al., 2007; Hori et al., 2002; Ngo and Davies, 2007, 2009; Pinti et al., 2011).

ClpXP

The second protein family of soluble proteases is the Clp protein family (caseinolytic protease), which was mainly studied in bacteria (Baker and Sauer, 2012). Whereas the human Lon protease has been extensively analysed, the ClpXP protein complex is one of the most understudied proteases in higher organisms. The missing knowledge is partly due to the fact that the yeasts *S. cerevisiae* or *S. pombe* do not contain any ClpXP homolog (Yu and Houry, 2007). ClpP forms a large homo-oligomeric ring-shaped protein complex composed of two stacked rings with 7 subunits each that serves as

proteolytic core. Additionally, ClpP needs to pair with its corresponding ClpX chaperone to form the fully active holo-protease (Santagata et al., 1999). The ClpX chaperone exerts three different functions: (i) recognition of the substrates, (ii) ATP-dependent substrate unfolding, and (iii) the translocation of the substrate proteins into the proteolytic chamber of the ClpP complex.

In prokaryotes, ClpXP serves as major quality control protease that degrades proteins under stress conditions (Baker and Sauer, 2012), and translation products that contain a SsrA-tag (Gottesman et al., 1998). Similar to the bacterial system, mammalian mitochondria contain a complete ClpXP system, whose structural properties have been studied *in vitro* (Bross et al., 1995; Kang et al., 2005; Kang et al., 2004). Even though similar activities in the degradation of model peptides and proteins such as casein were observed in bacteria and mammals, the endogenous substrate specificity, largely determined by the respective ClpX subunits, remains uncharacterized in mammals (Kang et al., 2002; Lowth et al., 2012). In general, structural differences between mammalian and prokaryote ClpX translate into differences in substrate specificities (Kang et al., 2002). Moreover, it has not been described so far, which recognition motifs are used by the mammalian ClpXP, therefore a detailed functional characterisation is required. However, it was suggested that it is implicated in protein quality control and the mitochondrial stress response signalling by its similarity to homologs in bacteria and *C. elegans*, respectively (see chapter 1.5.).

FtsH/membrane AAA proteases

In addition to the soluble chambered matrix proteases Lon and ClpXP, mitochondria harbour a separate proteolytic system that is responsible for the degradation of membrane-integrated substrate proteins (Gerdes et al., 2012). These enzymes have evolved from the bacterial FtsH (filament-forming temperature-sensitive) protein family that are present in the plasma-membrane facing the cytosol with their catalytic domain (Ito and Akiyama, 2005). These proteases comprise a zinc metallo-protease domain, a regulatory domain belonging to the AAA family, and a transmembrane domain that enables their insertion into the inner mitochondrial membrane (Voos, 2013).

In mitochondria, two forms of inner membrane bound AAA proteases with different membrane topology are present: (i) the m-AAA protease that is active in the matrix compartment, as well as (ii) the i-AAA protease that faces the intermembrane space (Leonhard et al., 1996). The m-AAA protease forms a ring-like hexameric structure, comprising a central cavity that serves as proteolytic core. In humans it is either present as heterooligodimer composed of the subunits Afg3l2 and paraplegin or as homooligodimer only composed of Afg3l2 (Koppen et al., 2007). In mice, the m-AAA protease incorporates an additional subunit, Afg3l1, that is able to form homooligomeric complexes or heterooligomeric complexes together with Afg3l2 and/or paraplegin (Koppen et al., 2007). In contrast, the i-AAA protease is build up only of a single subunit, Yme1l (*S. cerevisiae*: Yme1) (Weber et al., 1996).

Mitochondrial AAA proteases are implicated in different fundamental processes: (i) membrane protein quality control processes (mainly m-AAA protease) (Arlt et al., 1998; Augustin et al., 2005), (ii) assembly of respiratory chain complexes (both AAA proteases) (Arlt et al., 1998; Leonhard et al., 1999), and (iii) import and maturation of certain mitochondrial proteins (Nolden et al., 2005; Rainey et al., 2006). Furthermore, the i-AAA protease was found in yeast to be implicated in the maintenance of mitochondrial phospholipid levels (Potting et al., 2010), as well as in the regulation of mitochondrial fusion by cleavage of OPA1 (Griparic et al., 2007; Song et al., 2007). The crucial role of AAA proteases in protein quality control was highlighted by the finding that mutations in either paraplegin or Afg3l2 result in the neurological disorders hereditary spastic paraplegia (HSP) and spinocerebellar ataxia type 28 (SCA28), respectively (Di Bella et al., 2010; Martinelli et al., 2009; Martinelli and Rugarli, 2010; Rugarli and Langer, 2006). On the one hand, an autosomal recessive form of HSP caused by *SPG7* (paraplegin) mutations is highly progressive, mainly characterized by lower extremity spasticity (Rugarli and Langer, 2006). On the other hand, autosomal dominant mutations in *AFG3L2* cause SCA28, which is slowly progressive and mainly affecting the cerebellum and motor coordination (Cagnoli et al., 2010; Di Bella et al., 2010). It is quite striking that mutations in either subunit cause are quite tissue-specific, causing very different clinical outcomes. Remarkably, mutations in HSP60, another ubiquitously expressed mitochondrial quality control component, causes also tissue specific pathologies, such as autosomal dominant HSP (Hansen et al., 2007;

Hansen et al., 2002) or autosomal recessive hypomyelinating leukodystrophy (HML) (Magen et al., 2008).

1.5 The mitochondrial unfolded protein response (UPR^{mt})

Protein homeostasis, also termed proteostasis, is constantly challenged by the accumulation of unfolded proteins that might occur during biogenesis, disease and ageing (Jensen and Jasper, 2014). Unfolded proteins may aggregate to toxic intermediates that pose a serious risk not only for orgenellar function, but also for the entire cell. In each individual cellular compartment, chaperones aim at restoring protein homeostasis to counteract unfolded protein accumulation (Hartl et al., 2011). When the load of unfolded proteins exceeds the folding capacity of chaperones, it is sensed and signalled to the nucleus, where a specific proteostatic surveillance programme gets activated, a process termed "unfolded protein response".

To date, unfolded protein responses were found in the cytosol, the endoplasmatic reticulum (ER) and in mitochondria (Hetz et al., 2015; Lindquist, 1986; Pellegrino et al., 2013). The first unfolded protein response described was the cytosolic heat shock response (HSR) that induces the heat shock factor (HSF) transcription factors, thereby regulating Hsp70 and Hsp90 expression (Richter et al., 2010). The unfolded protein response in the ER (UPR^{ER}) also has been studied in great detail, where the response is determined by the transmembrane proteins inositol-requiring 1 (IRE-1), the activating transcription factor 6 (ATF6) and protein-like endoplasmic reticulum kinase (PERK) that together account for the induction of chaperones as BiP (GRP-78) (Buchberger et al., 2010; Mori, 2009; Walter and Ron, 2011). In contrast to HSR and UPR^{ER}, the mitochondrial unfolded protein response (UPR^{mt}) has been discovered rather recently.

The first direct evidence for a mitochondria-to-nucleus response triggered by unfolded/misfolded proteins was identified by the use of a folding impaired mutant mitochondrial protein (ΔOTC) that was found to stimulate the expression of Hsp60, Hsp10, the protease ClpP and the Hsp40 family chaperone mtDNAJ (Zhao et al., 2002). Even though the UPR^{mt} was initially found in mammalian cells, the molecular mechanisms

underlying this pathway have been mainly studied by the use of *C. elegans* models (Jensen and Jasper, 2014). The following chapters will summarize the UPR^{mt} signalling in *C.elegans* and mammals as well as highlights its role in broader cellular context.

1.5.1 The UPR^{mt} in C. elegans

By the use of *C. elegans* models, various stresses leading to UPR^{mt} induction as well as the UPR^{mt} signalling cascade itself could be studied in great detail. The UPR^{mt} induction can be monitored by transcriptional reporters that drive GFP expression under the control of either *hsp-6* (mammalian mtHsp70) or *hsp-60* (mammalian Hsp60) promoters (Yoneda et al., 2004).

Ethidium bromide, an inhibitor of mitochondrial translation, was the first stressor described to trigger UPR^{mt} signalling in *C. elegans* (Yoneda et al., 2004). It is generally believed that inhibition of mitochondrial transcription and replication results in an imbalance between nuclear- and mtDNA-encoded proteins that increase the load of unfolded and unassembled OXPHOS complexes (Houtkooper et al., 2013). In line with these findings it also has been shown that interference of mitochondrial translation either through inhibitors, such as doxycycline, or by knockdown of ribosomal proteins, induces UPR^{mt} signalling (Houtkooper et al., 2013). Moreover, the activation of mitochondrial biogenesis by rapamycin as well as by NAD$^+$ administration creates a mitonuclear imbalance, which activates the UPR^{mt} (Houtkooper et al., 2013; Mouchiroud et al., 2013; Pirinen et al., 2014). Another way to activate UPR^{mt} signalling is achieved by ETC mutants that perturb mitochondrial physiology by elevating ROS levels. For instance, this is true for mutations in nuo-6 (encoding NADH ubiquinone oxidoreductase) (Yang and Hekimi, 2010) or isp-1 (encoding cytochrome b-c1 complex subunit Rieske) (Feng et al., 2001). In addition, toxins such as rotenone or antimycin A that perturb ETC function also have been shown to trigger an UPR^{mt} response (Runkel et al., 2013). In line with that, administration of paraquat induces UPR^{mt} signalling in *C. elegans*, most likely as a consequence of ROS-induced protein damage (Runkel et al., 2013; Yoneda et al., 2004).

Signalling in *C. elegans*

In the past decade much progress was made to unravel the UPR^mt signalling events in *C. elegans* by the use of large-scale RNAi screens and UPR^mt reporter worms. Initially, it was found that knockdown of the mitochondrial matrix protease CLPP-1 prevented UPR^mt reporter gene expression during mitochondrial stress (Haynes et al., 2007). Based on this observation, it has been proposed that CLPP-1 degrades accumulated unfolded proteins into small peptides that might serve as initial signals for UPR^mt induction. In line with this assumption, the matrix exporter HAF-1 was found not only to be essential for UPR^mt induction and survival under proteotoxic stress, but also dependent on CLPP-1, suggesting that CLPP-1 acts upstream of HAF-1 (Haynes et al., 2010). In a first model, it was proposed that peptides produced by CLPP-1 are pumped out of the matrix via HAF-1 and subsequently reach the cytosol via passive diffusion.

Downstream of HAF-1, the bZip transcription factor ATFS-1 (Activating Transcription Factor associated with Stress, also described as ZC376.7) was found to be required for UPR^mt signalling (Haynes et al., 2010). Moreover, ATFS-1 translocates to the nucleus in a HAF-1 dependent manner, suggesting that peptides exported from mitochondria stimulate ATFS-1 (Haynes et al., 2010). A detailed mechanism that controls ATFS-1 translocation was recently described (Nargund et al., 2012). Apart from its nuclear localization sequence (NLS), this transcription factor also possesses a N-terminal mitochondrial targeting sequence (MTS). During normal mitochondrial function ATFS-1 is constantly translocated into mitochondria and degraded by the Lon protease (Nargund et al., 2012). Under mitochondrial stress the import machinery is impaired, which enables a translocation of ATFS-1 to the nucleus, where it can induce the UPR^mt (Haynes et al., 2010; Nargund et al., 2012) Through this mechanism the cell monitors the mitochondrial import efficiency via ATFS-1 and therefore the need of UPR^mt induction.
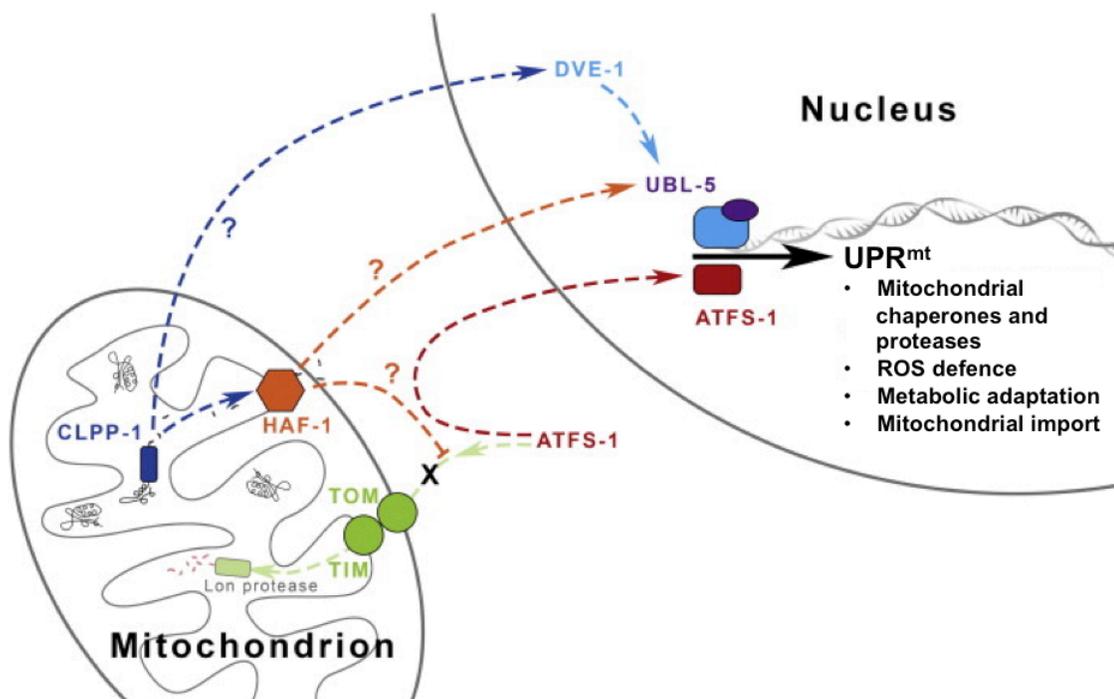
Figure 1.3: UPR^{mt} signalling in *C. elegans*.
The matrix protease CLPP-1 degrades misfolded/unfolded proteins to peptides that subsequently are exported by HAF-1. It has been suggested that high peptide efflux slows down import of the central UPR^{mt} mediator ATFS-1. During normal mitochondrial function the transcription factor ATFS-1 is constantly translocated into mitochondria and degraded by the Lon protease. Upon mitochondrial stress, the import machinery is impaired, which enables a translocation of ATFS-1 to the nucleus. In addition, the two transcription factors UBL-5 and DVE-1 form a complex in a HAF-1- or CLPP-1 dependent manner, respectively. Together, the transcription factors orchestrate the activation of protective factors such as mitochondrial chaperones and proteases, ROS-detoxification enzymes, glycolytic enzymes, as well as the mitochondrial import machinery. Reprinted with modifications from (Munkacsy and Rea, 2014).

In the nucleus, ATFS-1 enables a broad transcriptional response consistent with the proposed mechanism of UPR^{mt}, including upregulation of chaperones, proteases, ROS-scavenging enzymes and the TIM23 import complex (Harbauer et al., 2014; Nargund et al., 2012). A detailed mechanism by which HAF-1 exported peptides influence ATFS-1 is unknown, however, it has been suggested that the peptide export might hamper the import of ATFS-1 into mitochondria, thus favouring nuclear translocation (Nargund et al., 2012). The mitochondrial import machinery has a crucial role for the mitochondrial localization of ATFS-1, which is further supported by the finding that knockdown of either TIM-17 or

TIM-23 triggers UPR^mt activation in an ATFS-1-dependent manner (Nargund et al., 2015; Rainbolt et al., 2013). In addition, ATFS-1 regulates OXPHOS levels directly by matching the OXPHOS expression to the protein-folding capacity of mitochondria (Nargund et al., 2015).

Apart form ATFS-1, the transcription factors ubiquitin-like protein UBL-5 and the homeobox protein DVE-1 are also needed for transcriptional upregulation of the mitochondrial chaperone genes *hsp-6* and *hsp-60* (Benedetti et al., 2006; Haynes et al., 2007). Upon perturbation of mitochondrial proteostasis, DVE-1 undergoes nuclear re-distribution, whereas UBL-5 translocates to the nucleus to dimerize with DVE-1. On the one hand, nuclear re-distibution of DVE-1 is CLPP-1 dependent, but not HAF-1 dependent; on the other hand, UBL-5 expression is activated in a DVE-1 and HAF-1 dependent manner (Haynes et al., 2007; Haynes et al., 2010). It was suggested that both DVE-1 and UBL-5 might help in chromatin remodelling to enable ATFS-1 binding to specific UPR^mt target promoters, however, the importance of the UBL-DVE complex also in the context of ATFS-1 still needs to be further characterized.

1.5.2 The UPR^mt in mammals

In mammals, far less is known about the UPR^mt signalling events that occur during unfolded protein stress. Nevertheless, the first signs of a specific signalling in response to protein perturbations were found in mammalian cells upon treatment of ethidium bromide or by overexpression of a folding impaired mutant mitochondrial protein (ΔOTC) (Martinus et al., 1996; Zhao et al., 2002). The mitochondrial chaperones HSP60, HSP10 and mtDnaJ, as well as the matrix protease ClpP were shown to be specifically induced in response to unfolded protein stress in mammalian cells (Zhao et al., 2002). Moreover, the mitochondrial protease YME1L1, the import component TIMM17A and the enzymes NDUFB2, endonuclease G and thioredoxin 2 are induced upon UPR^mt signalling (Aldridge et al., 2007).

Promoters of these genes contain a mitochondrial stress responsive element that corresponds to the CHOP transcription factor consensus binding site as well as two

mitochondrial unfolded protein response elements (MURE1 and MURE2) (Aldridge et al., 2007; Horibe and Hoogenraad, 2007). Upon overexpression of ΔOTC, the transcription factor CHOP dimerizes with C/EBPβ, which has been proposed to induce mitochondrial chaperones, proteases, as well as the import machinery (Aldridge et al., 2007; Horibe and Hoogenraad, 2007; Zhao et al., 2002). Interestingly, CHOP is activated during the UPR^{ER} signalling and is found to mediate apoptosis under strong ER stress conditions (McCullough et al., 2001; Schroder, 2006; Szegezdi et al., 2006). However, it has been proposed that the UPR^{mt} specificity of CHOP and C/EBPβ is achieved through their selective expression due to activator protein-1 (AP-1) promoter elements that are not activated by UPR^{ER} signalling (Horibe and Hoogenraad, 2007). The AP-1 site is bound by the transcription factor c-Jun that is regulated by JNK2, implicating the JNK pathway in UPR^{mt} signalling (Jaeschke et al., 2006; Weiss et al., 2003).

Recently it was reported that overexpression of ΔOTC in intestinal epithelial cells induces phosphorylation of c-Jun in a ClpP and dsRNA-activated protein kinase (PKR) dependent manner (Rath et al., 2012). Interestingly, similar to GCN-2 in *C. elegans* the PKR phosphorylates eIF2α in mammals, thereby attenuating cytosolic translation during UPR^{mt} signalling (see section 1.5.3) (Baker et al., 2012; Rath et al., 2012). Nevertheless, how the transcriptional regulation of AP-1 is specifically triggered during UPR^{mt} signalling, remains elusive.

In addition to a bona fide UPR^{mt} response coming from the matrix, there is also evidence for a response to unfolded proteins occurring in the IMS, since overexpression of a mutant form of the IMS resided endonuclease G specifically induced the IMS protease HTRA2 (also known as Omi) as well as the proteasome (Papa and Germain, 2011, 2014; Radke et al., 2008). Protein aggregates in the IMS trigger ROS production and protein kinase B (AKT) phosphorylation, which leads to activation of the estrogen receptor α (ERα), boosting HTRA2, the nuclear respiratory factor 1 (NRF1), and the proteasome (Papa and Germain, 2011, 2014). Interestingly, this response is independent from CHOP-mediated signalling (Papa and Germain, 2011).

1.5.3 Crosstalk of the UPR^{mt} with other stress responses

Maintenance of mitochondrial proteostasis upon unfolded protein stress does not only induce overexpression of mitochondrial chaperones and proteases, but also orchestrates a broad transcriptional response including other cellular pathways (Jovaisaite and Auwerx, 2015). A gene expression analysis in *C. elegans* using ATFS-1 mutant and wild type worms revealed that among 685 differentially expressed genes in response to mitochondrial stress, only 391 genes were dependent on ATFS-1, suggesting the involvement of other pathways (Nargund et al., 2012). In line with these findings, the UPR^{mt} signalling seems to be interconnected with other cellular stress signalling pathways such as the integrative stress response (ISR) as well as the antioxidant response (Baker et al., 2012; Mouchiroud et al., 2013).

Cytosolic translational attenuation through eIF2α phosphorylation is activated during mitochondrial stress through the eukaryotic translation initiation factor 2 - kinase 4/GCN2-like protein in a ROS-dependent manner (GCN-2) (Baker et al., 2012). This is very similar to the situation found during ER stress that also triggers translational attenuation by phosphorylating eIF2α in parallel to the well-characterized UPR^{ER} (Shen et al., 2001). Both UPR^{mt} and UPR^{ER} seem to be interconnected through the regulation of eIF2α that is phosphorylated on the one hand by PEK-1 (PERK in mammals) during ER stress, and on the other hand by GCN-2 in response to mitochondrial stress (Baker et al., 2012; Harding et al., 1999). Organelle-specific stress responses depend on their corresponding kinases; however, inhibition of UPR^{mt} signalling during mitochondrial stress increases ISR signalling as determined by elevated eIF2α phosphorylation (Baker et al., 2012). It should be noted that the mechanism that defines one or the other pathway remains poorly understood.

Furthermore, levels of NAD$^+$ are crucial not only for the activation of sirtuins, but also activate UPR^{mt} signalling through mito-nuclear protein imbalance (Kincaid and Bossy-Wetzel, 2013; Mouchiroud et al., 2013). In both mice and *C. elegans*, application of nicotinamide riboside (NR), a NAD$^+$ precursor, induces CLPP-1, HSP-6, an antioxidant response, activating SOD-3 (SOD2 in mammals) as well as DAF-16 nuclear localization (FOXO3A in mammals) (Mouchiroud et al., 2013). Again both pathway share common

regulators since SOD-3 induction was dependent on UBL-5, a transcription factor involved in UPR^{mt} signalling (Mouchiroud et al., 2013).

Another pathway that shares feature, which seems to be interconnected with UPR^{mt} signalling is the mitophagy pathway (Burbulla et al., 2014; Jin and Youle, 2013). Damaged mitochondria are specifically eliminated via autophagic degradation, a process known as mitophagy (Youle and Narendra, 2011). Upon loss of mitochondrial membrane potential, the kinase PINK1 specifically accumulates on the outer membrane of mitochondria (Narendra et al., 2010). Subsequently, PINK1 labelled mitochondria recruit Parkin to the OMM, which then directs damaged mitochondria to the downstream autophagy machinery (Lazarou et al., 2012). Remarkably, it was reported that UPR^{mt} stresses ultimately also induce mitophagy. For instance, mtDNA depletion, overexpression of mutant OXPHOS subunits as well as application of the ROS-inducing agent paraquat resulted in both UPR^{mt} and mitophagy activation (Narendra et al., 2008; Suen et al., 2010). It is very likely that UPR^{mt} serves as a first line of defence upon mild stress; however, if mitochondrial damage becomes too heavy, the organelle undergoes mitophagy. Remarkably, it was recently described that overexpression of ΔOTC as well as knockdown of mitochondrial chaperones and proteases directly affects PINK1 levels on the OMM (Burbulla et al., 2014; Jin and Youle, 2013). These findings further illustrate that the UPR^{mt} cannot be just assessed as a single pathway, but rather ties various stress signalling pathways in response to mitochondrial stress.

1.6   Objectives

The molecular mechanism of the UPR^{mt} signalling in mammals especially *in vivo* is largely unknown. Therefore, the aim of this thesis was to decipher UPR^{mt} signalling in mammals using *in vitro* cell culture models on the one hand, and *in vivo* mouse models on the other hand.

Modelling UPR^{mt} signalling in *C. elegans* gave rise to many new insights into this fundamental process in recent years (Jensen and Jasper, 2014). However, only a limited number of findings has been transferred to the mammalian system. In order to fill that gap, a first objective was to assess the potential of the mitochondrial chaperones HSP60 and mtHSP70 as UPR^{mt} markers upon mitochondrial stress *in vitro*. Furthermore, the role of ATF5, a potential homolog of ATFS-1, the central mediator of the UPR^{mt} signalling in *C. elegans* (Nargund et al., 2012), was investigated in both *in vitro* and *in vivo*. Finally, novel UPR^{mt} markers and signalling components were analysed.

In addition, a mouse model that modulates factors implicated in UPR^{mt} signalling was developed. On the one hand, the heart-specific DARS2 knockout mouse model exhibits a high UPR^{mt} upregulation due to a strong dysregulation of mitochondrial protein synthesis (Dogan et al., 2014). On the other hand, the matrix protrease CLPP was shown to be part of the UPR^{mt} signalling in worms and in mammalian cell culture (Haynes et al., 2007; Rath et al., 2012; Zhao et al., 2002). In order to dissect the role of CLPP *in vivo*, heart-specific DARS2/CLPP double knockout mice were generated, since this allows the investigation of CLPP under activated UPR^{mt} conditions.

This work outlined here will be a necessary step towards the understanding of this fundamental process and might be instrumental for the development of new therapies for age-related pathologies as well as the cure of mitochondrial disorders.

2 Material & Methods

2.1 Cell culture

2.1.1 Cell lines

Table 2.1: Cell lines used in this study

Organism	Cell line	Reference
Mus musculus	Mouse embryonic fibroblasts (MEF)	(Xu, 2005)
	C2C12 myoblasts	(Yaffe and Saxel, 1977)
	Hepa 1-6 hepatoma cells	(Darlington et al., 1980)
Homo sapiens	Human Embryonic Kidney/Flp-In™ T-REx™ HEK293 (HEK293FT) cells	Invitrogen, Karsruhe, Germany
	Cervical cancer cell line from Henriette Lacks (HeLa)	(Scherer et al., 1953)
Simia aethiops	Immortalized kidney cells from the african green monkey (COS-7)	(Gluzman, 1981)

2.1.2   Culture and maintenance of mammalian cells

Cell lines (MEF, HEK293FT, C2C12, HeLa, Hepa 1-6, COS-7) were cultivated as monolayers in cell culture medium containing Dulbecco's modified Eagle's essential medium (DMEM) (4.5g/L glucose, with GlutaMAX/Glutamin and sodium pyruvate; Gibco Life Technologies, Karlsruhe, Germany), supplemented with 10% fetal bovine serum (FBS), penicillin 100 units/ml and streptomycin 100 mg/ml. As soon as cells reached 90% confluency, cells were split and again seeded in the ratio 1:6 to 1:20 depending on the cell type. Typically, adherent cells were split every 3 – 4 days using TrypLE Express (Gibco Life Technologies, Karlsruhe, Germany). Every second day a medium change was conducted. Cells were maintained at 37 °C in a humified atmosphere containing 5 % CO_2. For hypoxic treatment, cells were grown in a hypoxia chamber with a humidified gas containing 5% oxygen, 5% CO_2, and 90% nitrogen. The cells were exposed under hypoxic conditions for various time courses as indicated. For mitochondrial stress assays, cell culture medium was supplemented with 25 μM paraquat, 100 nM rotenone, 20 nM antimycin A, 50 μg/ml chloramphenicol or 30 μg/ml doxycycline. In all conditions, the medium was supplemented with 50 μg/ml uridine.

Cell lines were passaged according to their confluency. For this purpose, the medium was aspirated from the culture dish and cells were washed once using PBS. Subsequently, TrypLE Express was added to the cells. Cells were then incubated at 37°C until they detached from the culture dish – typically around 5 minutes. Carefully slapping the dish from time to time on each side can speed up trypsinization. The reaction was stopped using medium containing serum. In order to count the cells, a single cell suspension was prepared by carefully pipetting the cells. Thereafter cells were transferred into a 15 ml centrifuge tube and collected at 1000rpm ($\approx$ 170g) for 5 minutes at 4°C. Cell pellets were then re-suspended in fresh medium and seeded onto fresh plates.

In order to seed appropriate numbers of cells onto cell culture dishes, the cells were counted in advance. For this purpose, a cell suspension was prepared directly from the cell culture and depending on this density the suspension was further diluted. This suspension was mixed in a 1:1 ratio with 0.4% trypan blue (Gibco Life Technologies, Karlsruhe, Germany). Trypan blue is able to enter dead cells, which allows the

discrimination between blue stained dead cells and living cells. Approximately 10µl of the solution were transferred to a Countess™ counting chamber slide (Invitrogen, Karlsruhe, Germany) and the solution was aspirated by capillary force. Subsequently, cells were automatically counted using the Countess™ automated cell counter (Invitrogen, Karlsruhe, Germany) according to manufacturer's instructions.

For cryoconservation and long-term storage, the cells were trypsinized and resuspended in fresh medium to inactivate the trypsin. Therefore, the freezing medium (90% FBS + 10% DMSO) was added to the cell pellets and cells were re-suspended and transferred into a cryovial (Nunc, Langenselbold, Germany). Cryovials were stored at -80°C in a Cryo 1°C Freezing container (Nalgene, Roskilde, Denmark) filled with isopropanol enabling slow and gentle freezing of the cells. The next day cells were transferred into liquid nitrogen for long time storage. To thaw cells, cryovials were quickly transferred from liquid nitrogen into a 37°C water bath and thawed until only a small ice crystal in the middle of the cryovial remained. Cells were then transferred from the cryovial into a 15mL centrifugation tube containing pre-warmed cell culture medium. Cells were centrifuged at 800rpm ($\approx$ 110g) for 3 minutes at 4°C. The supernatant was aspirated and the cells were carefully resuspended and finally seeded on a cell culture dish.

2.1.3 Liposome-mediated transient transfection

Cells were plated 24 h prior to transfection at approx. 30-50% confluency. At 60 to 80 % confluency, cells were transfected using Lipofectamine 2000 (Invitrogen, Karsruhe, Germany) reagent according to manufacturer's instructions. The transfection mix was prepared in OptiMEM (Gibco Life Technologies, Karlsruhe, Germany) and added to the cells over night. Subsequently, the medium was replaced by fresh medium the next day and cells were analysed.

2.1.4 Cell harvest and lysis

For protein extraction, cells were washed twice with ice-cold PBS and directly lysed on the plate using RIPA buffer containing protease *SIGMAFAST*™ protease inhibitor

cocktail tablets (Sigma-Alderich, Seelze, Germany). In general, 150 µl RIPA buffer were added onto a 6 well plate whereas 70 µl onto a 12 well plate. A cell scraper was used to break the cells in presence of RIPA buffer and the suspension was kept on ice for 30 min. Afterwards, cell lysate was transferred into 1.5 ml tubes and centrifuged at full speed for 30 min to allow cell debris to be pelleted. The supernatant was then transferred to a new tube and kept on -80°C for long time storage.

Total RNA was isolated from cells using TRIzol reagent (Life Technologies GmbH, Darmstadt, Germany). To start with, cells were washed twice using PBS and 1 ml TRIzol was added directly to a growing 3.5 cm cell culture dish. Subsequently, the manufacturer's instructions were followed.

2.1.5   RNA interference

Cells were grown to 60-70% confluence and subsequently subjected to RNA interference (RNAi) that results in a transient reduction in gene expression. For this purpose, 50 pM of small interfering RNA (stealth siRNA from Eurogentec, Seraing, Belgium) were transiently transfected using Lipofectamine 2000 (Invitrogen, Karlsruhe, Germany) or Lipofectamine RNAiMAX (Invitrogen, Karlsruhe, Germany) according to manufacturer's instructions. Cells were harvested and lysed 72 hours after transfection.

Table 2.2: siRNA sequences

Oligoname	Sequence (Sense strand)
ATF5 siRNA (1)	CAGAUGGAAGACUUCUUCCTT
ATF5 siRNA (2)	GCUCGUAGACUAUGGGAAATT
LONP1 siRNA (1)	CACUGCUCAUCAAGCAAUATT
LONP1 siRNA (2)	CCACUCCUCUGAGUUCAAUTT
HSP60 siRNA	CAUCACAACUAGUGAAUAUTT
mtHSP70 siRNA	CACCACUAUUCCAACCAAATT

2.1.6   Colocalization imaging

Cells were grown on coverslips over night and the next day transfected with eGFP-tagged factors (Section 2.1.3) to assess a possible import into mitochondria. Again 24 hours later cells were additionally stained for mitochondria by incubation with MitoTrackerRed CMXRos (Invitrogen, Karlsruhe, Germany), (dilution 1:10,000 in cell culture medium – see Section 2.1.2) for 15 minutes at 37 °C in a humified atmosphere containing 5 % CO_2. After exchanging the staining medium with fresh cultivation medium, cells were incubated for additional 15 minutes in the incubator to destain the background. Cells were then washed and subsequently fixed using 4% PFA for 20 min. After another washing step, the samples were finally mounted with one drop Mowiol (Sigma-Alderich, Seelze, Germany) with 2.5 μg/ml DAPI (AppliChem, Darmstadt, Germany). Mitochondrial colocalization was analysed using the DeltaVision microscope system equipped with Softworx software (Applied Precision).

2.2   Mouse experiments

2.2.1   Animal care

Mice (Mus musculus, C57Bl/6) were housed in the pathogen-free animal facility of the CECAD (Cologne, Germany) in groups of 3-5 mice per cage at 22-24°C ambient temperature at a 12-hour light / 12-hour dark cycle. All animal had unlimited access to standard rodent chow diet (NCD; Teklad Global Rodent 2018; Harlan, IN, USA) containing 53.5% carbohydrates, 18.5% protein, and 5.5% fat (12% of calories from fat)) as well as water (*ad libitum*). Animals were handled in accordance with the guidelines of the institutional animal care committee. Every animal experiment or procedure was carried out in compliance with protocols, approved by local government authorities (Bezirksregierung Köln, Cologne, Germany) and were in accordance with NIH guidelines. Mice were sacrificed by cervical dislocation.

2.2.2 Mouse handling and breeding

Laboratory mice were maintained and handled in accordance to guidelines gathered from "Mouse Genetics" by Lee M. Silver (Silver, 1995).

2.2.3 Experimental mouse models

On the one hand, the mitochondrial aspartyl-tRNA synthetase (*Dars2*) gene targeting was carried out as part of the International Knockout Mouse Consortium (KOMP) that was described earlier (Dogan et al., 2014)(additional information available at http://www.knockoutmouse.org, Project ID: 41773). On the other hand, the caseinolytic peptidase, ATP dependent proteolytic subunit (*Clpp*) gene targeting was conducted from Taconic Artemis, Germany, in Art B6/3.5 embryonic stem cell line on a C57BL/6 NTac genetic background (for a detailed targeting scheme and information see section 3.2.1). Double deficient heart and skeletal muscle specific knockout mice were generated by mating double floxed mice (Dars2$^{L/L}$; ClpP$^{L/L}$) with transgenic mice expressing cre recombinase under the control of muscle creatine kinase promoter (*Ckmm-cre*) (Larsson et al., 1998). To reduce the overall mouse litter numbers, experiments were performed using ClpP KO and Dars2 KO that were heterozygous for *Dars2* and *ClpP*, respectively (For detailed mating scheme see section 3.2.1). However, additional control animals were obtained from the following matings: (i) Dars2-deficient animals - *Dars2$^{+/L}$, Ckmm-Cre$^{+/T}$* mated with *Dars2$^{L/L}$* and (ii) ClpP-deficient animals - *ClpP$^{+/L}$; Ckmm-Cre$^{+/T}$* mated with *ClpP$^{L/L}$*.

2.3 Molecular biology

2.3.1 Isolation of genomic DNA from mice tissues

Mice ear clips/tails/tissues were incubated overnight in *tissue lysis buffer* at 55 °C under agitation using a thermoshaker (Eppendorf, Hamburg, Germany). Subsequently, DNA was precipitated using equal volumes of pure isopropanol and centrifuged at 12.000 g

for 20 min in a benchtop centrifuge (Eppendorf, Hamburg, Germany). The supernatant was carefully removed and the DNA pellet was washed with ice-cold 70% (v/v) ethanol and centrifuged again at 12.000 g for 15 min in a benchtop centrifuge. Finally, the supernatant was removed completely and the DNA pellet was dried under a hood for 10 min. The pellet was resupended in 50-100 μl H_2O and shook at 37°C for 30 min to allow complete dissolving.

2.3.2   Isolation of total RNA from mice tissues

Fresh tissue samples were either snap frozen using liquid nitrogen or directly subjected to RNA isolation. RNA was isolated from tissues using TRIzol reagent (Life Technologies GmbH, Darmstadt, Germany) according to the manufacturer's protocol. In general, 50-100 mg tissues (approx. 3 mm^3 tissue cube) were placed into a Precellys CK 14 (Bertin Technologies, Versailles, France) 2 ml tubes with beads in the presence of 1 ml TRIzol. Subsequently, tissues were homogenized using a pre-chilled Precellys 24 Homogenizer (PeqLab, Erlangen, Germany) at 5500 rpm for 2 x 30 seconds, before continuation with the regular protocol.

2.3.3   Quantification of Nucleic Acids

The concentration of DNA or RNA was quantified using a NanoDrop ND-1000 UV-Vis spectrophotometer (Peqlab, Erlangen, Germany). Both DNA and RNA will absorb at 260 nm. The purity of the solution was assessed by the ratio of absorbance between 260 nm and 280 nm (protein absorbance). A ratio of 1.8 is considered pure for DNA, whereas a ratio of 2.0 correlates with pure RNA.

2.3.4   Polymerase chain reaction (PCR)

The polymerase chain reaction (PCR) is a method to amplify double-stranded DNA fragments of a defined length (Saiki et al., 1985). A typical PCR program consists of

a denaturing step (95 - 98 °C), an annealing step (45 – 65°C) and an elongation step (72 °C). At the beginning, the double stranded DNA is denatured by high temperatures (95-98°C). The following annealing step enables hybridization of the oligonucleotide primers to the single stranded DNA. The used primer pair is complementary to the 3' ends of each of the sense and anti-sense strands of the DNA target. The annealing temperature of the primers depends on their length and composition. The annealed oligonucleotides are the starting point for the elongation by a thermostable DNA polymerase, which uses the free 3' hydroxyl termini for the synthesis of the new strands. Desoxynucleotides (dATP, dCTP, dGTP, dTTP) in the reaction mix are incorporated while elongation. These steps are repeated in cycles until an adequate amount of DNA is produced. The PCR reactions were carried out using a Veriti Thermal Cycler (Applied Biosystems, Life Technologies GmbH, Darmstadt, Germany).

Genotyping PCR

PCR reactions were carried out to determine the correct genotype of mutant mice. Based on the tissue specific approach we distinguished between wild type (WT) alleles, floxed (LoxP flanked) alleles as well as knock out (KO) alles. In addition, genotyping for the transgenic cre-recombinase (Cre) allele, was performed. Primers (purchased from Sigma-Alderich, Seelze, Germany) used are found in Table 2.3.

All PCR amplifications were conducted using the GoTag® DNA polymerase (Promega, Mannheim, Germany) in a total reaction volume of 20 μl. For all Dars2 and ClpP PCRs, 12.35 μl of dH_2O, 4 μl of 5x GoTaqBuffer (Promega), 1 μl of dNTPs (1.25 mM each), 0.8 μl of each primer (10 μM), and 0.05 μl of GoTaq (5 U/μl, Promega) were added to 1 μl of sample DNA. For Cre PCR, 10.5 μl of dH_2O, 4 μl of 5x GoTaqBuffer, 3.2 μl of dNTPs (1.25 mM each), 0.6 μl of each primer (10 μM) and 0.1 μl of GoTaq (5 U/μl) were added to 1 μl of sample DNA.

Table 2.3: Genotyping PCR primer sequences

Primer	Sequence
Dars2-Forward-WT	ATGAATTCTAGGCCAGCCAC
Dars2-Reverse-WT	TGGCAATCTCTTAGGACTAAG
Dars2-Forward-KO	CGCTACCATTACCAGTTGGT
Dars2-Reverse-KO	TGACTGGCTATAATGCTGAAG
ClpP-Forward-WT	GTGGATGATGGTCAGTAGAATCC
ClpP-Reverse-WT	CCCAGACATGATTCCTAGCAC
ClpP-Forward-KO	TGTGCATTCTTACCATAGTCTGC
Cre-Forward	CACGACCAAGTGACAGCAAT
Cre-Reverse	AGAGACGGAAATCCATCGCT

PCR cycling conditions for **Dars2** and **ClpP**

1. Initial denaturation at 95°C for 5 minutes
2. Denaturation at 95°C for 30 seconds
3. Annealing at 60°C for 30 seconds
4. Extension at 72°C for 45 seconds (Dars2) or 1 minute (ClpP)
5. Final extension at 72°C for 7 minutes
6. Hold at 4°C

Steps 2 - 4 were repeated 30 times.

PCR cycling conditions **Cre**

1. Initial denaturation at 95°C for 5 minutes
2. Denaturation at 95°C for 30 seconds
3. Annealing at 53°C for 30 seconds
4. Extension at 72°C for 30 seconds
5. Final extension at 72°C for 7 minutes
6. Hold at 4°C

Steps 2 - 4 were repeated 35 times.

Cloning PCR

To amplify on the one hand, the ATF5 or XBP1 open reading frame (ORF) from a cDNA mouse library for cloning; and on the other hand, the promoter fragments of *Hspd1* and *Hspa9* from genomic DNA to generate promoter reporter constructs, the Phusion®

41

High-Fidelity DNA polymerase kit (New England Biolabs (NEB), Ipswich, USA) was used. Primer pairs can be found in Table 2.4.

All PCR amplifications were conducted in a total reaction volume of 50 μl, with the following composition: 24.5 μl of dH$_2$O, 10 μl of 5x GC-Phusion buffer (NEB), 6.5 μl of dNTPs (1.25 mM each), 2.5 μl of each primer (10 μM), 1.5 ul DMSO and 0.5 μl of Phusion®Taq (2 U/μl, NEB) were added to 1 μl of sample DNA.

Table 2.4: Cloning PCR primer sequences

Primer	Sequence
Atf5-Forward-EcoRI	GATAGAATTCATGTCACTCCTGGCGACCCT
Atf5-Reverse-SalI	GATAGTCGACGGTGCTGCGGGTCCTCTG
Xbp1-Forward-HindIII	GACAAAGCTTATGGTGGTGGTGGCAGC
Xbp1-Reverse-SalI	GACAGTCGACGAGGCTTGGTGTATACATGG
Hspd1-Foward-AseI	GACAATTAATTTCCCTGTCTGGTGTGTGT
Hspd1-Reverse-EcoRI	GACAGAATTCTTCTGGGGAAGGAAAAAAGA
Hspa9-Foward-PciI	GACAACATGTATGCTCCTCCTGCCTCAGTAT
Hspa9-Reverse-BamHI	GATAGGATCCTGGACAGAGGGGGTTACG

PCR cycling conditions:

1. Initial denaturation at 98°C for 30 seconds
2. Denaturation at 98°C for 20 seconds
3. Annealing at 60°C for 20 seconds
4. Extension at 72°C for 45 seconds
5. Final extension at 72°C for 7 minutes
6. Hold at 4°C

Steps 2 - 4 were repeated 35 times.

2.3.5   Reverse transcriptase PCR (gene expression analysis)

Total RNA was isolated either from cell culture or tissue samples as described before. Subsequently, DNA contaminations were removed using DNase digestion (DNA-free Kit, Ambion, Life Technologies GmbH, Darmstadt, Germany). Afterwards, 2 μg RNA were subjected to reverse transcription using the High capacity reverse transcription kit

(Applied Biosystems, Life Technologies GmbH, Darmstadt, Germany). The resulting cDNA was used for quantitative real-time PCR, in which 50 ng of cDNA was amplified using either Taqman Assay-on-Demand kits (Applied Biosystems, Life Technologies GmbH, Darmstadt, Germany; see Table 2.5) or Brilliant III Ultra-Fast SYBR Green QPCR Master Mix (Agilent Technologies, Waldbronn, Germany, see Table 2.6). Real-time PCR analysis was carried out in an ABIPRISM 7700 Sequence detector (Applied Biosystems, Life Technologies GmbH, Darmstadt, Germany). The target gene expression was assessed relative to the endogenous control genes: Hypoxanthine-guanine phosphoribosyltransferase (*Hprt*) or Peptidyl-prolyl cis-trans isomerase A (*Ppia*). Relative mRNAs levels were calculated using the comparative $2^{-\delta\delta CT}$ method according to the ABI Relative Quantification Method.

Table 2.5: Primers used for SYBR Green quantitative real-time PCR

Gene	Primer forward	Primer reverse
human *Hsp60*	CTACTGTACTGGCACGCTCTA	CAACAGCTAACATCACACCTCTC
mouse *Hsp60*	GCCTTAATGCTTCAAGGTGTAGA	CCCCATCTTTTGTTACTTTGGGA
human *mtHsp70*	TGGTGAGCGACTTGTTGGAAT	ATTGGAGGCACGGACAATTTT
mouse *mtHsp70*	ATGGCTGGAATGGCCTTAGC	ACCCAAATCAATACCAACCACTG
human *Lonp1*	GTTCCCGCGCTTTATCAAGAT	GTAGATTTCATCCAGGCTCTC
mouse *Lonp1*	ATGACCGTCCCGGATGTGT	CCTCCACGATCTTGATAAAGCG
mouse *Chop*	CTGGAAGCCTGGTATGAGGAT	CAGGGTCAAGAGTAGTGAAGGT
human *Atf5*	TGGCTCGTAGACTATGGGAAA	ATCAACTCGCTCAGTCATCCA
mouse *Trap1*	CAGGACAGTTATACAGCACACAG	CTCATGTTTGGAGACAGAACCC
mouse *Nppa*	ATGGGCTCCTTCTCCATCA	CCTGCTTCCTCAGTCTGCTC
mouse *Nppb*	GGATCTCCTGAAGGTGCTGT	TTCTTTTGTGAGGCCTTGGT
mouse *Afg3l2*	GTTGATGGGCAATACGTCTGG	GACCCGGTTCTCCCCTTCT
mouse *Atf4*	GCAAGGAGGATGCCTTTTC	GTTTCCAGGTCATCCATTCG
mouse *Ppia*	GAGCTGTTTGCAGACAAAGTTC	CCCTGGCACATGAATCCTGG
human *Hprt*	TGACACTGGCAAAACAATGCA	GGTCCTTTTCACCAGCAAGCT
mouse *Hprt*	GCCCCAAAATGGTTAAGGTT	TTGCGCTCATCTTAGGCTTT

Table 2.6: Taqman probes used for quantitative real-time PCR

Gene	Product number
Atf5	Mm00459515_m1
Fgf21	Mm00840165_g1
Nd1	Mm04225274_s1
Nd5/Nd6	Mm04225315_s1
Cytb	Mm04225271_g1
Cox1	Mm04225243_g1
Cox2	Mm03294838_g1
Atp6	Mm03649417_g1
Hprt	Mm00446968_m1

2.3.6 DNA gel extraction and PCR clean up

After running the gel at standard conditions the desired band was cut out under UV light using a scalpel. The extraction was performed with the QIAquick Gel Extraction Kit (Qiagen, Hilden, Germany) according to manufacturer's instructions. With this technique the gel fragment is dissolved at 50 °C under slight acidic conditions. Subsequently, the DNA binds to a sepharose column and after a washing step; the DNA can be eluted under alkaline conditions.

The PCR clean up was carried out using the QIAquick PCR Purification Kit (Qiagen, Hilden, Germany). An equal volume of acidic buffer was added to the PCR reaction mixture and samples were processed as mentioned above.

2.3.7 Restriction hydrolysis of DNA

For digestion of DNA exclusively type II restriction endonucleases (NEB, Ipswich, USA) were used at a concentration of 2 to 5 units of enzyme per μg of DNA. The restriction reaction was performed using an appropriate NEB buffer supplemented with 1% BSA if needed at the temperatures recommended by the manufacturer. Incubation time varied between 1 to 2 hours for analytical purposes, whereas for preparative approaches the incubation time was extended up to 4 hours.

2.3.8 Ligation of DNA

Genomic DNA fragments were blunt-end cloned using the Zero Blunt® TOPO® PCR Cloning Kit (Invitrogen, Karlsruhe, Germany) generating intermediate cloning products. After restriction digest, corresponding DNA fragments were re-ligated using the DNA T4 ligase (NEB, Ipswich, USA), which catalyses the formation of phosphodiester bonds between juxtaposed 5'phosphate and 3'hydroxyl termini of DNA. The ligation reaction was incubated for 1 to 2 hours at room temperature or over night at 16 °C. Subsequently, the T4 ligase was heat-inactivated for 15 minutes at 65 °C. Target vector peGFP-N3 was obtained from Clontech, Saint-Germain-en-Laye, France.

2.3.9 Transformation into E. coli

Generation of competent *E. coli*

For the generation of competent *E.coli*, an adapted version of the protocol published by Chung & Miller was used (Chung and Miller, 1988). It is important to use only prechilled (0 - 4 °C) buffers, pipettes, tubes and glassware.

A 5 ml LB medium culture was inoculated with DH5α *E.coli* bacteria and incubated over night at 37 °C. The next day, 100 – 200 ml LB medium were inoculated with the overnight culture in the ratio 1:100 and again cultivated at 37 °C under shaking (120 rpm). When the suspension reached an OD_{600} of 0.40 - 0.45 the culture was incubated on ice for 5 minutes and was transferred into prechilled 50 ml Falcon tubes. The cells were spinned down for 8 minutes at 4500 g and 4 °C. The supernatant was discarded and the pellet was carefully resuspended in ice-cold TSS buffer using 1/10 volumes of the original culture volume. The competent cells were finally shock frozen in liquid nitrogen as 100 μl aliquots. Competent cells can be stored at -80 °C.

Transformation of competent *E. Coli*

An aliquot of 100 μl competent bacterial cells was thawed on ice for 10 minutes. Subsequently, about 100 ng of the desired plasmid was added to the competent bacteria. After carefully flipping the tube, the solution was incubated for 30 minutes on ice.

Thereafter, cells were heat-shocked at 42 °C for 40 - 60 seconds in a water bath. Again, cells were incubated on ice for 2 minutes. After incubation 900 μl SOC medium were added and the cells were grown for 1 hour at 37 °C while shaking. Cells were then collected by centrifugation for 3 minutes at 3000 g and 90% of the supernatant was discarded. The remaining medium was used to re-suspend the bacteria. The bacterial solution was dispersed on a LB-agar plate containing the appropriate antibiotic.

2.3.10 Preparative and analytical scale plasmid DNA preparation

Preparation of large amounts of Plasmid DNA out of *E. coli*

An overnight culture of 300 mL LB medium containing an appropriate antibiotic was inoculated with bacteria, either from LB-agar plate or directly with transformed cells. Cells were incubated overnight at 37°C using a bacterial shaker (New Brunswick Scientific, Nürtingen) at 120 rpm. The next day plasmid DNA was extracted using the QIAfilter Plasmid Midi/Maxi Kit (Qiagen, Hilden, Germany). The purification was performed according to the manufacturer's instructions.

Preparation of small amounts of Plasmid DNA out of *E. coli*

An overnight culture of 3 mL LB medium supplemented with the appropriate antibiotic was inoculated with bacterial colonies cultivated on a LB-agar plate. Cells were grown at 37°C and 120 rpm. After incubation the bacteria were harvested by centrifugation and pellets were processed using the StrataPrep Plasmid Miniprep Kit (Agilent Technologies, Waldbronn, Germany) according to the manufacturer's protocol. The plasmid DNA was eluted with 50 µl H_2O.

2.3.11 Agarose gel electrophoresis

DNA fragments were separated according to their size by agarose gel electrophoresis. Through application of an electrical field the DNA moves towards the anode due to the negative charge of its phosphate backbone. The velocity of the DNA fragment is inversely proportional to the logarithm of its molecular weight. The

intercalating fluorescent dye GelRed (Biotium, Hayward, CA) is used to visualize the DNA within the gel using short-wave UV light. The actual size can be determined by including a DNA ladder, which consists of defined DNA fragments. Depending on the size of the expected fragments, different concentrations of agarose (0.5% - 2% [w/v]) were boiled in 0.5X TBE buffer. After cooling of the agarose solution, GelRed was added in a ratio of 1:50.000 and subsequently poured into a gel chamber with slot combs. The solidified agarose gel was put into an electrophoresis chamber and covered with 0.5X TBE buffer. Before applying the samples to the gel, they were either diluted 1:6 with an agarose gel loading buffer or non-diluted, when the PCR mix already contained a loading dye. After running the gel, it was analysed on a UV table or with the GelDoc system from Biorad (Munich, Germany).

2.3.12 DNA sequencing

The sequencing and analysis was carried out by the company GATC (Köln, Germany). For that, 400 – 500 ng pure DNA ($A_{260:280}$: ~1.8) and 25 pmol sequencing primers had to be prepared in a volume of 5 μl.

DNA sequencing was performed using a technique based on the chain-terminator method through fluorescent dye-labelled nucleotides. For that, nucleotides are labelled at their 3' hydroxyl termini with fluorescent dyes, each of which emits light at different wavelengths. Labelled nucleotides and non-labelled nucleotides are mixed and used for the sequencing polymerization. If a labelled nucleotide is incorporated into the DNA fragment, the following nucleotide cannot be attached to the previous nucleotide due to the missing 3' hydroxyl terminus and the synthesis reaction will stop. The probability that a longer strand is synthesized increases towards the end, because the amount of non-bond labelled nucleotides decreases. Automated DNA sequencing instruments carry out capillary electrophoresis for size separation, detection and recording of dye fluorescence, which results in fluorescent peak trace chromatograms, which are translated into a DNA sequence.

2.4 Biochemistry

2.4.1   Protein isolation from tissues

Proteins from mice tissues were extracted using organ lysis buffer. At first, a tissue cube of 3 mm^3 was cut off the respective tissue and transferred into Precellys CK 14 (Bertin Technologies, Versailles, France) 2 ml tubes with beads (500 µl of organ lysis buffer). The tissues were homogenized using a pre-chilled Precellys 24 Homogenizer (PeqLab, Erlangen, Germany) at 5500 rpm for 2x30 seconds. Subsequently, samples were incubated for 10 minutes on ice and centrifuged at 13000 rpm for 45 minutes at 4 °C. Next, the supernatant was transferred into a fresh tube and the protein concentrations were determined using the Bradford reagent (Sigma Aldrich, Seelze, Germany) according to the manufacturer's protocol. At last, protein solutions were stored at -80 °C.

2.4.2   Isolation of mitochondria from heart

Mice were sacrificed by cervical dislocation and dissected. Subsequently, the heart was transferred into a 50 ml falcon tube containing pre-chilled mitoisolation buffer (MIB). Next, the tissue was passed onto a petri dish and cut into small pieces using a razor blade. Tissue was weighed and transferred into a glass homogenizer tube and combined with 5 ml MIB containing Subtilisin A (1 mg per 1g tissue). The tissue pieces were homogenised using a Potter S (Santorius, Göttingen, Germany) homogenizer at 1000 rpm (approx. 20 long strokes). Then, the homogenate was passed into a 50 ml falcon and centrifuge at 8500 g at 4 °C for 5 minutes. The supernatant was removed and the pellet was resuspended in 30 ml MIB by shaking. Again the homogenate was centrifuged at 800 g for 5 minutes at 4°C. Afterwards, the supernatant was transferred into a tube and mitochondria were pelleted at 8500 g at 4 C for 5 minutes. Subsequently, the supernatant was discarded and the residual pellet was resuspended in 50 μl MIB. Mitochondria were either processed directly or snap frozen in liquid nitrogen for long term storage. The concentration was determined using Bradford reagent (Sigma Aldrich, Seelze, Germany) according to the manufacturer's protocol.

2.4.3 SDS-PAGE

Sodium dodecyl sulfate polyacryamide gel electrophoresis (SDS-PAGE) was used to separate proteins according to their size. The separation of the proteins was performed using a discontinuous gel electrophoresis (Laemmli, 1970). The SDS gel is split into two parts. The upper part, called stacking gel exhibits bigger pore sizes due to the low amount of (bis)acrylamide used, and all proteins concentrate in a small part of the stacking gel before uniformly entering the separating gel. In addition, both parts exhibit different pH values, which is also important for a clear separation of the proteins. The high amount of (bis)acrylamide in the separating gel possesses smaller pores, which enables separation of the proteins according to their mass. After the discontinuous gel was solidified, it was transferred into a gel chamber containing SDS-PAGE running buffer. SDS-PAGE loading buffer was added to 30-50 μg whole protein lysate and subsequently boiled at 95°C for 10 minutes. After loading the samples as well as the PageRuler™ Prestained Protein Ladder (Thermo Fisher Scientific Inc., Schwerte, Germany) onto the gel, electrophoresis was carried out at a voltage of 200V for 1 hour. Afterwards, the gel was incubated either with a coomassie staining solution to visualize the protein bands or processed in a Western blot in order to detect specific proteins.

Stacking Gel

- 4% Acryamide-Bisacrylamide (37.5:1)
- 125 mM Tris-HCl (pH 6.8)
- 0.1% SDS
- 1.25 % APS
- 0.125% TEMED

Separating Gel

- 10-15% Acryamide-Bisacrylamide (37.5:1)
- 375 mM Tris-HCl (pH 8.8)
- 0.1% SDS
- 1.25 % APS
- 0.125% TEMED

2.4.4 BN-PAGE and in-gel activity of respiratory chain complexes I and IV

Separation of protein complexes was performed with a blue native polyacrylamide gel electrophoresis (BN-PAGE) using the Novex Bis-Tris system (Life Technologies GmbH, Darmstadt, Germany) according to the manufacturer's protocol. *In-gel* activities were assessed by incubating the BN-PAGE gel in either 0.1 mg/ml NADH, 2.5 mg/ml

nitrotetrazolium blue (NTB) diluted in 5mM Tris-HCl (pH 7.4) for complex I; or in 0.24 unit/ml catalase, 10% Cytochrome C and 0.1% Diaminobenzidine tetrahydrochloride (DAB) diluted in 50 mM Tris-HCl (pH 7.4) for complex IV. Both solutions were kept on individual gels for 1 hour at room temperature for complex I and at 37°C for complex IV. For immunodection of mitochondrial protein complexes, the proteins were transferred from the gel onto a PVDF membrane and detected via specific antibodies (see section 2.4.5).

2.4.5   Western blot analysis

Western blot analysis was performed using the Criterion™ blotting system (Biorad, Munich, Germany). After the SDS-PAGE the gel was transferred into Western blot transfer buffer and incubated for several minutes. Subsequently, the Western blot was assembled in a way that the black side of the cassette was down followed by a fiber pad and 3 Whatman filter papers (GE Healthcare, Munich, Germany). The gel was placed on top followed by a nitrocellulose (GE Healthcare, Munich, Germany) or PVDF membrane (Biorad, Munich, Germany). The assembly was completed by 3 additional Whatman filter papers and another fiber pad. All components were incubated in Western blot transfer buffer for several minutes prior to assembling. Thereafter, the assembly was closed and put into the Criterion™ blotter (Biorad, Munich, Germany) and placed in the cold room. Western blot transfer buffer was filled inside the buffer tank and an electrical current of 600 mA was applied for 1 hour. Then the blot was disassembled and nitrocellulose membrane were transiently stained with PonceauS (Sigma-Alderich, Seelze, Germany). Subsequently, the membrane was put into blocking solution (5% milk powder in TBS-T) and incubated for 1 hour at room temperature. Blocking solution can vary, which depends on the antibody used and the corresponding instructions of the manufacturer. After blocking the membrane was washed 3 times for 5 minutes in TBS-T. Then, the membrane was incubated for 2 hours at room temperature or over night at 4°C either with the respective antibody (Table 2.7) each dissolved in TBS-T with 0.5% milk powder. Again, 3 washing steps each for 5 minutes with TBS-T are needed in order to continue with the secondary antibody (α-mouse 1:2000 & α-rabbit 1:2000 (Sigma-Alderich, Seelze, Germany); α-goat 1:20000 (Acris, Herford, Germany)) typically in TBS-T for 1 hour at room temperature. Finally, the

membrane was washed 3 times for 5 minutes in TBS-T and analysed by applying a substrate solution, which enabled a specific detection reaction. ECL solution (GE Healthcare, Munich, Germany) was used depending on the relative abundance of the protein. The chemiluminescence was evaluated using the Imagequant LAS 4000 (GE Healthcare, Little Chalfont, United Kingdom). Western blots were quantified relative to control levels of housekeeping proteins using the ImageJ software as intensity per mm^2.

Table 2.7: Primary antibodies used for Western blot analysis

Antigen	Distributor	Dilution
ACTIN	Santa Cruz (Dallas, USA)	1:5000
AFG3L2	Polyclonal antisera made by Prof. Elena I. Rugarli	1:1000
ATP5A1	Mitosciences (Abcam, Cambridge, UK)	1:1000
CLPP	Sigma Aldrich, Seelze, Germany	1:1000
DARS2	Proteintech (Chicago, USA)	1:1200
HSC70	Santa Cruz (Dallas, USA)	1:4000
HSP60	StressMarq (Victoria, Canada)	1:10000
LONP1	Abcam (Cambridge, UK)	1:1000
MnSOD	Millipore (Merck, Darmstadt, Germany)	1:500
mtHSP70	Abcam (Cambridge, UK)	1:1000
p62/SQSTM1	Abnova (Taipei, Taiwan)	1:1000
SDHA	Invitrogen (Karlsruhe, Germany)	1:10000
TFAM	Polyclonal antisera made by Prof. Nils-Göran Larsson	1:1000
TRAP1	BD Biosciences (East Rutherford, USA)	1:1000
eIF2α	Abcam (Cambridge, UK)	1:1000
P-eIF2α	Santa Cruz (Dallas, USA)	1:1000
VDAC	Cell Signalling (Cambridge, UK)	1:1000
TOM20	Santa Cruz (Dallas, USA)	1:1000
ATF5	Abcam (Cambridge, UK)	1:500
NDUFA9	Invitrogen (Karlsruhe, Germany)	1:1000

NDUFB6	Invitrogen (Karlsruhe, Germany)	1:1000
NDUFS3	Mitosciences (Abcam, Cambridge, UK)	1:1000
UQCRC1	Invitrogen (Karlsruhe, Germany)	1:1000
UQCRFS1	Mitosciences (Abcam, Cambridge, UK)	1:1000
COX1	Invitrogen (Karlsruhe, Germany)	1:1000
COX4I1	Invitrogen (Karlsruhe, Germany)	1:1000

Immunoblot stripping

In order to analyse another protein of interest on the same membrane with different primary and secondary antibodies, it is possible to remove the initially used antibodies from the membrane. This procedure is called stripping. For this the nitrocellulose membrane was incubated with pre-warmed stripping buffer for 30 minutes at 55°C in water bath under agitation. The combination of heat and strong denaturing agents as SDS and β-mercaptoethanol strip the antibodies off the blot. Subsequently, the membrane was rinsed 5-7 times with TBS-T for 5 min each in order to remove denaturing agents. The immunoblot could then be treated as a freshly blotted membrane.

2.4.6 Oxygen consumption rates

Mitochondria were isolated from heart (section 2.4.2) and oxygen consumption rates were assessed using the OROBOROS Oxygraph-2k for high-resolution respirometry (Oroboros Insturments, Vienna, Austria). Firstly, the mitochondrial complex I respiration was measured by applying 2 mM ADP, 5 mM pyruvate, 2 mM malate, and 20 mM glutamate. Subsequently, the combined complex I + complex II respiration was determined by further adding 10 mM of succinate. Next, coupling of mitochondria was analysed by inhibition of the ATP synthase by supplementing 1.5 μg/ml oligomycin and uncoupling by a multiple-step carbonylcyanide p-trifluoromethoxyphenylhydrazone (FCCP) titration. All measurements were conducted using 25 μg of purified mitochondria.

2.4.7 *In organello* translation

In organello translation was performed using 1-2 mg of freshly isolated mitochondria that were incubated in "hot" translation buffer containing 0.25 mCi/ml ^{35}S-met for 1 hour (Pulse) at 37°C on a rotating wheel. Next, half of mitochondria were lysed using SDS-PAGE loading buffer, whereas the other half was incubated for another 3 h in "cold" translation buffer containing all aminoacids, including non-radioactive methionine (chase). Subsequently, chased mitochondria were also lysed and both fractions were separated using SDS-PAGE. To assess loading, the gel was stained with coomassie staining solution. The gel was then incubated in 5% glycerol as well as Amplify solution (GE Healthcare, Munich, Germany) and dried at 80 °C for 2 hours using a Model 583 Gel Dryer (Biorad, Munich, Germany). Finally, newly produced polypeptides were detected using autoradiography.

Quantification of *de novo* protein synthesis rate was assessed by analysis of densitometric profiles obtained from scanned films in each condition. Either the whole range (overall rate) or only fractions (proficient or abortive) of newly synthetized proteins were quantified and normalized to their respective control conditions. The turnover rate of *de novo* protein synthesis was assessed as ratio of chase/pulse for the whole range of proteins (overall rate) or only for full-length polypeptides (Proficient). Individual fractions were also correlated with each other to determine their relative production rates.

2.5 Histological analysis

2.5.1 Cryostat sections

For cryostat sections, mice were sacrificed and hearts were isolated and immediately embedded in Tissue-Tek (Sakura, Alphen aan den Rijn, The Netherlands). The trays containing the embedded heart were then place onto dry ice that allowed freezing of the Tissue-Tek. Subsequently, hearts were stored at -80 °C. Hearts were sectioned on a Leica CM1850 cryostat with a thickness of 7 μm. Heart sections were immediately mounted on glass slides and kept at -20 °C.

2.5.2 COX-SDH staining

Mounted cryosections were subjected to COX/SDH staining. First, sections were dried at room temperature for 1 hour and a hydrophobic circle was drawn around the slide-mounted tissue using a PAP pen (Sigma-Aldrich, Seelze, Germany). Subsequently, slides were incubated in COX solution (0.8 ml 3,3 diaminobenzidine tetrahydrochloride, 0.2 ml 500 μM cytochrome c, a few grains of catalase) at 37 °C for 40 minutes in a humid chamber. After a washing step in PBS, the sections were incubated in SDH solution (0.8 ml 1.875 mM Nitroblue tetrazolium, 0.1 ml 1.3 M sodium succinate, 0.1 ml 2 mM Phenazine methosulphate, 0.01 ml 100 mM Sodium azide) for 90 minutes at 37 °C in a humid chamber. Next, sections were washed again in PBS and dehydrated with increasing ethanol concentration (75% for 2 minutes, 95% for 2 minutes, 100% for 10 minutes). Finally, stained sections were air dried and mounted in DPX Mountant (VWR, Darmstadt, Germany). Light microscopic imaging was performed using a Leica SCN400 slide scanner (Leica Microsystems, Wetzlar, Germany).

2.5.3 Masson's trichrome staining

Masson's trichrome staining was conducted on slide-mounted tissue sections using the Trichrome Stain (Masson) kit (Sigma Aldrich, Seelze, Germany), according to the manufacturer's protocol. Light microscopic imaging was carried out using a Leica SCN400 slide scanner (Leica Microsystems, Wetzlar, Germany).

2.6 Label-free quantification of the mitochondrial proteome

In-gel digestion

Mitochondrial protein extracts were separated by SDS-PADE and subsequently stained with a coomassie staining solution to visualize the protein bands. In general, the *in-gel* digestion was performed according to a previously published protocol (Shevchenko et al., 2006). In brief, each gel lane was divided into 6 parts and cut into small 1mm^2 cubes using a razor blade. Subsequently, gel pieces were washed several times and proteins were

reduced (10 mM DTT at 56 °C for 30 minutes) and alkylated (IAA, 30 minutes, room temperature in the dark). After another washing step, a dehydration step using ethanol and a rehydration step using 50 mM Ammonium bicarbonate. Afterwards, trypsin (40 μl of 12 ng/μl stock solution) was added to each tube, followed by 30 minutes incubation on ice. Next, gel pieces were covered with 50 mM Ammonium bicarbonate solution and incubated overnight at 37°C. Increasing amounts of acetonitrile were used to extract the generated peptides and further concentrated using a vacuum concentrator (Eppendorf, Hamburg, Germany). Peptides were primed using the STAGE tip technique before LC-MS/MS analysis was conducted (Rappsilber et al., 2003).

Liquid chromatography and mass spectrometry

The liquid chromatography and mass spectrometry (LC-MS/MS) device was made up of an EASY n-LC (Thermo Scientific, Waltham, USA) linked via a nano-electrospray ionization source (Thermo Scientific, Waltham, USA) to an ion-trap based bench top LTQ Discovery instrument (Thermo Scientific, Waltham, USA). An in-house packed 15 cm column (3 μm C18 beads, Dr. Maisch, Ammerbuch-Entringen, Germany) was loaded with 4 μl of peptide mixture. Peptides were separated using a binary buffer system consistent of 0.1% acetic acid (buffer A) and 0.1% acetic acid in acetonitrile (buffer B). Buffer B content was linearly increased from 7% to 20% within 220 minutes and further elevated to 40% within 60 minutes more. Subsequently, the column was washed with 95% buffer B and incubated for 20 minutes. The flow-rate was set to constant 200 nl/min throughout the complete gradient. To blank and re-equilibrate the column, it was washed after each run with 5% buffer B.

Peptides were ionized during elution from the column by an applied voltage of 1.8 kV. The capillary voltage was adjusted to 44 V and Multipole RF Amplifier (Vp-p) was set to 400. For the first MS scans a resolution of 30.000 (400 m/z), a maximal injection time of 500 milliseconds, and an automatic gain control (AGC) target of 2E5 was used. The 10 most pronouced peaks were used for the second MS level scans. A resolution of 7.500 (400 m/z), an AGC target of 1E54, an isolation window of 3.0 Th, and a maximal injection time of 200 milliseconds was applied. The normalized collision energy for CID scans was 35

and the activation time for second MS scans was 30 milliseconds. The waveform setting was enabled for both scan types.

MaxQuant processing and data analysis

Raw data were analysed and processed by MaxQuant 1.5.1.0 and the integrated Andromeda search engine (Cox and Mann, 2008; Cox et al., 2011). MS/MS spectra were blasted against the mouse Uniprot database (downloaded February 2015) including a list of common contaminants. Search criteria were applied as the following: minimal peptide length: 7 amino acids, mass tolerances for MS/MS spectra was 0.5 Dalton. The implemented decoy algorithm estimated the false discovery rate (FDR) to 1%. Label-free quantification intensities were $\log_2$ transformed and evaluated for using a two-sided t-test. To further correct multiple testing errors the FDR was calculated by a permutation-based algorithm using a FDR cut off of 5% and fudge-factor s0 of 0.1. To determine significantly enriched GO terms we applied the 1D enrichment tool in Perseus (Cox and Mann, 2012). Data were visualized in the statistical environment R.

2.7   Densitometry analysis

In order to measure the optical density as intensity (dynamic range of grey scale) per mm^2 of scanned films or CCD camera obtained pictures the public domain software Image J (National Institutes of Health (NIH) Image for Macintosh) was used. Densitometric values were normalized relative to control conditions.

2.8   Statistical analysis

Statistical calculations were conducted using Microsoft Excel (Microsoft Corp., Redmond WA, USA) and GraphPad Prism (GraphPad Software, Inc., La Jolla CA, USA). In general, a two-tailed unpaired student's t-test was used to determine statistical significance unless otherwise specified in the respective experiment. All p values below 0.05 were considered significant. Error bars represent standard error of the mean (S.E.M.). $*p<0.05$; $**p<0.01$; $***p<0.001$; $****p<0.0001$.

2.9 Chemicals and biological material

Table 2.8: Cell culture

Name	Supplier
DMEM (Dulbecco's Modified Eagle Medium) Glutamax	Gibco Life Technologies, Karlsruhe, Germany
Fetal bovine serum (FBS)	Merck, Darmstadt, Germany
Lipofectamine RNAiMAX	Invitrogen, Karlsruhe, Germany
Lipofectamine 2000	Invitrogen, Karlsruhe, Germany
MitoTrackerRed CMXRos	Invitrogen, Karlsruhe, Germany
OptiMEM	Gibco Life Technologies, Karlsruhe, Germany
PBS	Gibco Life Technologies, Karlsruhe, Germany
Penicillin-Streptomycin	Gibco Life Technologies, Karlsruhe, Germany
Trypan blue	Gibco Life Technologies, Karlsruhe, Germany
TrypLE Express	Gibco Life Technologies, Karlsruhe, Germany

Table 2.9: Enzymes, Markers and kits

Name	Supplier
Amplify solution	GE Healthcare, Munich, Germany
Bradford reagent	Sigma Aldrich, Seelze, Germany
Brilliant III Ultra-Fast SYBR Green QPCR Master Mix	Agilent Technologies, Waldbronn, Germany
Catalase, bovine liver	Sigma Aldrich, Seelze, Germany
Creatine Phosphokinase Type III, bovine	Sigma Aldrich, Seelze, Germany
Cytochrome C, bovine heart	Sigma Aldrich, Seelze, Germany
DNA T4 ligase	NEB, Ipswich, USA
DNase digestion (DNA-free Kit)	Ambion, Life Technologies GmbH, Darmstadt, Germany
DPX Mountant	VWR, Darmstadt, Germany
ECL solution	GE Healthcare, Munich, Germany
GelRed	Biotium, Hayward, CA
GoTag DNA polymerase	Promega, Mannheim, Germany
High capacity reverse transcription kit	Applied Biosystems, Life Technologies GmbH, Darmstadt, Germany
Mowiol	Sigma-Alderich, Seelze, Germany

Novex Bis-Tris system	Life Technologies GmbH, Darmstadt, Germany
PageRuler Prestained Protein Ladder	Thermo Fisher Scientific Inc., Schwerte, Germany
Phusion High-Fidelity DNA polymerase kit	NEB, Ipswich, USA
Proteinase k	AppliChem, Darmstadt, Germany
QIAfilter Plasmid Midi/Maxi Kit	Qiagen, Hilden, Germany
QIAquick Gel Extraction Kit	Qiagen, Hilden, Germany
QIAquick PCR Purification Kit	Qiagen, Hilden, Germany
Sigmafast protease inhibitor cocktail tablets	Sigma-Alderich, Seelze, Germany
StrataPrep Plasmid Miniprep Kit	Agilent Technologies, Waldbronn, Germany
Subtilisin A	Sigma Aldrich, Seelze, Germany
Taqman Assay-on-Demand kits	Applied Biosystems, Life Technologies GmbH, Darmstadt, Germany
Trichrome Stain (Masson) kit	Sigma Aldrich, Seelze, Germany
TRIzol	Life Technologies GmbH, Darmstadt, Germany
trypsin	Sigma Aldrich, Seelze, Germany
type II restriction endonucleases	NEB, Ipswich, USA
Zero Blunt TOPO PCR Cloning Kit	Invitrogen, Karlsruhe, Germany

Table 2.10: Chemicals

Name	Supplier
3-Indoleacetic acid (IAA)	Sigma Aldrich, Seelze, Germany
^{35}S-met	Perkin-Elmer, Waltham, USA
Acetic acid	AppliChem, Darmstadt, Germany
Acetonitrile	Sigma Aldrich, Seelze, Germany
Acryamide-Bisacrylamide 40	Carl Roth, Karlsruhe, Germany
Adenosine 5'-diphosphate sodium salt	Sigma Aldrich, Seelze, Germany
Adenosine 5'-triphosphate disodium salt (ATP)	Sigma Aldrich, Seelze, Germany
Agarose LE	Ambion, Life Technologies GmbH, Darmstadt, Germany
Albumin from bovine serum fatty acid free (BSA)	Sigma Aldrich, Seelze, Germany
Amino acids	Sigma Aldrich, Seelze, Germany
Ammonium bicarbonate	Sigma Aldrich, Seelze, Germany

Ammonium persulfate (APS)	Sigma Aldrich, Seelze, Germany
Antimycin A	Sigma Aldrich, Seelze, Germany
Boric Acid	Sigma Aldrich, Seelze, Germany
Bromophenol blue	Merck, Darmstadt, Germany
Carbonyl cyanide-4-(trifluoromethoxy) phenylhydrazone (FCCP)	Sigma Aldrich, Seelze, Germany
Chlormaphenicol	Sigma Aldrich, Seelze, Germany
Coomassie Brilliant Blue R-250	Merck, Darmstadt, Germany
DAPI	AppliChem, Darmstadt, Germany
Diaminobenzidine tetrahydrochloride (DAB)	Sigma Aldrich, Seelze, Germany
Diethyl Malate	Sigma Aldrich, Seelze, Germany
Dimethylsulfoxide (DMSO)	Sigma Aldrich, Seelze, Germany
Disodium phosphate (Na_2HPO_4)	Sigma Aldrich, Seelze, Germany
Dithiothreitol (DTT)	Sigma Aldrich, Seelze, Germany
Doxycycline monohydrate	Sigma Aldrich, Seelze, Germany
Ethanol	AppliChem, Darmstadt, Germany
Ethylenediaminetetraacetic acid (EDTA)	Sigma Aldrich, Seelze, Germany
Glucose	Merck, Darmstadt, Germany
Glycerol	Sigma Aldrich, Seelze, Germany
Glycine	AppliChem, Darmstadt, Germany
Guanosine 5'triphosphate sodium salt hydra	Sigma Aldrich, Seelze, Germany
HEPES	AppliChem, Darmstadt, Germany
Hydrochloric acid (HCl)	VWR, Langenfeld, Germany
Isopropanol	AppliChem, Darmstadt, Germany
L-Glutamic Acid	Sigma Aldrich, Seelze, Germany
Magnesium chloride hexahydrate	Sigma Aldrich, Seelze, Germany
Magnesium sulfate ($MgSO_4$)	Merck, Darmstadt, Germany
Methanol	AppliChem, Darmstadt, Germany
Methyl viologen dichloride hydrate (Paraquat)	Sigma Aldrich, Seelze, Germany
Milk powder	AppliChem, Darmstadt, Germany
Monopotassium phosphate (KH_2PO_4)	Sigma Aldrich, Seelze, Germany
Nicotinamide adenine dinucleotide reduced Sodium salt (NADH)	Sigma Aldrich, Seelze, Germany
Nitrotetrazolium blue (NTB)	Sigma Aldrich, Seelze, Germany

Oligomycin	Sigma Aldrich, Seelze, Germany
Paraformaldehyde	Sigma Aldrich, Seelze, Germany
Peptone from meat	Merck, Darmstadt, Germany
Phenazine methosulphate (PMS)	Sigma Aldrich, Seelze, Germany
Phosphocreatine disodium salt hydrate enzymatic	Sigma Aldrich, Seelze, Germany
Polyethylenglycol	Sigma Aldrich, Seelze, Germany
PonceauS	Sigma Aldrich, Seelze, Germany
Potassium chloride (KCl)	AppliChem, Darmstadt, Germany
Rotenone	Sigma Aldrich, Seelze, Germany
Sodium azide	Sigma Aldrich, Seelze, Germany
Sodium chloride (NaCl)	Sigma Aldrich, Seelze, Germany
Sodium deoxycholate	Sigma Aldrich, Seelze, Germany
Sodium dodecyl sulfate (SDS)	AppliChem, Darmstadt, Germany
Sodium fluoride (NaF)	AppliChem, Darmstadt, Germany
Sodium hydroxide (NaOH)	Sigma Aldrich, Seelze, Germany
Sodium orthovanadat	AppliChem, Darmstadt, Germany
Sodium pyruvate	Sigma Aldrich, Seelze, Germany
Sodium succinate dibasic hexhydrate	Sigma Aldrich, Seelze, Germany
Sucrose	Sigma Aldrich, Seelze, Germany
Tetramethylethylenediamine (TEMED)	Sigma Aldrich, Seelze, Germany
Tris	Sigma Aldrich, Seelze, Germany
Triton X-100	Sigma Aldrich, Seelze, Germany
Tryptone Biochemica	AppliChem, Darmstadt, Germany
Tween-20	VWR, Langenfeld, Germany
Uridine	Sigma Aldrich, Seelze, Germany
Yeast extract granulate for Microbiology	Merck, Darmstadt, Germany
β-mercaptoethanol	Sigma Aldrich, Seelze, Germany

Table 2.11: Buffers and solutions

Name	**Composition**
Coomassie staining solution (1l)	1g Coomassie Brilliant Blue R-250 500 ml Methanol 100 ml Acetic acid 400 ml H_2O

LB medium (1 l)	10g Tryptone/Peptone 5g Yeast extract 10g NaCl Solve ingredients in 800mL dH2O and adjust pH to 7.5 with NaOH. Thereafter fill up to 1L with dH2O and sterilize by autoclaving.
Mitoisolation buffer (MIB)	100 mM sucrose 50 mM KCl 1 mM EDTA 20 mM TES 0,2% BSA free from fatty acids adjust pH to 7.2
Organ lysis buffer	50 mM HEPES (pH 7.4) 50 mM NaCl 10 mM EDTA 1% Triton X-100 10 mM sodium orthovanadat 100 mM NaF 0.1% SDS 1 tablet of protease inhibitor cocktail
PBS	1.5mM KH_2PO_4 2.7mM KCl 8.1mM Na_2HPO_4 137mM NaCl
RIPA buffer	50 mM Tris-HCl (pH 7.4) 150 mM NaCl 0.5% Sodium deoxycholate 0.1% SDS 1 mM EDTA 10 mM NaF
SDS-PAGE loading buffer	50 mM Tris-HCl (pH 6.8) 2% SDS 10% Glycerol 1% β-Mercaptoethanol 12.5 mM EDTA 0.02% Bromophenol Blue

SDS-PAGE running buffer	25 mM Tris-HCl (pH 8.3) 250 mM Glycine 0.1% SDS
SOC medium	0.5% Yeast extract 2% Tryptone/Peptone 10mM NaCl 2.5mM KCl 20mM Glucose 10mM $MgCl_2$ 10mM $MgSO_4$ Dissolve in nanopure water and autoclave.
Stripping buffer	62.5 mM Tris (pH 6.7) 2% SDS 0.78% β-Mercaptoethanol
TBE buffer	89 mM Tris-HCl (pH 8) 89 mM Boric acid 2 mM EDTA
TBS-T	50 mM Tris-HCl (pH 7.6) 150 mM NaCl 0.05% Tween-20
Tissue lysis buffer	50 mM Tris-HCl (pH 8.0) 2.5 mM EDTA 0.5% SDS 0.1 M NaCl 10 mg/ml Proteinase K
TSS medium	10% Polyethylenglycol 5% DMSO 50mM $MgCl_2$ Dissolve in LB medium (pH 6.5) and sterile filter it.
Western blot transfer buffer	25 mM Tris-HCl 192 mM glycine 0.1% SDS 20% methanol

3 Results

3.1 Modelling UPR^mt signalling *in vitro*

3.1.1 HSP60 and mtHSP70 are not suitable as markers for UPR^mt induction *in vitro*

Mutant mitochondrial proteins have no effect on HSP60 & mtHSP70 levels

The mitochondrial chaperones HSP-60 and HSP-6 are used in *C. elegans* as markers to measure the induction of UPR^mt signalling (Yoneda et al., 2004). The corresponding mammalian homologues are HSP60 and mtHSP70. HSP60 (also known as CPN60) was also observed to be upregulated in ρ^0 cells and upon transfection of a defective mitochondrial matrix protein, a truncated ornithine decarboxylase (ΔOTC) (Martinus et al., 1996; Zhao et al., 2002). No effect was reported on mtHSP70 levels. To study the effects of mutant mitochondrial proteins on the levels of HSP60 & mtHSP70, the ΔOTC plasmid (kindly provided by Nicolas Hoogenraad) was also transfected into COS-7 cells mimicking the original experiment (Figure 3.1A). On the protein level of the indicated markers no difference was observed compared to control conditions in contrast to what was reported before (Zhao et al., 2002). To further explore the potential of ΔOTC to induce UPR^mt, its

reactivity in HEK293FT cells was tested and HSP60 as well as mtHSP70 were measured on both protein and mRNA level (Figures 3.1B-C). No changes were detected on the protein level, whereas a slight upregulation in *mtHSP70* mRNA levels were found. A second question arising was whether disturbing the mitochondrial import machinery has an impact on the load of unfolded proteins in the intermembrane space as well as on the functionality of matrix proteins. To answer this question, the effect of a mutant TIM14/DNAJC19 (TIM14ΔH3) form (kindly provided by Thomas Langer) was investigated that is a part of the TIM23 import machinery shown to directly interact with mtHSP70 in yeast (Mokranjac et al., 2003). Moreover, in *C. elegans* it was found that downregulation of TIM-23 or TIM-17 strongly induced *hsp-60::gfp* expression (Nargund et al., 2012; Rainbolt et al., 2013). Transfection of HEK293FT cells with a plasmid carrying TIM14ΔH3 did not change the levels of HSP60 and mtHSP70 on both protein and mRNA level (Figures 3.1B-C). Taken together, no elevation of HSP60 and mtHSP70 was observed upon transfection of mutant mitochondrial proteins. As for both HSP60 and mtHSP70 very high endogenous levels were found, it could be concluded that those proteins are rather stably expressed, and hence are not very amenable to transient stress induction.
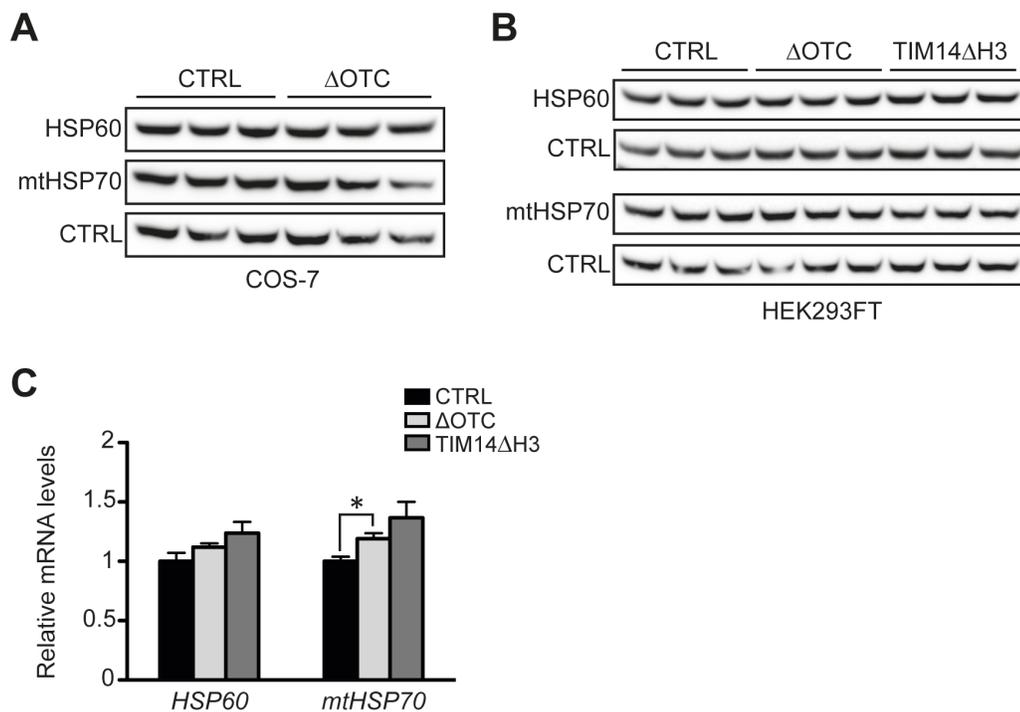
Figure 3.1: Mutant mitochondrial proteins do not affect HSP60 and mtHSP70 levels.

Figure 3.1: Mutant mitochondrial proteins do not affect HSP60 and mtHSP70 levels.
(A) COS-7 cells were transfected with a ΔOTC containing plasmid and incubated for 48 hours. Subsequently, proteins were isolated and subjected to Western blot analysis. (B-C) HEK293FT cells were transfected with either a ΔOTC or TIM14ΔH3 containing plasmid and incubated for 48 hours. Subsequently, proteins and mRNAs were isolated and subjected to Western blot analysis or realtime PCR, respectively. HSC70 serves as control (CTRL). mRNA levels were normalised to *HPRT*. Bars represent mean ± S.E.M. (Student's t test, *p < 0.05), (n=3).

Stress induction had mild or no effects on HSP60 & mtHSP70 levels

In order to find potential factors that upregulate UPR^{mt} signalling *in vitro*, different chemical compounds compromising mitochondrial function were applied and screened for induction of HSP60 and mtHSP70 in various cell lines. In *C. elegans* it was shown that the ROS generating complex I inhibitor paraquat triggered the UPR^{mt} as displayed by induction of *hsp-60::gfp* as well as *hsp-6::gfp* reporters (Yoneda et al., 2004). Also rotenone, targeting ubiquinone of complex I, and antimycin A, preventing electron transfer from coenzyme Q to cytochrome C, have been found to activate ROS-induced UPR^{mt} (Runkel et al., 2013). On the other hand, inhibition of mitochondrial translation by exposure to low doses of chloramphenicol and doxycycline also induced UPR^{mt} signalling in worms (Houtkooper et al., 2013). Based on these observations, the same set of chemicals was applied to different cell lines for 48 hours and measured HSP60 and mtHSP70 protein levels (Figure 3.2). Unlike what was described in *C. elegans*, only little or no effects were observed on the levels of these two suggested markers using a direct readout by Western blot. Having no effect on MEFs and HeLa cells (Figure 3.2A and 3.2F), a slight decrease in protein levels was found in C2C12, Hepa 1-6 and COS-7 cells (Figures 3.2 B-D). The only minor upregulation was observed in HEK293FT cells (Figure 3.2 E). Taken together, on protein level HSP60 and mtHSP70 barely respond to the previously described chemicals in cell lines of human, mouse and monkey origin.
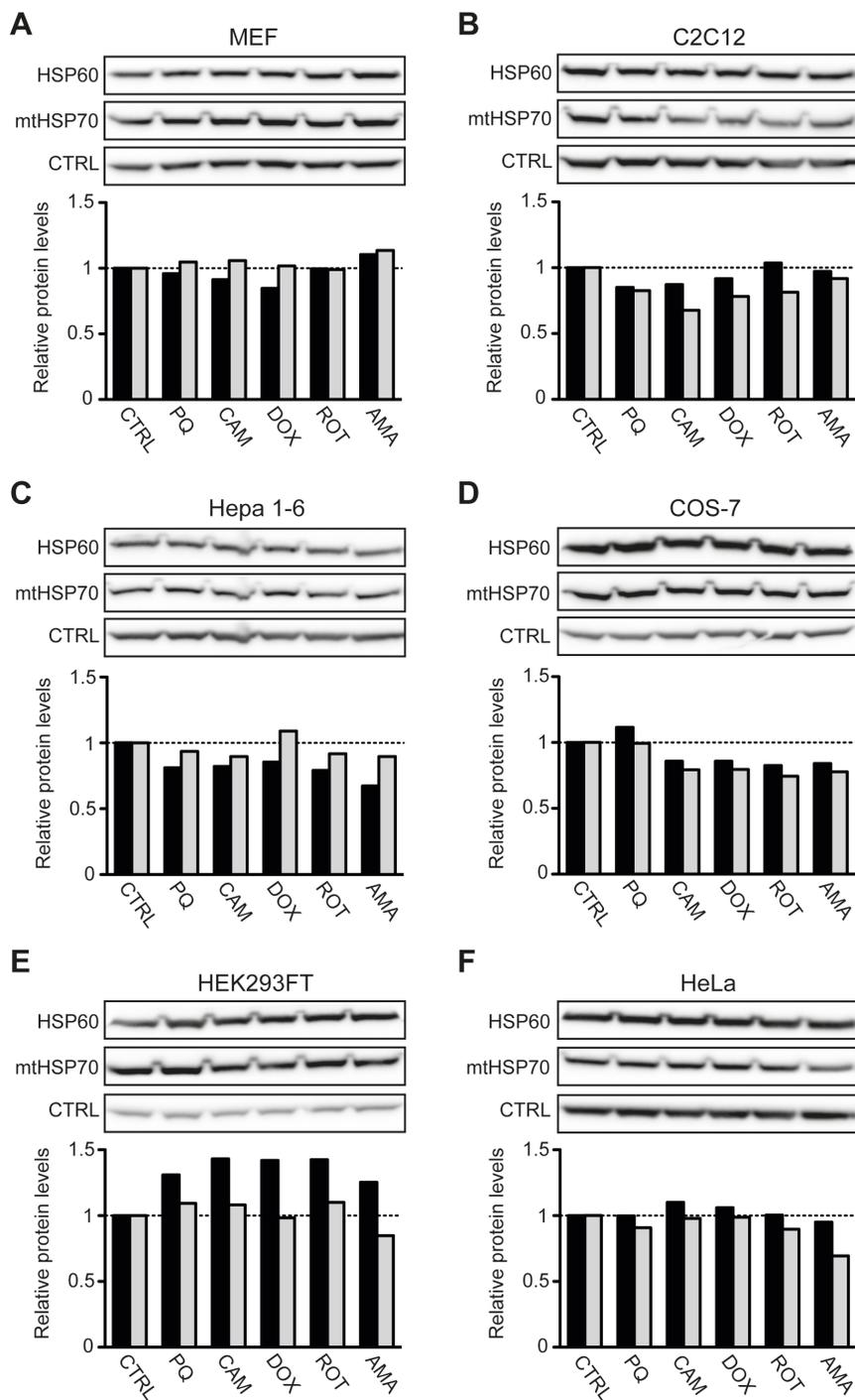
Figure 3.2: UPR^{mt}-inducing agents do not affect HSP60 and mtHSP70 levels.
Different cell types were treated with ROS-inducing agents (25 µM paraquat (PQ), 100 nM rotenone (ROT), 20 nM antimycin A (AMA)) or mitochondrial translation inhibitors (50 µg/ml chloramphenicol (CAM) or 30 µg/ml doxycycline (DOX)) for 48 hours. The medium was supplemented with 50 µg/ml uridine, since it is known that cells without full mitochondrial gene expression become auxotrophic for pyrimidines (King and Attardi, 1989). Cell lysates were subjected to Western blot analysis. ACTIN serves as control (CTRL). The quantification relative to the CTRL levels can be found in the diagrams below. Black bars display the HSP60 levels, whereas grey bars display the mtHSP70 levels. This small-scale screen was only performed once.

Hsp60 and *mtHsp70* transcriptional reporters are constitutively active *in vitro*

In *C. elegans* the readout for transcriptional activation of the *hsp-6* or *hsp-60* gene, hence the induction of UPR^mt signaling, is measured by transcriptional reporters that drive GFP expression (Yoneda et al., 2004). Also for cell culture studies transcriptional reporters driving luciferase (LUC) or chloramphenicol acetyltransferase (CAT) were used to measure UPR^mt induction (Zhao et al., 2002). Typically, a transcriptional reporter consists of a promoter fragment of a few kilobases upstream of the start codon that harbours a significant amount of the *cis*-regulatory information necessary to provide expression pattern of the endogenous gene under study. To examine the transcriptional activation in cell culture reporter constructs were generated under the control of the *Hspd1* (*Hsp60*) or *Hspa9* (*mtHsp70*) promoter fragment of approx. 2 kb size driving GFP expression (Figures 3.3, 3.4 and 3.5A). Promoter sequences were retrieved and predicted transcription start sites (TSS) assigned using the TRED database (Zhao et al., 2005). For both *Hspd1* and *Hspa9* three possible TSSs were found (Figure 3.3 and 3.4). The *Hspd1* gene is co-regulated with the *Hspe1* (*Hsp10*) gene sharing one bidirectional promoter (Hansen et al., 2003). *Cis*-acting transcriptional elements were analysed and assigned to the respective promoter sequence (Figure 3.3 and 3.4). Apart from regular promoter motifs, both contained a heat shock element (HSE) that is activated by specific transcription factors upon heat shock or protein folding perturbations (Ryan et al., 1997). In addition, the *Hspd1* promoter contains a CHOP responsive element that cannot be found in *Hspa9* promoter region. Instead, the *Hspa9* promoter harbours a motif associated to the tricarboxylic acid cycle (TCA motif) (Cora et al., 2004). Reporter constructs that detect transcriptional activation of *Hspd1* (pHSPD1-GFP) and *Hspa9* (pHSPA9-GFP) were transfected into COS-7 as well as HEK293FT cells without further stress application (Figure 3.5B). A moderate to strong GFP expression was observed in both COS-7 and HEK293FT cells using the *Hspd1* as well as the *Hspa9* reporter that was comparable to the CMV promoter driven GFP expression (Control). Given the fact that no stress was applied to the cells, the data suggest that both genes are constitutively active in both cell types under regular cell culture conditions.

-1930

↰

TTTCATTTCCCTGTCTGGTGTGTGTGTGTGTGTGGTGGTGGTGGTGGGGGGGGGGTCTTCATTACTAATCAGCA
Hspe1 ORF

ATCGCCACCTTGATCTATTCCAAGGTCAAACATTTCTTTAATTTTTTTAAAAATTCGAATAACGGGGGAGTGG

CGTCACTTTTCGAGCCTGGATCTTAGTCTTTCTCCAACATAGGACACATCCACTGAAGCCCTGCCAGGGCAGG

TGGGCTTCTGCGTGTGCATCGGGTTCCCGCCCCCTGCCCCAGACGCTTTGTCGCA**CACGTG**CGTGCGGCAAAG
E-box

CCATGGTGGAGAGAGAAATGGCCTCGCTTCTGCAGAGCCATGGGCGGACACCGGACACTGACCAGACCCCGGA

CCCCTGTCCTATTAGTCCCAAAGCGCACAAGGGTTCGCCGTGGGCCGCAGGCCGAACTGGACCCGCAGGCCTG

CCAACCACGAGACACTCACCATGACTCTCGCCTTCGCCGCCACCACCGCAGCTCCGGACTCTGAACTCGGGCC

GCTGCTGCA**A**GGAGAGTCCTGCTGGCCGGCTGGGA**CACGTG**AAAAGGCCGCGCAGCGCGCAGGCGCACTCAGC
　　　　　TSS1　　　　　　　　　　　　**E-box**

CCCCCGAGCGTGAGAGGGGGCGGCCACGCCGACGCGCGCGCCGATTGGTGGCGAGGGCTCCGCGCAAGG**GGGC**
　　GC-box

CGACGCGGGCGGCCGGAGGCGGAAGAAAAGGGGAGCACTTTCTAGGCTTTTCCAGGCCGGCCGCCGAGGTGAA

AGAACGAGCCCCCCTCCCGGAAATGACGCCACTTGACCTTTCACCCACG**GGACG**CGCGGGGCCTTCCGGAAGG
　　　　　　　　　　　　　　　　　　　　　　　　　　　　　　DPE

T**TCTAGAA**CGGACCGTGGCCCAGGAACCAGCGTAGGGCGGCGGGAGAGGGCTGAGGCCGCAGAGCTGAGGCGG
　HSE

CTCTGGTACGGAGGGCGGGGCCGCGCGCGCCGCATGCA**GATTGCA**GGGCCCCGGCGTGGGAGAGAGCGGGGGG
　　　　　　　　　　　　　　　　　　　　　　　CHOP

CGCGCGCGCGCA**CACGCG**GGGCCGCGGGGCGGGGCGGGGAGGGAGGGGACTCGGGCTCATTGCGGTGCGCGCC
　　　　　　　N-Box

CA**G**AGCTGGGTCCCTCACTCGCCGC**AGACG**GCCTGCCTCGCCTCGTGCTCTCCTGCCGCCGCCCCGCAGGTAC
　TSS2　　　　　　　　　**DPE**

GCGGCCTCGGCGTGCA**GGGCGCC**CCGGCGCTCGCGGGGGGCTGCTTGCAGCGCGGACCGAGCACGGAGGACTA
　　　　　　　　　　BRE

GGGGGAGAAGTCTGGCAGCGACGCCGCAGGCTCGGCTCACTTGTCCAGGCCCAGCGGGGCCACGCTGGTTTCA

T**CACGTG**TGGCGGGGAC**CACGCG**ATCCAGGCCGAGCGCCGGAGCAAGGGCGGGCTAGGGTGGAAGCAACTTGG
　E-box　　　　　　　**N-Box**

GCCCTCTGGTGCCACCTGCGCCTGGCGCACTGCAGGACTCTGTGGGAGGGTGGTCGGGGTCCTTTAGTCCCCG

GTGGCCGCGGCGGTCCGGTGTTCACTTTGACCTTGCTCGGGGCTCCTGGTCGGGAAGA**CACGTG**GGGCCGCGA
　　　　　　　　　　　　　　　　　　　　　　　　　　　　　　　　　　E-box

GGCTGGACTGACCTACTGTCTTTTCCTCCGGCCTTGCTAGCTGCTGTGTTACCGTAGCTTCGGGTGGATACCT

GGCGACACACTCAGAGGGTTTTGCACCGTCATGAGTACTTCTG**T**AGTTCTCTAGGCAATTGCATTTAGAACCT
　　　　　　　　　　　　　　　　　　　　　　　　　　TSS3

GCCTTGCTTGCACCAACTTGATTTTTTTCCTTTGGACACTTTTCGGAGTGGATCTGCTCCCAAGGCCGCTTTG

GCAGTGAAAGATTAACTTGAGAGGGCAGAGTGGGTGGCCATGGGGATGTGGTTTTCTGTGCTTTGTGCTTATG

CTGTTGGTCAGGCTTGGGGTCAGCCTCCATGATCAGTTGGCTAGCAGATTATGCCCTGAATCTGCAGCGCCCA

GGCATGGTGGTTAGCAGAGGACAGCCCAGCT**CCAAT**CTAGCCTCCCATGTTTTGAAGCACCGTTGGACAAGTT
　　　　　　　　　　　　　　　　　　C/EBP

TGTAGTGATTTTTCTTTTTTCCTTCCCCAGAA**ATGCTT**
　　　　　　　　　　　　　　　　　↳+1

Figure 3.3: Sequence of the mouse *Hspd1/Hspe1* promoter region.
The nucleotide position +1 corresponds to the start of the open reading frame (ORF) of *Hspd1*. Predicted transcription start sites (TSS) are depicted in red. Potential *cis*-acting elements of interest are shown underneath the sequence. *Cis*-regulatory elements were assigned according to (Aldridge et al., 2007; Cora et al., 2004; Smale and Kadonaga, 2003).

-1963

ATGCTCCTCCTGCCTCAGTATCCTGAGAGCTGGGATGAAGTGTGCCACTAAACCTGATTGATGGGATGATGAG

GATGGAACTCTGACCTAGCACATTCTAGGCTAGCACACTCCCAACTGAAATATGATTCTAGTCCTTTTACTTT

TTGAGACAGAGGCTTACTGTGTAGCTGTGTTAAAATCAGACCCTCCACACATCTTTGATAGATCACAAGCATT

TATCACCAGGCCCCTTTTTCTTTTAATGCATTATCTATCACTAATTGAAATGCAATGTCTGTCCTGTTTAACT

TAATTTTATTAACTTGTTAAAAAAGAGGTTCACAGACTCTTAGTGTCATCGAGCTGGTTC**CCAAT**TCATTTTA
                                                            C/EBP

TCACCAAAGGTGACCTTGCATTTCTGGTTCAACCTCACCCAAGTGCTGGAGGCTGACAGCACCATTCCCAGCT

ACCTTCCATTCCCTTCTACTTTCTTTTATAATATAACTGTATTTTATCTCCTAATTTCCCCACACGTTCTTCA

TAACTTGTTACAGTGATGACCACCATTACTTCTTTTTGAGATAGTTTCATGTAGCTCTTGTTGGCCTGGAACG

AATGATGGGGTCAAAGATGACCGGTGGAATTACAAGCCTGTATGAGCACTTCCTACCCAACTATTTTCTCTTG

CTATCAAACTGCTACCTCCAAAACCAAGTTCTACTTCACTGTCTTTGAATCCCTGTTTTTACAACCGTCGAGA

AAATCCTGACACAACATTTGTTCCAAGGTTTTGTCCCTAAAAGTCTCTCAGTACCTCCCATCTGTAATTCAGA

CATTTGAAAGGGTCCGGCAGTAGAGCCTTGAGTGTGAGGACAACTAAGGCTAGTAAAACCCTGGGGTTGGGTG

GGGTGGCGCAGGCCTTTAATTCCAGCGT**TCTAGAA**GTACACTGGTGGGATCAAGGCCAGCCTGGTC**TATAAA**T
                            HSE   **TATA-Box**
CTAGTTCTGTGACAGC**CGGCGCC**CGCCATTCATACCCCGTCGGAAACCTTGTCTTTGAAAAAAAAAAAAAATCG
                TCA motif

TCACATTATAATCAACATCTGGCAAGCGCAAGGTTTGAAAAAGAGGCGCCCCTGGCCTTGCAAACCGGGCAAT

AAGAGCTCATGTAGTTCTCCCCTCATCGTTCCCAAGGCAGCCTTAAAAGTGACTCGAAGCTTCGTGAATCCGA

TGCTGCCCTAGAGCTTAGGAACCTAACCCGACCGAAGCAATGCGCTGCCCAAATTTGTGTGAGACCGCGCACA

TTCAGGTGTGCACATTTCAAGCGGCGAACAAACAGCGATGGAGAACAAAGGTCCCCGAAACAACGCCTCAGGA

CAAGATGGCGACCGCAGCAAGTCGCGGCCTCCGGGGACAACGCCCACGCGCCTGCCAGTGAGCGCGCGAGCTC

GCGCCCCCGGCACTCGCCCGCAAATTCGCGTGCACTGGAGCAT**CCAAT**AAACGCTACAGTTAAACCCGAACCC
                                           C/EBP
GTTTTCT**CCACGCC**CCTCACACATGCGCTT**CACGAC**CTCTGTCCGGAGCGGAGAACGCAGGCGCAGAACGCAC
        BRE   **N-Box**
CTCCTTCTGCGCAACTGACGCAAGGAGACTGTAATCTGTTCGTAATTTATCCCGTGTGACCTTGAGTCTTTCC

CGTCCTAAGGACCGGGACTGTCCGAAGCGATGCCTGTCCACCTCTCTTCTCTCTTTCCCTTCTCCCTGCTCCC

ACAGCCCTGGAAACCGTGATGAGAGAACGGGAACTTTCAACGATTAATGCTGAGAGGCGTGCTGGCGGCGTGC

GCCGATCCCGGGAGCAGCGGACACGTAGTCTCTAGTCAGGCAGCACGTCGGGCGCCTCAGCAGAAGAGCGGGC

TTCATTGCTGCAGCGGCCAGCCCCCGCCCCC**A**CCC**CACGTG**GT**T**GGAGGTTTCCAGAAGCGTAGC**C**ACCACCG
                                TSS1   **E-box** TSS2   TSS3
TGCACGCAGCTCCGGGCCCGTGGGGTGTTGGTTCTTGCCCTCGTAACCCCCTCTGTCCAGCCACC**ATGATA**
                                                                    ↳+1

Figure 3.4: Sequence of the mouse *Hspa9* promoter region.
The nucleotide position +1 corresponds to the start of the open reading frame (ORF) of *Hspa9*. Predicted transcription start sites (TSS) are depicted in red. Potential *cis*-acting elements of interest are shown underneath the sequence. *Cis*-regulatory elements were assigned according to (Aldridge et al., 2007; Cora et al., 2004; Smale and Kadonaga, 2003).

A

pEGFP-N3   -589 ———— CMV_{pr} ———| GFP |

pHSPD1-GFP   -1930 ———— $Hspd1_{pr}$ ———| GFP |

pHSPA9-GFP   -1963 ———— $Hspa9_{pr}$ ———| GFP |

B
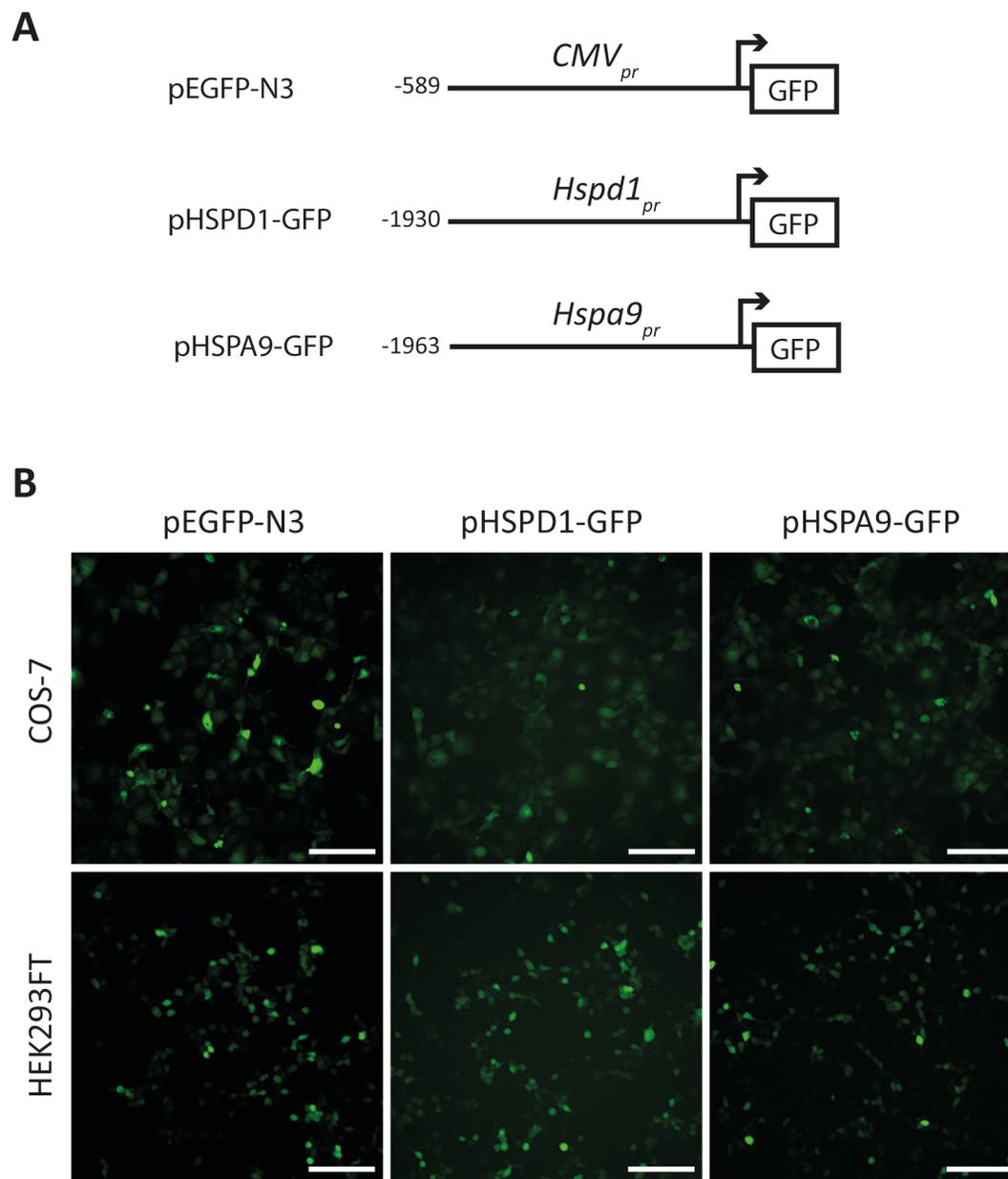
Figure 3.5: *Hspd1* and *Hspa9* reporters are active under regular cell culture conditions.
(A) Schematic outline of the reporter assay. A *CMV* promoter upstream of the GFP coding sequence was used as control. Numbers indicate the size of the assigned promoter regions upstream of the respective ORF that was cloned upstream of the GFP gene. (B) COS-7 and HEK293FT cells were transfected with pEGFP-N3 (*CMV::*GFP); pHSPD1-GFP and pHSPA9-GFP respectively and incubated for 24 hours. Levels of GFP expression were analysed using fluorescence microscopy. White scale bars, 100 µm.

3.1.2   Downregulation of UPR^{mt} signalling

Based on the observation that HSP60 and mtHSP70 are highly expressed in regular cell culture and stress induction did not further increase their levels, the question was asked vice versa whether reduction of UPR^{mt} signalling affects their levels, thereby yielding new insights into this fundamental process.

3.1.2.1   Physiological oxygen conditions do not influence the HSP60 & mtHSP70 levels

Cells are routinely cultured under atmospheric oxygen conditions (approx. 21%) in the majority of cell culture laboratories. However, *in vivo*, the oxygen concentrations range from 1-12% rather than the 21% *ex vivo*. These differences already alter cellular functions, especially challenging mitochondria and oxidative metabolism. It has been shown that reduction of oxygen levels to more physiological conditions improves the mitochondrial network and shape as well as lowers the ROS production (Tiede et al., 2011). On the other hand hypoxic conditions (0.1%-5%) also perturb mitochondrial energy metabolism and induce ROS production (Solaini et al., 2010). To explore whether the high oxygen conditions in regular cell culture are the primary cause for the high levels of HSP60 and mtHSP70, hence the UPR^{mt} induction, different cell lines were cultivated at 5% oxygen for 1 week and HSP60 and mtHSP70 levels were measured (Figure 3.6A and 3.6 B). Only in C2C12 cells we a slight decrease in HSP60 levels could be detected. However, mtHSP70 levels were not affected. Taken together, no general reduction in the levels of HSP60 and mtHSP70 was found under more physiological oxygen conditions.
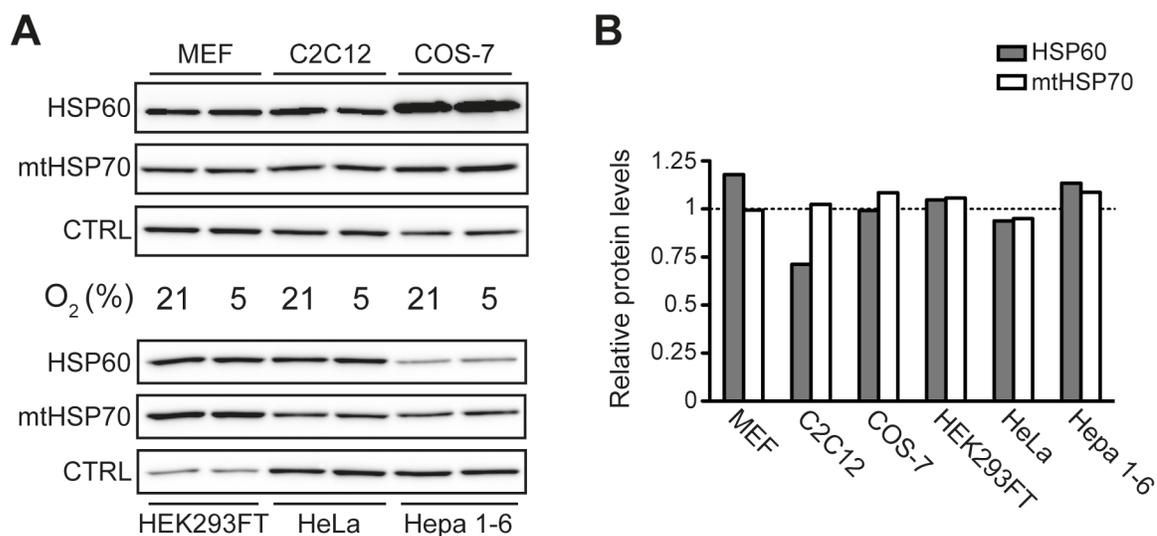
Figure 3.6: Physiological oxygen conditions do not reduce HSP60 & mtHSP70 levels.
(A) Different cell lines were incubated for 1 week under 5% oxygen conditions. Subsequently, proteins were isolated and subjected to Western blot analysis. ACTIN serves as control (CTRL). (B) Protein levels obtained in (A) were quantified relative to CTRL levels. Bars represent the 5% oxygen condition, whereas the dashed line corresponds to the 21% oxygen condition. This experiment was only performed once.

3.1.2.2 Knockdown of ATF5 mildly reduces UPR^{mt} markers

By the use of reporter worms and large-scale RNAi screens, the bZIP transcription factor ATFS-1 was found to be the central player in mediating the UPR^{mt} *in C. elegans* (Nargund et al., 2012). To date no mammalian homologue has been found. However, ATFS-1 contains a C-terminal basic leucine zipper domain that comprises a distant similarity to the mammalian ATF4 and ATF5 as determined by the gene ontology software PANTHER (Mi et al., 2010) (Figure 3.7). Knowing that ATF4 is the key transcription factor of the integrated stress response (Harding et al., 2003), the further analysis focused on ATF5. The hypothesis that ATF5 exerts a similar role in the mammalian system as ATFS-1 does in *C. elegans* was tested by performing a knockdown of ATF5 and subsequent analysis of HSP60 and mtHSP70 levels. The idea behind this was that downregulation of the potential UPR^{mt} signal should affect the UPR^{mt} marker levels. Based on the observation that both HSP60 and mtHSP70 are highly upregulated in cell culture, a

decrease in the marker levels upon knockdown of ATF5 was expected, if ATF5 is transmitting the signal. Indeed, a slight downregulation of HSP60 and mtHSP70 was found after 3 days knockdown of ATF5 using 2 different siRNAs (Figure 3.8A and 3.8B). Moreover, CLPP, a potential UPR^{mt} marker, was slightly reduced upon ATF5 knockdown. *ATF5* mRNA levels after siRNA treatment generally correlated with the observed effects of HSP60, mtHSP70 and CLPP (Figure 3.8C). Therefore, these data indicate that reducing the ATF5 level does translate into a reduction of UPR^{mt} markers as well. It should be noted that although the knockdown efficiency of *ATF5* siRNA (1) was lower compared to *ATF5* siRNA (2), the effect on the UPR^{mt} markers was comparable or even more pronounced (Figures 3.8 B-C). It was reported that detection of siRNA-mediated knockdown by realtime PCR is highly dependent on the primers used (Holmes et al., 2010). Thus, it is possible that residual mRNA fragments are detected, although the knockdown is present.
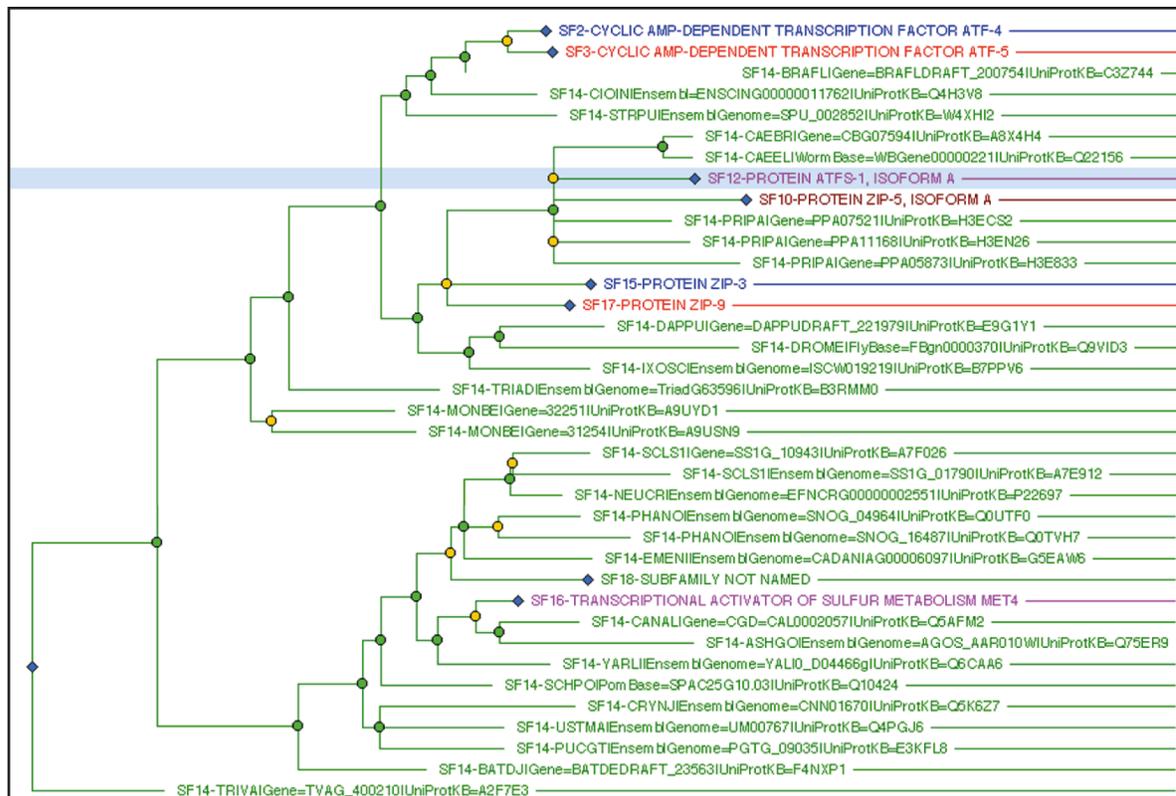
Figure 3.7: Tree panel of the phylogenetic relationship among the ATF4/5 family.
The longer the (horizontal) branch length, the more distant the groups joined by those branches. There are 3 types of nodes in the phylogenetic tree: blue diamonds (subfamily nodes); orange circles (gene duplication nodes) and green circles (speciation nodes). ATF4 and ATF5 can be found at the top of the chart. ATFS-1 is highlighted with a blue background.

A

HSP60

CLPP

CTRL

mtHSP70

CTRL

B

Relative protein levels

■ CTRL siRNA
□ *ATF5* siRNA (1)
▦ *ATF5* siRNA (2)

HSP60 mtHSP70 CLPP

C

Relative mRNA levels

■ CTRL siRNA
□ *ATF5* siRNA (1)
▦ *ATF5* siRNA (2)

**
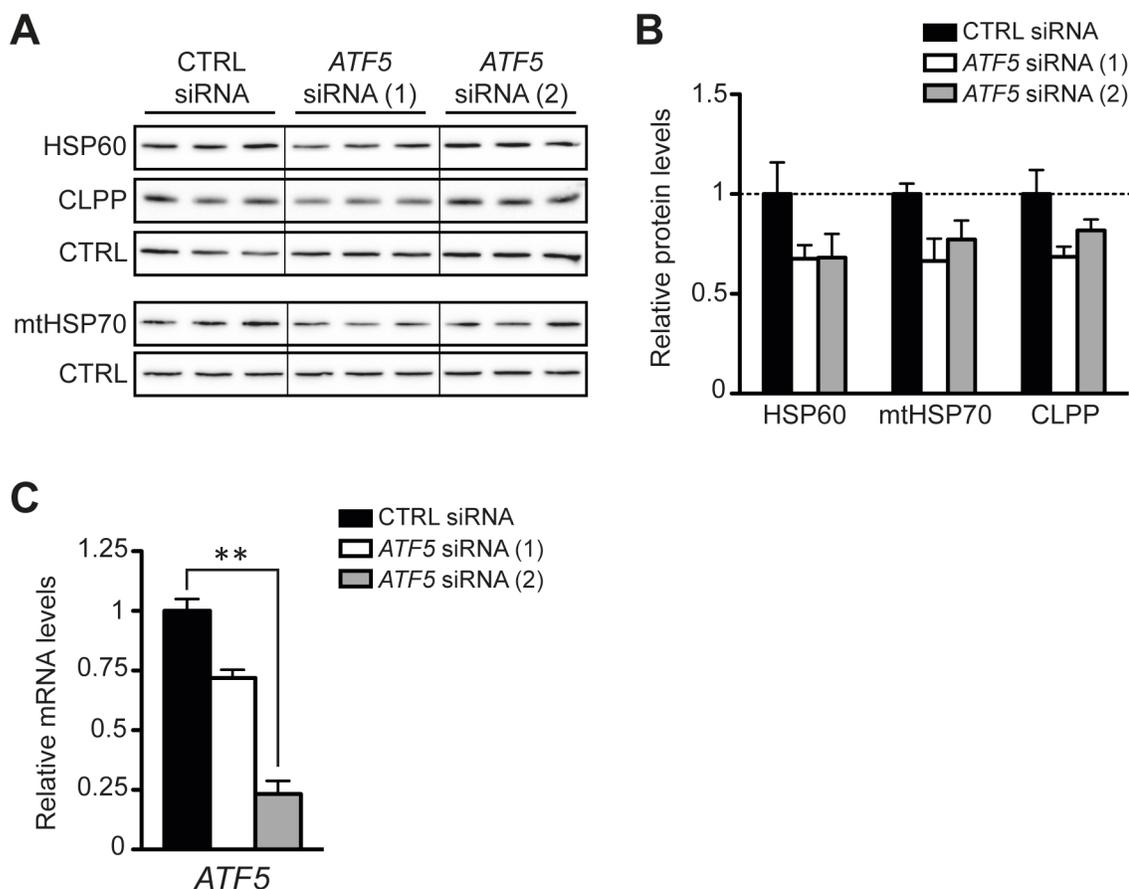
ATF5

Figure 3.8: Knockdown of ATF5 reduces UPR^mt marker levels.
HEK293FT cells were transfected with the indicated siRNA for 3 days. Subsequently, proteins and mRNA were isolated and subjected to Western blot analysis (A) or realtime PCR (C). (B) Relative quantification of UPR^mt markers to control conditions. Actin level serves as control (CTRL). Bars represent mean ± S.E.M. (Student's t test, **$p < 0.01$), (n=3).

3.1.3 ATF5 is localized to the nucleus under regular cell culture conditions

In *C. elegans* the transcription factor ATFS-1 accumulates in the nucleus during mitochondrial stress since it comprises a nuclear localization sequence (NLS). In addition, it consists of a mitochondrial targeting sequence (MTS) allowing the translocation to mitochondria under non-stressed conditions (Nargund et al., 2012). The MTS was found using a protein sequence prediction algorithm, called Mitoprot II (Claros and Vincens, 1996). The same algorithm was used here to assess ATF5 for its potential to enter mitochondria (Table 3.1). A probability of 0.2907 for ATF5 to be imported into

mitochondria was found, however, no cleavage site and therefore no cleaved sequence. In contrast, ATFS-1 had a probability of 0.8658 to end up in mitochondria, but also no cleavage site was predicted. Interestingly, we obtained a high probability of 0.7052 and also a cleavage site for XBP1, the central factor of the UPR^{ER} (Ron and Walter, 2007). Mitoprot II analyses indicate a trend for mitochondrial proteins to be imported into mitochondria. However, false positives or false negatives are retrieved quite frequently, therefore experimental validation is inevitable.

Table 3.1: Mitoprot II analysis of ATF5, ATFS-1 and XBP1

Transcription factor	Length	Cleavage site	Cleaved sequence	Probability of export to mitochondria
ATF5	283 AA	n/a	n/a	0.2907
ATFS-1	472 AA	n/a	n/a	0.8658
XBP1	267 AA	41	MVVVAAAPSAATAAPKVL LLSGQPASGGRALPLMVP GPRA	0.7052

To examine experimentally whether ATF5 is imported into mitochondria, colocalization studies using fluorescence microscopy were performed. A GFP-tagged versions of ATF5 and XBP1 (Control) were generated (Figure 3.9A). Both constructs were transfected into MEFs for 24 hours and subsequently stained with MitoTracker and DAPI. Fluorescence microscopy revealed that ATF5 is exclusively found in the nucleus (Figure 3.9B). XBP1, however, did not colocalize with mitochondria or the nucleus, but was detected in a structure likely to be the ER as it was described before. Based on the observation that regular cell culture conditions constitutively induce the UPR^{mt} markers one would also expect that ATF5 is found in the nucleus, if it acts in the same way as ATFS-1 upon stress induction. Therefore, it was difficult to examine in cell culture whether ATF5 is able to translocate to mitochondria or not.

A

B
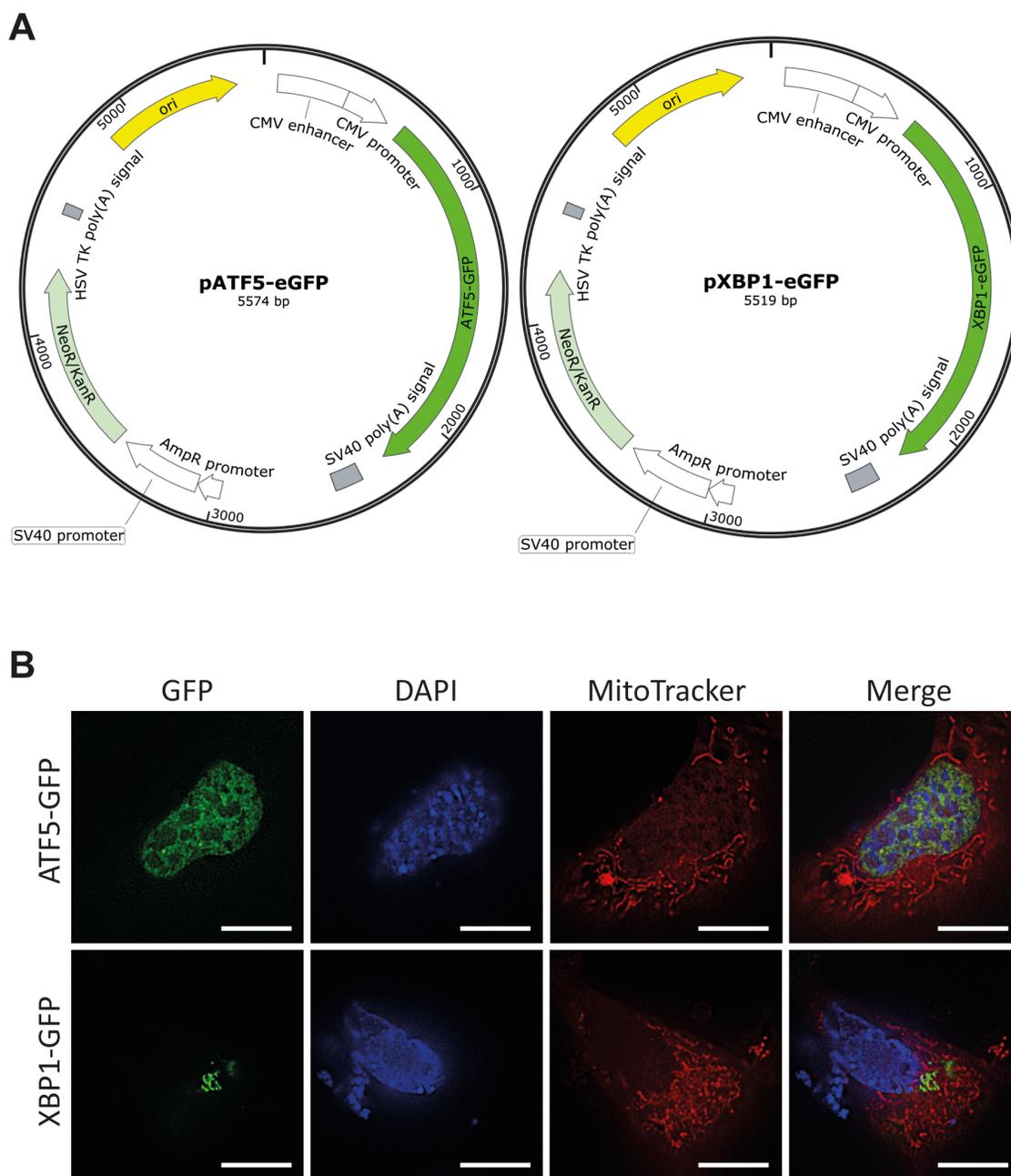
Figure 3.9: ATF5 is localized to the nucleus under regular cell culture conditions.
(A) Vector maps of cloned eGFP-tagged factors. Vector maps were generated using the SnapGene software (from GSL Biotech; available at snapgene.com). (B) Colocalization analysis of MEFs transfected with GFP-tagged constructs for ATF5 and XBP1 incubated for 24 hours. Cells were stained with DAPI and MitoTracker and analysed by fluorescence microscopy. White scale bars, 10 µm.

3.1.4 Knockdown of HSP60 and mtHSP70 affect the levels of mitochondrial matrix proteases

Knockdown of HSP-6 and HSP-60 induced UPR^{mt} signalling in *C. elegans* as shown by the activation of both the *hsp-6::gfp* and the *hsp-60::gfp* reporter (Yoneda et al., 2004). Knowing that the pHSPD1-GFP and pHSPA9-GFP reporter constructs are activated in cell culture without further stress application (see section 3.1.1), it was not possible to use the same approach to investigate the mammalian UPR^{mt} signalling. Instead, a knockdown of HSP60 and mtHSP70 in HEK293T cells was performed and endogenous protein and mRNA levels were analysed. A strong knockdown efficiency of *mtHSP70* siRNA of approx. 80% was found on the protein levels, while only 25% in the case of *HSP60* siRNA (Figure 3.10A-B). No effect was observed of HSP60 knockdown on mtHSP70 levels and vice versa, contrary to what was described in *C. elegans*. The protein quality control system in mitochondria relies not only on chaperones but also on proteases to degrade unfoldable polypeptides. Based on this fact, it was hypothesized that increased unfolded protein stress should not only affect the levels of chaperones, but also proteases. Thus, the levels of the matrix proteases CLPP and LONP1 were assessed, both reported to deal with the degradation of unfolded proteins (Voos, 2009). Interestingly, CLPP was found reduced upon increased unfolded protein stress, which is also in contrast to what was described before (Figure 3.10A-B) (Zhao et al., 2002). Unlike CLPP, LONP1 was induced upon HSP60 and mtHSP70 knockdown on protein level (Figure 3.10A-B). On mRNA level only mtHSP70 knockdown strongly increased *LONP1* expression levels (Figure 3.10C). As a next step, *ATF5* mRNA levels were examined upon HSP60 or mtHSP70 knockdown. Increased expression levels of *ATF5* were found using both siRNA species, however, upregulation failed to be significant (Figure 3.10D). Taken together, these data demonstrate that knockdown of HSP60 and mtHSP70 indeed trigger the UPR^{mt}, using LONP1 and ATF5 as novel readout, rather than the proposed UPR^{mt} markers HSP60, mtHSP70 and CLPP.
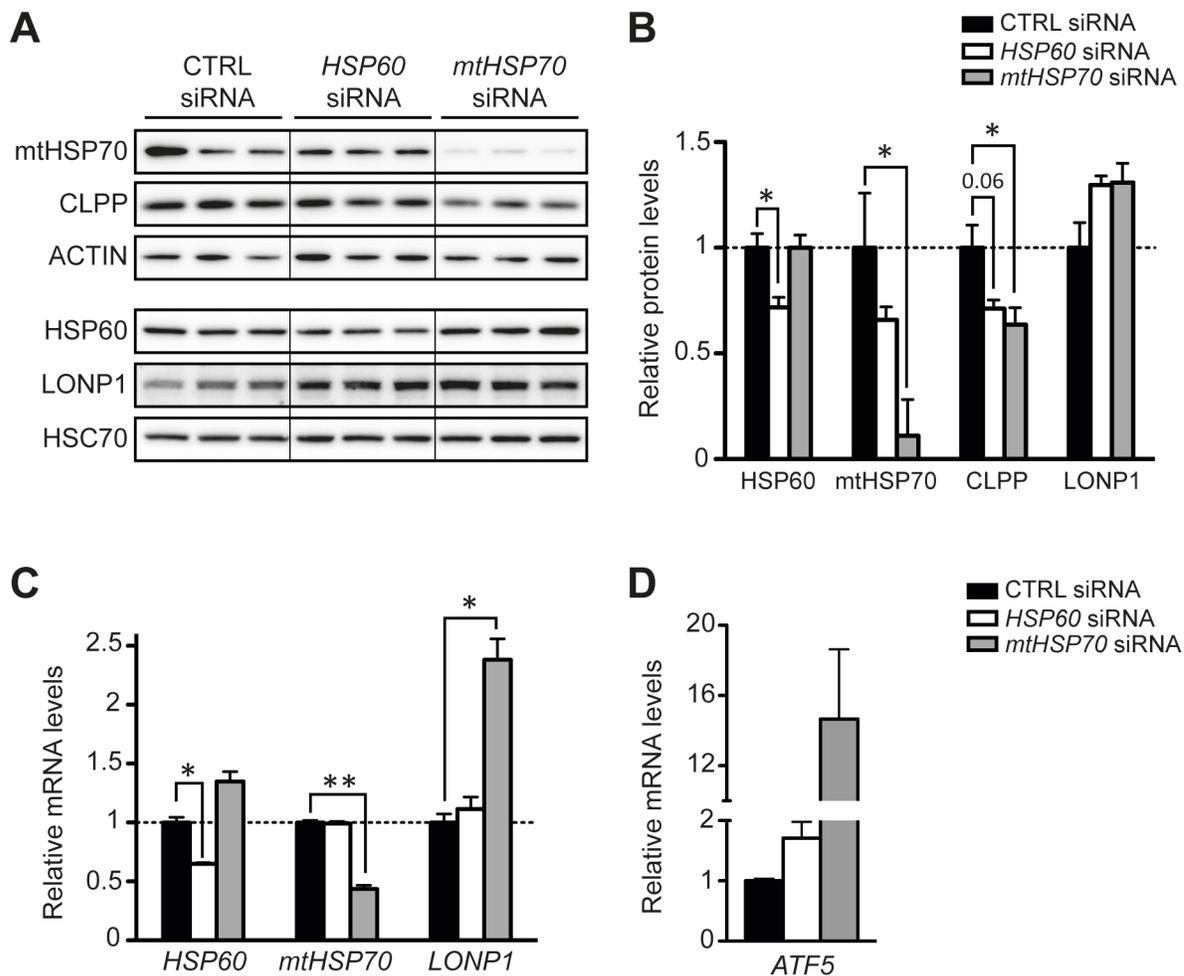
Figure 3.10: Knockdown of HSP60 and mtHSP70 affect the levels of mitochondrial proteases.
HEK293FT cells were transfected with the indicated siRNA and incubated for 3 days. Subsequently, proteins and mRNA was isolated and subjected to Western blot analysis (A-B) or realtime PCR (C-D). (B) Protein levels were quantified relative to the control levels (ACTIN or HSC70). Bars represent mean ± S.E.M. (Student's t test, *p < 0.05; **p < 0.01), (n=3).

3.1.5 UPR^{mt} markers depend on LONP1, a novel UPR^{mt} marker itself

Based on the observation that LONP1 was induced upon HSP60 and mtHSP70 knockdown, the question arose whether this upregulation is also dependent on ATF5. To study the effect of ATF5 on LONP1, a knockdown of ATF5 in HEK293FT cells was performed and LONP1 protein and mRNA levels were analysed. A significant induction of LONP1 was found on both protein as well as mRNA level upon ATF5 knockdown, showing that reduction of ATF5 levels increase mitochondrial stress *in vitro* (Figure 3.11A-C). Furthermore, these data demonstrate that activation of LONP1 was independent of ATF5. Since LONP1 instantly reacts to mitochondrial perturbations, it was checked whether LONP1 is upstream of known UPR^{mt} markers. To test this, LONP1 was knocked down in C2C12 cells, since siRNA against mouse *Lonp1* mRNA was available, and the effect on ATF5 was examined (Figure 3.11D). A strong correlation between the LONP1 and ATF5 expression levels was observed upon LONP1 knockdown, showing that ATF5 expression is dependent on LONP1. In addition, expression levels of mitochondrial chaperones as well as CHOP, a multifunctional transcription factor involved in both UPR^{mt} and UPR^{ER}, were assessed (Horibe and Hoogenraad, 2007; Nishitoh, 2012; Zhao et al., 2002). A general reduction was found in all UPR^{mt} markers analysed (Figure 3.11E). The knockdown efficiency of *Lonp1* mRNA levels strongly correlated with the reduction of *mtHsp70*, *Trap1*, implicated in the UPR^{mt} signalling in *Drosophila melanogaster* (Baqri et al., 2014), as well as *Chop*. For *Hsp60* only a minor effect was found on the expression levels, which is in line with previous experiments, indicating that HSP60 is a high abundant protein, difficult to regulate (see section 3.1.1). Taken together, these data show that LONP1 regulates the levels of UPR^{mt} markers, whereas mitochondrial unfolded protein stress can be sensed by LONP1 independent of ATF5.
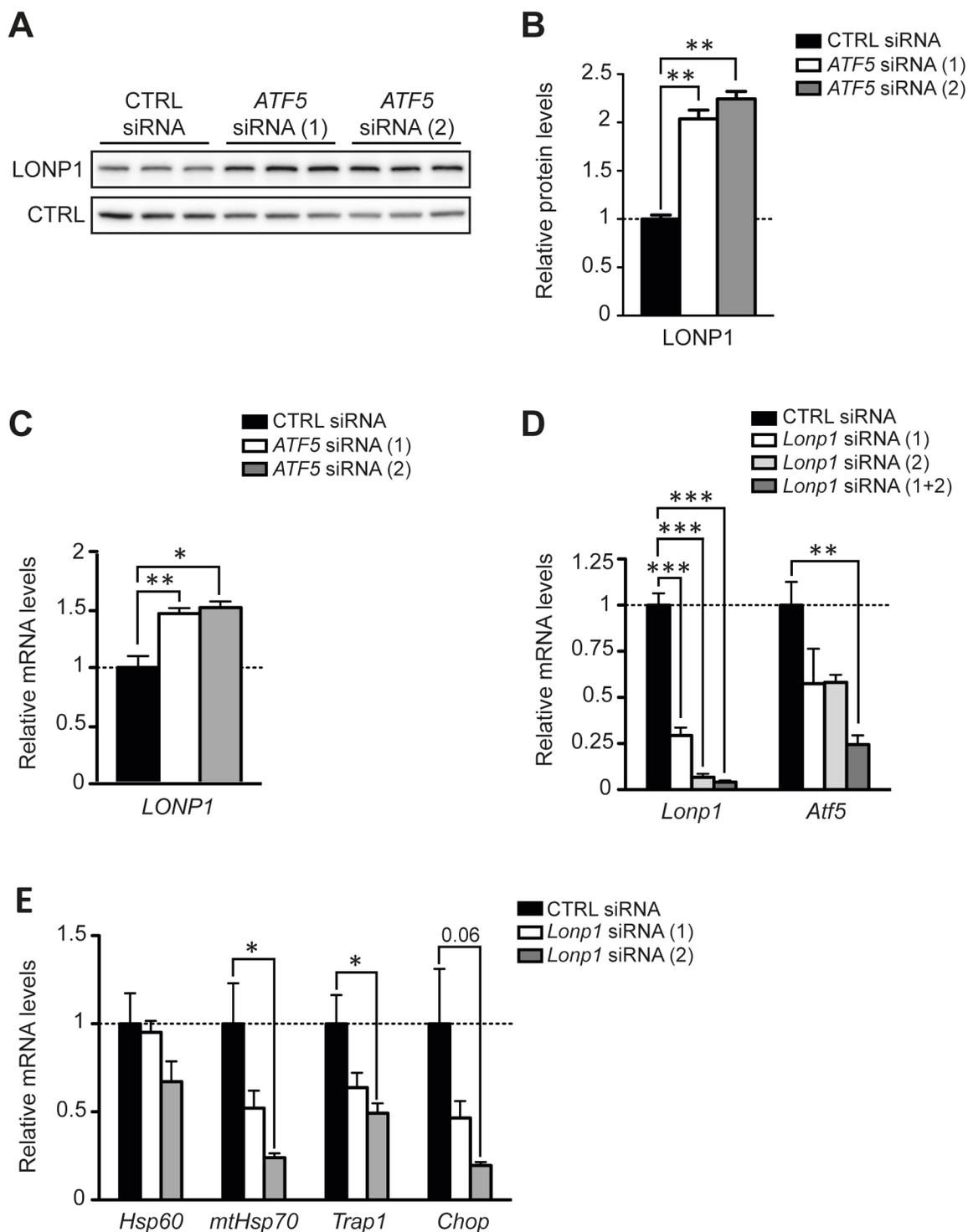
Figure 3.11: LONP1, a novel UPR^mt marker, regulates other UPR^mt markers.
(A) Western blot analysis and (B) relative protein levels of LONP1 upon ATF5 knockdown in HEK293FT cells. HSC70 serves as control (CTRL). (C) Relative mRNA levels of *Lonp1* upon ATF5 knockdown in HEK293FT cells. (D-E) Relative mRNA levels of UPR^mt markers upon LONP1 knockdown in C2C12 cells. Bars represent mean ± S.E.M. (Student's t test, *p < 0.05; **p < 0.01; ***p < 0.001), (n=3).

3.2 Modelling UPR^(mt) signalling *in vivo*

3.2.1 Generation of tissue specific DARS2/CLPP double deficient mice

To decipher the *in vivo* role of CLPP under mitochondrial protein perturbations, CLPP was selectively deleted in DARS2-deficient heart and skeletal muscle using a muscle creatine kinase promoter driven Cre-recombinase (*Ckmm-Cre*). On the one hand, *Dars2* conditional gene targeting was conducted in the context of the International Knockout Mouse Consortium (KOMP) as previously reported (Dogan et al., 2014). On the other hand, conditional targeting of the *Clpp* gene was performed at Taconic Artemis (Germany), which was achieved by flanking the exons 3 to 5 with loxP sites, while also introducing a Frt flanked puromycin resistance (PuroR) selection marker into intron 5 (Figure 3.12). Upon successful germline transmission the resulting heterozygous $Clpp^{+/PuroR-L}$ mice were intercrossed to Flp deletor mice, removing the PuroR selection cassette. Eventually, mice were bred with Cre expressing animals that led to the knockout of exons 3 to 5, resulting in both the deletion of the protease domain as well as a frameshift from exon 2 to 6.
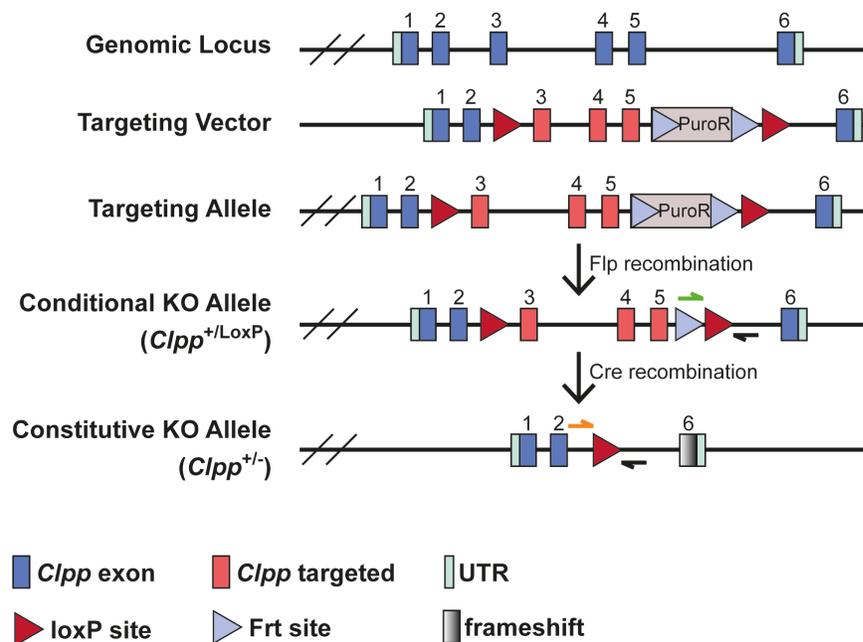
Figure 3.12: Targeting strategy for conditional disruption of the *Clpp* gene.
Puromycin resistance cassette was used as positive selection marker (PuroR). Arrows display the primers used for genotyping PCR; forward primer for loxP allele (green arrow); forward primer for KO allele (orange arrow) and shared reverse primer (black).

The resulting ClpP-floxed mice (*ClpP^{L/L}*) were then intercrossed with *Dars2*-floxed mice (*Dars2^{L/L}*) to generate double floxed animals (*Dars2^{L/L}; ClpP^{L/L}*). Subsequently, those animals were bred with mice expressing the *Ckmm-Cre* transgene to obtain triple transgenic mice (*Dars2^{+/L}; ClpP^{+/L}; Ckmm-Cre^{+/T}*). Double floxed mice (*Dars2^{L/L}; ClpP^{L/L}*) were crossed to triple transgenic animals (*Dars2^{+/L}; ClpP^{+/L}; Ckmm-Cre^{+/T}*) to generate wildtype (WT), ClpP KO (*Dars2^{+/L}, ClpP^{L/L}, Ckmm-Cre^{+/T}*), Dars2 KO (*Dars2^{L/L}, ClpP^{+/L}, Ckmm-Cre^{+/T}*) and DKO (*Dars2^{L/L}, ClpP^{L/L}, Ckmm-Cre^{+/T}*) mice (Figure 3.13). To minimize the overall mouse litter numbers, experiments were performed using ClpP KO and Dars2 KO that were heterozygous for *Dars2* and *ClpP*, respectively. However, additional control animals were obtained from the following matings: (i) Dars2-deficient animals - *Dars2^{+/L}, Ckmm-Cre^{+/T}* mated with *Dars2^{L/L}* and (ii) ClpP-deficient animals - *ClpP^{+/L}; Ckmm-Cre^{+/T}* mated with *ClpP^{L/L}*.
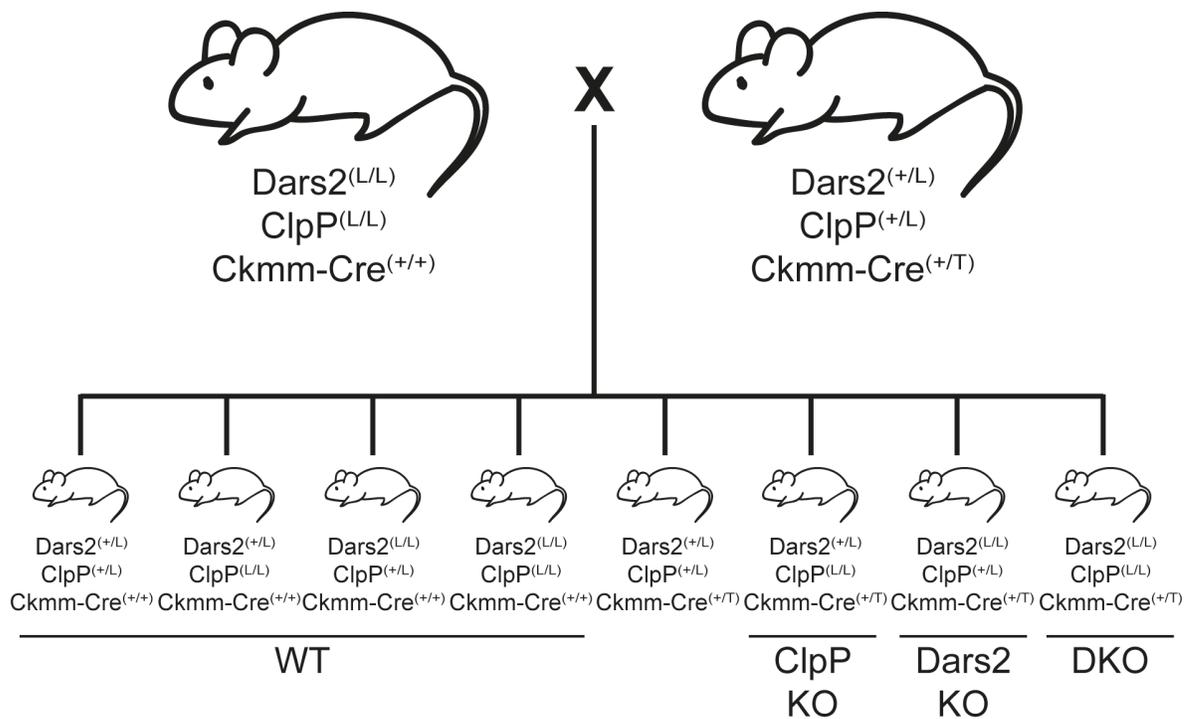
Figure 3.13: Breeding scheme to generate WT, ClpP KO, Dars2 KO and DKO animals.
Note that ClpP KO and Dars2 KO animals are heterozygous for *Dars2* and *ClpP*, respectively. Allele nomenclature: wild type (+), floxed (L) and transgene (T).

3.2.2 Phenotypic changes caused by DARS2 deficiency can be alleviated by the loss of CLPP

Tissue specific deletion in heart and skeletal muscle was mediated by the *Ckmm* promoter that triggers activation of Cre after embryonic day 15.5 (E15.5) (Lyons et al., 1991). It has been shown that DARS2 deletion in heart leads to a severe progressive cardiomyopathy starting at 3 weeks of age leading to the ultimate death of the animal at approx. 7 weeks of age (Dogan et al., 2014). Based on this observation, it was not very likely that additional knockout of a mitochondrial matrix protease would give rise to living animals. However, mice of all different genotypes were born at the expected Mendelian ratios (data not shown). Moreover, it turned out that DKO mice were not only born, but also significantly increased their lifespan of about 35%, from approx. 7 to 10 weeks of age (Figure 3.14A). In stark contrast, ClpP KO mice displayed no signs of lethality at that time and also did not appear to be compromised later (Figure 3.14A). To decipher the phenotype observed in DKO mice, all following experiments were conducted using 6-week-old mice. As described before Dars2 KO mice displayed a strong increase in heart size accompanied by a decrease of body weight (Figure 3.14B-H) (Dogan et al., 2014). Surprisingly, DKO heart morphology and weight revealed a significant reduction in heart size compared to Dars KO animals (Figures 3.14B-C, 3.14F). Additionally, DKOs exhibited normal body weight that was significantly elevated compared to Dars2 KO mice (Figures 3.14D, 3.14G). Expressed as heart-to-body weight ratios, a clear reduction could be observed at the level of cardiomyopathy in DKOs compared to Dars2 KOs (Figure 3.14E, 3.14H). Interestingly, a very mild, but significant increase in the heart-to-body weight ratio of ClpP KO could be found compared to WT animals, indicating a possible, low-level cardiac hypertrophy (Figure 3.14E). Since no phenotypical changes were observed in skeletal muscle due to loss of CLPP, neither in DARS2 nor in WT background, no further experiments were conducted in this respect (data not shown).
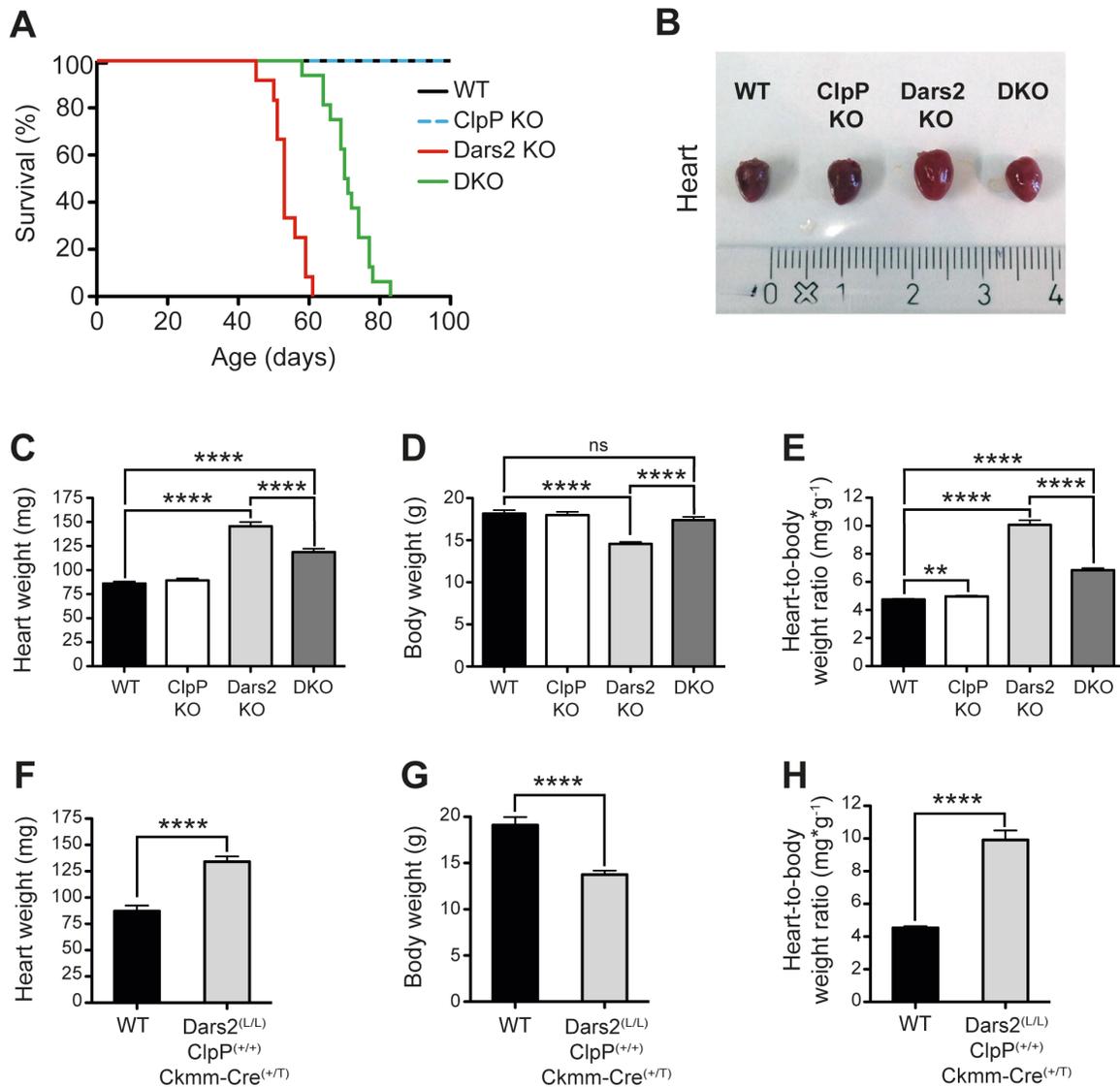
Figure 3.14: Lifespan analysis and phenotypic characterization of DKO mice.
(A) Kaplan-Meier survival curves for WT, ClpP KO, Dars2 KO and DKO (n = 12 - 16). Lifespan is significantly increased between DKO and Dars2 KO (ρ = 0,0000014679 (****)). Lifespan of ClpP KO animals are comparable to WT. (B) Heart gross morphology. (C) Heart weight; (D) Body weight and (E) Heart-to-body weight ratio of WT, ClpP KO, Dars2 KO and DKO (n = 28-40). (F-H) Heart weight (F), Body weight (G) and Heart-to-body weight ratio (H) of Dars2 KO mice that are homozygous for the *ClpP* allele (n = 10 - 14). Bars represent mean ± S.E.M. (Student's t test; **$p < 0.01$, ****$p < 0.0001$).

The observed milder phenotype in DKOs hearts compared to Dars2 KOs suggested an additional measurement of the expression levels of molecular hypertrophy markers in these hearts. The Natriuretic peptides B (*Nppb*) expression levels were significantly decreased upon CLPP depletion in DARS2-deficient animals, but still elevated compared to WT and ClpP KO (Figure 3.15A). *Nppa* levels did also display a trend

towards less expression in DKO, which was insignificant to WT and ClpP KO (Figure 3.15A). To further visualize the mitochondrial respiratory function in hearts sections, an enzyme histochemical double staining was performed for cytochrome c oxidase/succinate dehydrogenase (COX/SDH). Remarkably, COX/SDH staining demonstrated a strong increase in COX activity in DKO compared to Dars2 KO heart sections, which is in line with reduced interstitial fibrosis shown by Masson's trichrome staining (Figures 3.15B-C). In agreement with the previously reported increase in mitochondrial mass and hypertrophy in DARS2 deficient hearts (Dogan et al., 2014), a strong correlation could be found between the amount of SDH positive cells (blue staining) and the heart size as determined by the whole sections displayed (Figure 3.15B). Taken together, the data demonstrate that CLPP deficiency in the context of high mitochondrial stress, as detected in DARS2-deficient hearts, clearly alleviates mitochondrial cardiomyopathy and sustains animals healthier for a longer period of time.
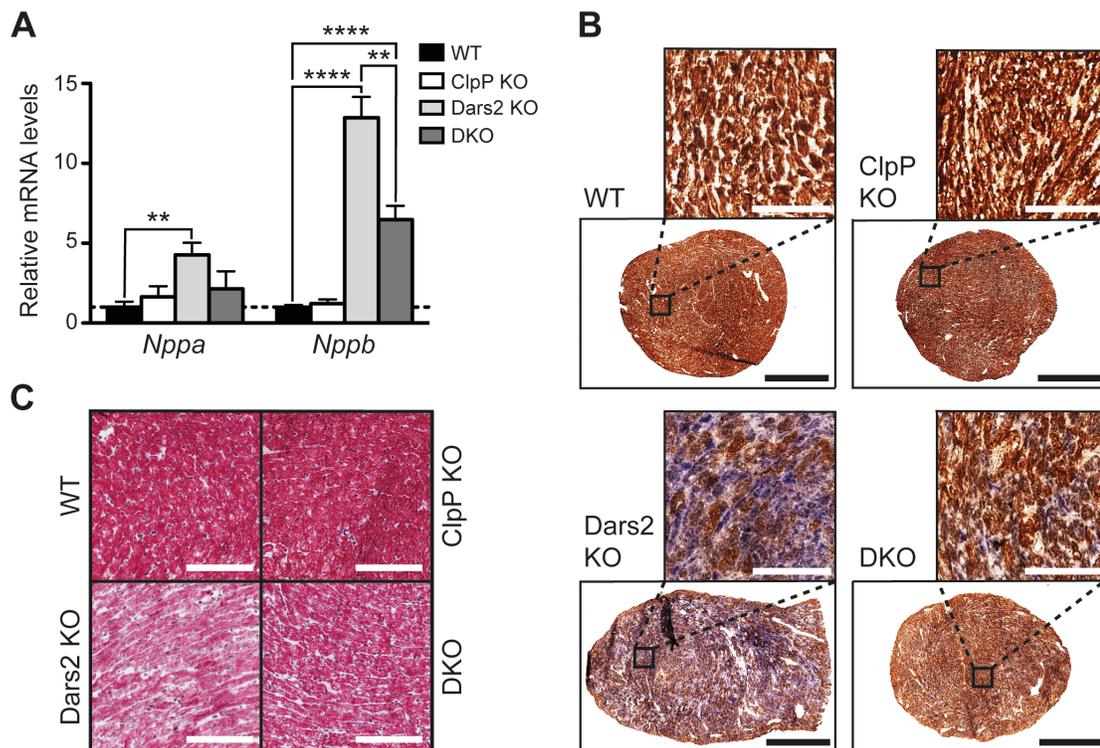
Figure 3.15: Molecular characterization and immunohistochemical analysis of mutant hearts.
(A) Relative expression levels of cardiac hypertrophy markers (*Nppa* and *Nppb*) (n = 5). Bars represent mean ± S.E.M. (Student's t test; **p < 0.01, ****p < 0.0001). (B) Enzyme histochemical double staining for COX and SDH activities. (n = 4). (C) Assessment of cardiac fibrosis by Masson's trichrome staining (n = 4). White scale bars, 100μm; black scale bars, 1 mm. Stainings were performed with Steffen Hermans.

3.2.3 Mitochondrial and cellular stress responses do not depend on CLPP under proteotoxic stress

A mouse model deficient for DARS2 and CLPP was created to elucidate the role of CLPP in UPR^{mt} signalling *in vivo*, since CLPP has been described to be a central player in mediating the UPR^{mt} response in *C. elegans* and to be activated upon mitochondrial protein perturbations in mammalian cells (Haynes et al., 2007; Zhao et al., 2002). Based on the observation that CLPP mitigates the strong cardiomyopathy in DARS2 deficient heart, the question how loss of CLPP could actually be beneficial for the animal was investigated if needed for the UPR^{mt} activation. Initially, the levels of mitochondrial chaperones and proteases were examined that are commonly used as markers to show activation of UPR^{mt} signalling. The mitochondrial chaperones mtHSP70 and TRAP1 were clearly elevated on protein level in both Dars2 KO and DKO hearts, while HSP60 was only slightly increased (Figures 3.16A-B). Interestingly, CLPP deficiency itself induced mitochondrial protein perturbations as observed by an activation of the mitochondrial chaperones mtHSP70 and TRAP1 (Figures 3.16A-B). In contrast, the mitochondrial proteases, LONP1 and AFG3L2 were only found activated in Dars2 KO and DKO hearts (Figures 3.16A-B). Since Dars2 and ClpP KO animals were heterozygous for the *Clpp* and *Dars2* allele, respectively, the UPR^{mt} marker levels were also assessed in their single mutant counterparts. Nevertheless, similar changes of mitochondrial chaperones and proteases were observed in hearts of both genotypes (Figure 3.16C-D). To explore whether a mitochondrial biogenesis effect causes the upregulation of chaperones and proteases, the steady state levels of all UPR^{mt} markers were assessed in isolated mitochondria. Here, similar levels of the UPR^{mt} markers could be found in both whole tissue lysate and isolated mitochondria (Figure 3.16A-B). On the one hand, the mitochondrial biogenesis marker TFAM (mitochondrial transcription factor A) (Virbasius and Scarpulla, 1994) was decreased in ClpP KO and DKO mitochondria, although being unchanged in whole tissue lysates (Figure 3.16E, and data not shown). On the other hand, DARS2 depletion in the heart itself increased mitochondrial biogenesis to compensate for the respiratory chain deficiency as previously described (Figure 3.16E) (Dogan et al., 2014). A hallmark of UPR^{mt} activation is the increase in transcript levels of mitochondrial chaperones and proteases, which is also present in Dars2 KO and DKO hearts, as shown by increased *mtHsp70*, *Lonp1* and *Afg3l2* mRNA levels (Figure 3.16F). In

contrast, *Hsp60* mRNA levels were not elevated in any condition, corresponding to the very slight increase in the steady-state protein levels (Figures 3.16A, 3.16F). Taken together, the results clearly demonstrate that the activation of the mammalian UPR^{mt} *in vivo* does not depend on CLPP.
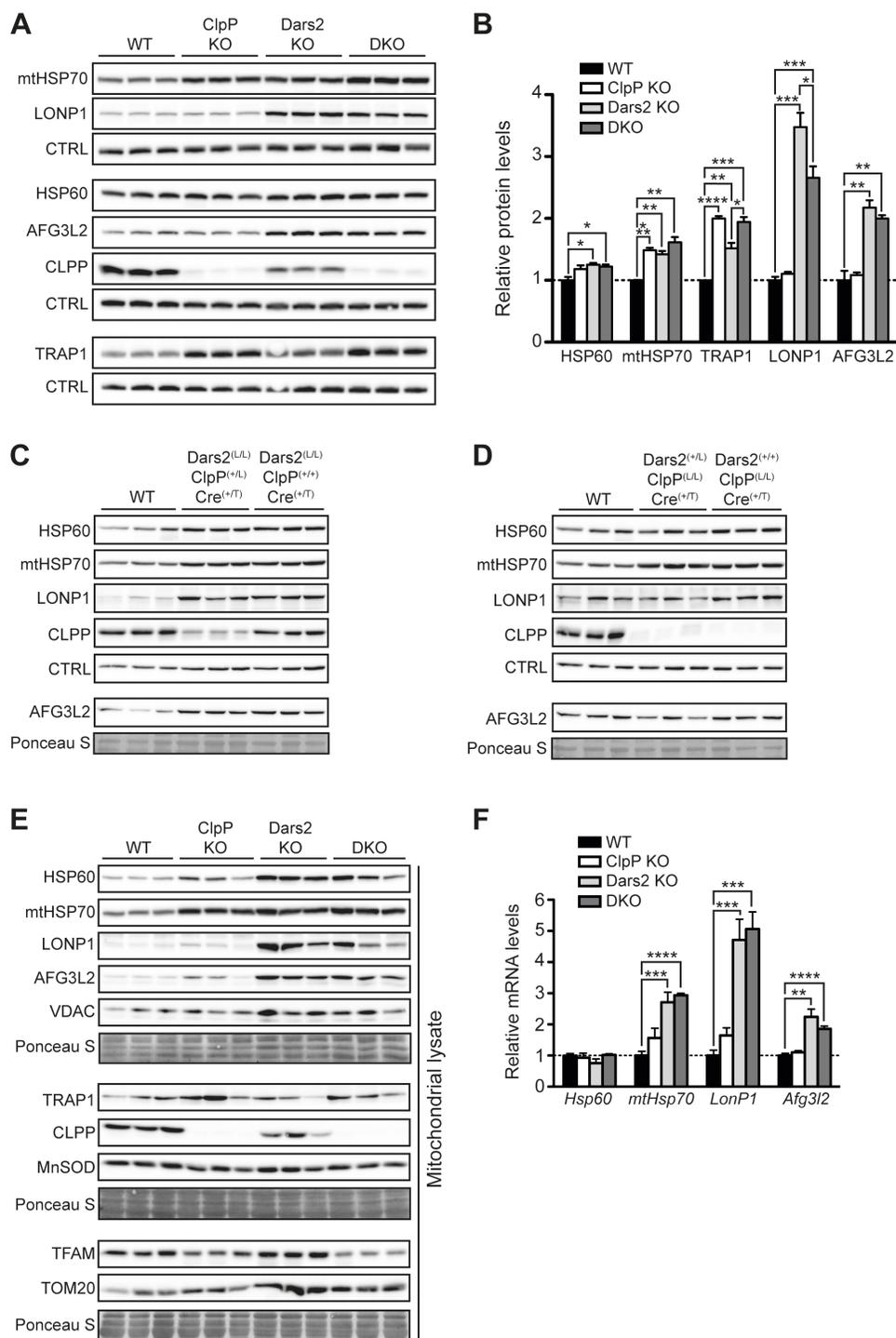
Figure 3.16: UPR^{mt} markers do not depend on CLPP under proteotoxic stress.

Figure 3.16: UPR^{mt} markers do not depend on CLPP under proteotoxic stress.

(A) Western blot analysis and (B) Relative quantification of UPR^{mt} markers in heart extracts. HSC70 is used as a loading control (CTRL), (n = 3). (C and D) Western blot analysis of UPR^{mt} markers in (C) Dars2 KO with heterozygous vs. homozygous ClpP background and in (D) ClpP KO with heterozygous vs. homozygous Dars2 background. HSC70 and PonceauS staining serve as loading controls. (E) Western blot analysis of mitochondrial chaperones, proteases and maintenance markers in isolated heart mitochondria. PonceauS staining serve as loading control. (F) Relative expression levels of UPR^{mt} markers in heart extracts (n = 5). Bars represent mean ± S.E.M. (Student's t test, *p < 0.05, **p < 0.01, ***p < 0.001, ****p < 0.0001).

It is known that mitochondrial dysfunction also comprises cellular function, which causes cellular stress responses such as autophagy or the integrated stress response (ISR) to be affected in response to mitochondrial stress aimed at restoring homeostasis (Dogan et al., 2014; Evstafieva et al., 2014; Marzetti et al., 2013). Since DARS2 deficiency has been shown to influence both autophagy and the ISR (Dogan et al., 2014), it was examined whether the loss of CLPP has any impact on these cellular stress responses. On the one hand, inhibition of autophagy is characterized by accumulation of p62, which was present in both Dars2 KO and DKO, but not in WT and ClpP KO hearts (Figures 3.17A-B). On the other hand, ISR activation is defined by induction of the activating transcription factor 4 (ATF4) upon phosphorylation of the α subunit of the eukaryotic initiation factor 2 (eIF2α) that was observed in DARS2 deficient hearts and not compromised by the loss of CLPP (Figures 3.17A-B, 3.17C). In addition, the expression levels of the transcription factors *Chop* and *Atf5* (potential mammalian homolog of *C. elegans* ATFS-1) that are implicated in the activation of the UPR^{mt} signalling (Horibe and Hoogenraad, 2007; Nargund et al., 2012) were greatly increased in DKO and Dars2 KO hearts, showing that loss of CLPP does not impair UPR^{mt} signalling in mammals (Figure 3.17C). Interestingly, using heart extracts, no clear pattern of up- or downregulation of ATF5 could be found on the protein level (Figure 3.17D). However, using isolated mitochondria, it was observed that (i) ATF5 was clearly localized to mitochondria and (ii) ATF5 levels within mitochondria negatively correlate to the level of chaperones and/or proteases, hence the stress inside mitochondria (Figure 3.17D). Thus, these data suggest a similar mechanism of ATF5 in mammals to ATFS-1 in *C. elegans*, where the level of mitochondrial stress is sensed via the import efficiency of ATFS-1 (Nargund et al., 2012). The fibroblast growth factor 21 (FGF21) was recently found to be a stress sensor that serves as a "mitokine" upon mitochondrial dysfunction

(Tyynismaa et al., 2010). Loss of DARS2 in the heart also leads to a huge upregulation of *Fgf21* mRNA levels (Dogan et al., 2014) that was again not altered upon deletion of CLPP (Figure 3.17E). In conclusion, the overall data show that both mitochondrial and cellular stress responses are not affected by loss of CLPP in mammals.
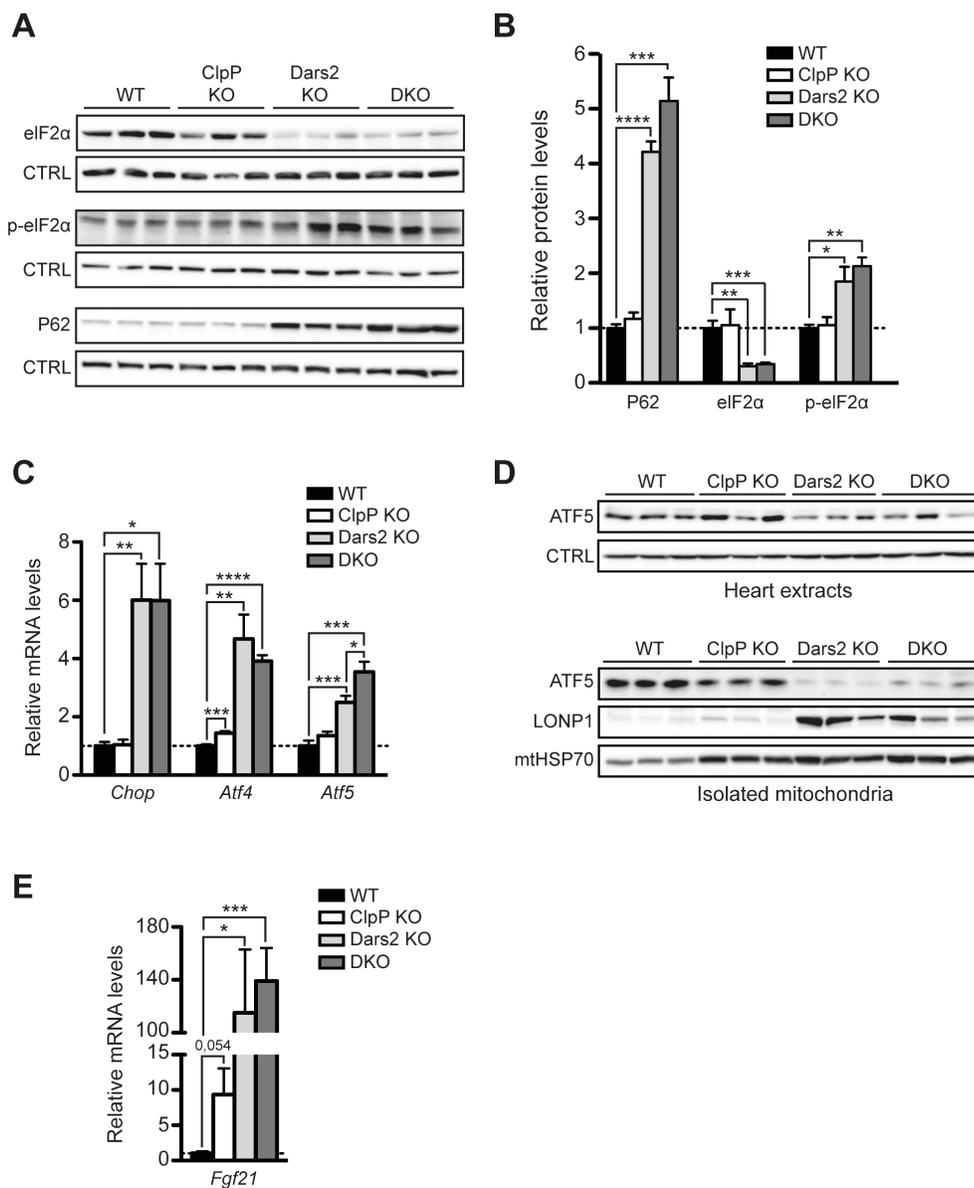
Figure 3.17: Cellular stress markers do not depend on CLPP.
(A) Western blot analysis and (B) Relative quantification of cellular stress markers in heart extracts. HSC70 is used as a loading control (CTRL), (n = 3). (C) Relative expression of transcription factors involved in UPR[mt] and ISR in heart extracts (n = 5). (D) Western blot analysis of ATF5 levels in heart extracts (upper) and isolated mitochondria (lower). HSC70 serves as loading control (CTRL, upper), while relative levels of LONP1 and mtHSP70 are shown with respect to isolated mitochondria (lower). (E) Relative expression of *Fgf21* in heart extracts (n = 5). Bars represent mean ± S.E.M. (Student's t test, *p < 0.05, **p < 0.01, ***p < 0.001, ****p < 0.0001).

3.2.4 Loss of CLPP in DARS2-deficient heart mitochondria increases mitochondrial respiratory activity

Since DKO animals live longer and show less signs of cardiac dysfunction compared to Dars2 KOs (Figure 3.14, 3.15), it was investigated whether the mitochondrial respiratory activity was also improved in these mice. First, the steady-state levels of individual OXPHOS subunits were examined to allocate potential improvements upon loss of CLPP. Remarkably, a general correction in the steady-state levels of individual complex I, III and IV subunits in DKO compared to Dars2 KO hearts was observed, including the mtDNA-encoded complex IV subunit COXI/MT-CO1 (Figure 3.18A). It seems reasonable that the increased availability of mtDNA-encoded subunits impacts the levels of C I, C III and C IV nDNA-encoded subunits since both sets of proteins need to be assembled in correct stoichiometry, as it was found before in the mtDNA mutator mouse (Edgar et al., 2009). Nevertheless, complex II (SDHA) and complex V (ATP5A1) subunits were stably expressed in all mutants analyzed, hence not influenced by the loss of CLPP or DARS2 (Figure 3.18A). Next, the levels of complexes by BN-PAGE and subsequent Western Blot analysis were determined using different antibodies against individual OXPHOS subunits. As previously described, Dars2 KO animals exhibit a strong reduction of complex I, III, IV levels in the heart, while complex V is not affected (Dogan et al., 2014). Lack of ClpP in the DARS2-deficient hearts increased the levels of complex I and IV, while having a minor effect on the amount of other OXPHOS complexes (Figures 3.18B, 3.18C and 3.18D). Interestingly, in ClpP KOs a slight increase in complex III levels was found, but no change for the other complexes (Figure 3.18B).
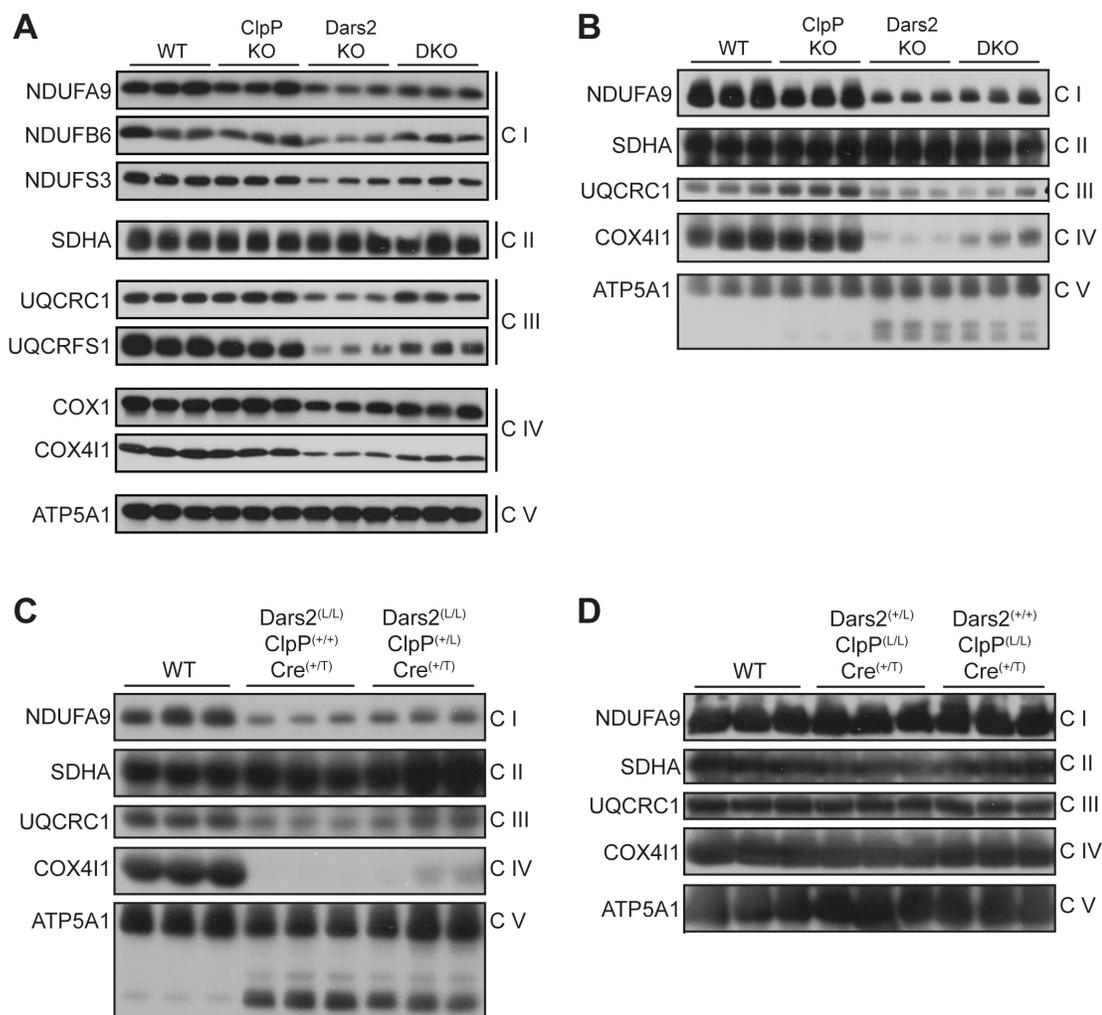
Figure 3.18: Lack of CLPP in DARS2-deficienct hearts corrects mitochondrial OXPHOS complex levels.
(A) Western blot analysis of individual OXPHOS subunits in isolated mitochondria. (B) BN-PAGE and subsequent Western blot analysis for OXPHOS complexes in isolated mitochondria. (C and D) BN-PAGE and subsequent Western blot analysis of OXPHOS complexes in isolated mitochondria: (C) Dars2 KO with heterozygous vs. homozygous ClpP background and (D) ClpP KO with heterozygous vs. homozygous Dars2 background. Antibodies against individual OXPHOS subunits (on the left) were used to detect OXPHOS complexes (on the right). Experiments were performed with Katharina Senft.

Having found an increase of complex levels in DKOs, it was examined whether the activity of these complexes is also elevated. Here, in-gel activity assays were performed for complex I and IV. Collectively, both assays showed higher activities in DKO compared to Dars2 KO, showing that loss of ClpP not only increases the level of individual complexes, but also their activity in a state of disrupted mitochondrial proteostasis (Figures

3.19A and 3.19B, respectively). Thereafter, the analysis of the bioenergetic consequences of the increased complex I and complex IV activity was continued by assessing the mitochondrial respiratory capacity in freshly isolated cardiac mitochondria using a high-resolution respirometer (Figure 3.19C). Therefore, mitochondria were incubated with a physiological substrate combination feeding electrons into complex I (pyruvate, glutamate, malate) or II (succinate) and recorded the oxygen consumption rate in the phosphorylating (state 3: ADP and Pi), non-phosphorylating (state 4: oligomycin) and uncoupled state (FCCP) using a SUIT protocol (Lemieux et al., 2011). Respiration (state 3: ADP and Pi) through complex I significantly improved in DKO compared to Dars2 KO (Figure 3.19C). Furthermore, combined respiration, feeding electrons though complex I and II simultaneously, was almost significantly elevated ($\varrho = 0{,}053$) (Figure 3.19C). However, respiration in DKOs still remained lower than in WT (Figure 3.19C). Non-phosphorylating (state 4: oligomycin) respiration as well as electron transfer system (ETS) capacity (uncoupled state: FCCP) did not improve in DKO compared to Dars2 KO (Figure 3.19C). Taken together, the overall respiratory capacity was improved in DARS2-deficient mice when CLPP was missing.
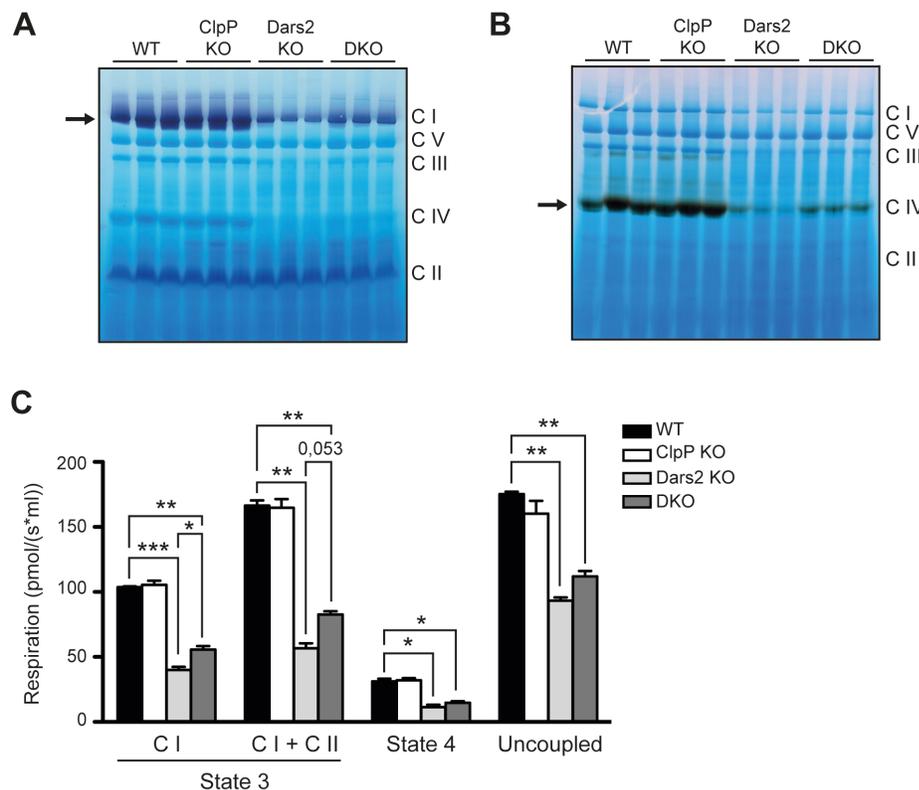
Figure 3.19: Lack of CLPP in DARS2-deficienct hearts increases mitochondrial respiratory activity.

Figure 3.19: Lack of CLPP in DARS2-deficienct hearts increases mitochondrial respiratory activity.
(A and B) *In gel* activity of complexes I (A) and IV (B) performed after BN-PAGE. (C) Oxygen consumption rates in intact heart mitochondria in the presence of pyruvate-glutamate-malate (C I) and pyruvate-glutamate-malate + succinate (C I + C II) as substrates. State 3 (substrates+ADP); State 4 (+oligomycin); Uncoupled (+FCCP). (n = 3). Bars represent mean ± S.E.M. (Student's t test, *p < 0.05, **p < 0.01, ***p < 0.001). Experiments were performed with Katharina Senft and Christina Becker.

3.2.5 Label-free mass spectrometric analysis of the mitochondrial proteome reveals a partial correction of the DARS2 phenotype upon loss of CLPP

Mass spectrometric analysis of the mitochondrial proteome was performed to establish a quantitative map of mitochondrial protein abundance to further understand the impact of loss of CLPP on DARS2-deficient mitochondria (carried out together with Hendrik Nolte, CECAD Proteomics Facility, Cologne). To do so, quantitative proteomics of mouse heart mitochondria were performed using a label-free approach. It was possible to quantify 483 of approx. 1000 annotated mitochondrial proteins in the mitochondrial fraction of all mutants analysed. The low coverage observed was due to (i) low resolution of the mass spectrometric device as well as (ii) the fact that only proteins that had been quantified in at least two samples out of three were used for comparative analysis. The following analysis mainly focused on respiratory chain subunits, proteins involved into mitochondrial translation as well as proteins, which are part of the protein quality control, processing or transport, since these processes were key to the previously described phenotypes. In ClpP KO mitochondria significant changes of only 18 quantified proteins were found, which is in line with our previous findings that ClpP KO mitochondria are phenotypically close to WT mitochondria (Figure 3.20A and Table 3.2). However, an increase of mitochondrial chaperones TRAP1, HSPA9 and GRPEL1 was found as well, which is consistent with previous findings (Figure 3.16). The complex I subunit NDUFA11, shown to be involved in assembly of the complex I membrane arm (Andrews et al., 2013), was highly downregulated upon loss of CLPP. On the other hand, MTIF2, an essential component for mitochondrial translation initiation, was upregulated upon CLPP deletion (Figure 3.20A and Table 3.2). Proteomic changes upon DARS2 deletion were more dramatic with respect to mitochondrial-encoded as well as nuclear encoded subunits

of the respiratory chain (Figure 3.20B and Table 3.2). All the subunits quantified were highly reduced upon DARS2 depletion. Both the amount of subunits affected as well as the decreasing fold change could be alleviated by the loss of CLPP (Figures 3.20B, 3.21A and Table 3.2). Similarly, direct correlation of protein abundance between DKO and Dars2 KO mitochondria revealed a strong increase of mitochondrial as well as nuclear encoded subunits in DKO mitochondria (Figure 3.22 and Table 3.3). Although the abundance of most OXPHOS subunits still remained lower in DKO compared to WT, some were also found to be insignificant, showing a partial correction of the respiratory defects in DKO mitochondria (Figures 3.21A and 3.22; Table 3.2 and 3.3). By the use of a scatter plot, a general trend of proteins that migrate towards WT levels when comparing Dars2 KO to DKO mitochondria could be found (Figure 3.21B, green area). Furthermore, it was observed that components of the large mitoribosomal subunits were highly enriched in both Dars2 KO as well as DKO mitochondria, most likely as a compensatory mechanism for the strong translational defect caused by DARS2 deficiency (Figures 3.20B and 3.21A; Table 3.2). Interestingly, there was also a fraction of large mitoribosomal subunits that was upregulated either in Dars2 KO or DKO mitochondria, showing that both translational machineries differ from each other with respect to the large mitoribosomal subunit (Table 3.2). Mitochondrial UPR^{mt} markers such as HSPE1 and LONP1 were elevated in both Dars2 KO and DKO mitochondria (Figures 3.20B and 3.21A; Table 3.2). In addition, HSPA9 and GREPEL1 were found to be upregulated in both ClpP KO and Dars2 KO and to have an additive effect in DKO (Figure 3.21A and Table 3.2). The major UPR^{mt} chaperone Hsp60 was found to be slightly elevated (log$_2$ fold change: 0.74) in DARS2 deficient mice only, which further supports the hypothesis that it is a rather stable protein not very suitable for the UPR^{mt} readout. Interestingly, the chaperone DNAJA33 was highly elevated exclusively in DKO mitochondria (log$_2$ fold change: 3.37). As expected, all these changes were similar to what was found earlier using western blot analysis and realtime PCR (Figure 3.16). Taken together, mitochondrial proteomic analysis revealed a partial correction of the OXPHOS defects in DKO mitochondria and further supports the idea that mitochondrial stress responses are regulated independent of CLPP.
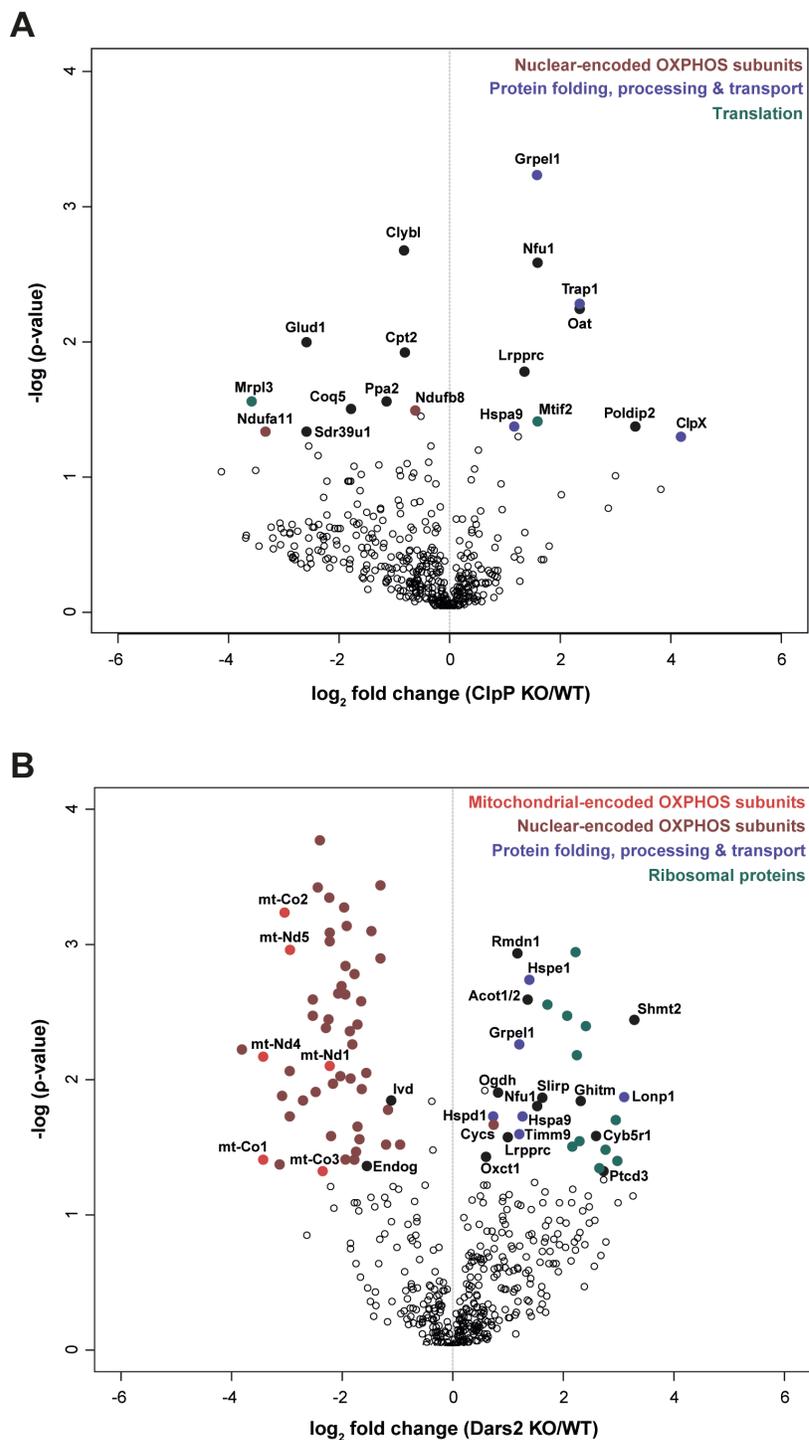
Figure 3.20: Quantitative assessment of proteomes of purified mitochondria (1).
Proteins are ranked in a volcano plot according to their statistical ρ-value (y-axis) and their relative abundance ratio (log_2 fold change) between (A) ClpP KO and WT or (B) Dars2 KO and WT. Highlighted dots represent both a high fold change (log_2 fold change: ±0,5849 corresponds to a fold change of ±1.5) as well as high statistical significance (-log ρ-value: >1.3 corresponds to a ρ-value: <0.05).
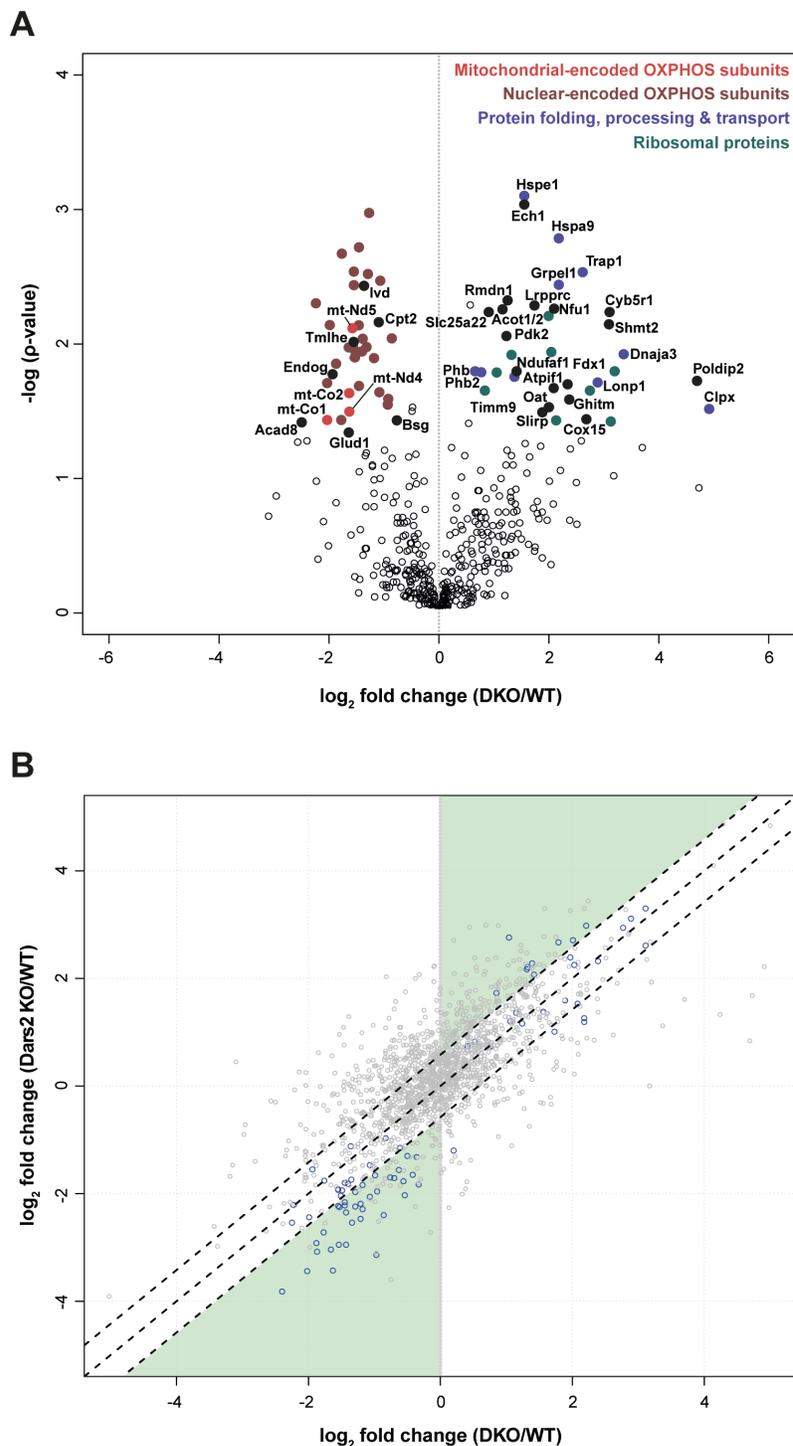
Figure 3.21: Quantitative assessment of proteomes of purified mitochondria (2).
(A) Proteins are ranked in a volcano plot according to their statistical ρ-value (y-axis) and their relative abundance ratio ($\log_2$ fold change) between DKO and WT. Highlighted dots are represented as in Figure 3.21. (B) Scatter plot of $\log_2$ fold changes of DKO to WT versus $\log_2$ fold changes of Dars2 KO to WT. Blue circles display a high statistical significance (-log ρ-value: >1.3 corresponds to a ρ-value: <0.05), whereas dashed lines represent the $\log_2$ fold change thresholds of ±0,5849 that corresponds to a fold change of ±1.5. The green area displays the partial convergence of DKOs towards WT compared to Dars2 KO.

96

Table 3.2: Relative protein changes determined by quantitative proteomics.

Proteins are clustered according to their changes that occurred only in a single mutant (left table) or to those that appeared in multiple mutants (right table). Values are calculated relative to WT. All proteins listed have a fold change cut-off ≥1.5 and $p<0.05$ (log$_2$ fold change: ≈ ±0,58 and -log ρ-value: >1.3).

Gene Name	ClpP KO p-Value	ClpP KO log2 fold change	Dars2 KO p-Value	Dars2 KO log2 fold change	DKO p-Value	DKO log2 fold change
Ndufa11	1.34	-3.36				
Sdr39u1	1.34	-2.57				
Coq5	1.51	-1.79				
Ppa2	1.56	-1.15				
Clybl	2.67	-0.84				
Mtif2	1.41	1.60				
Cox7c			2.22	-3.82		
Cox6a2			1.89	-3.08		
Ndufb2			2.59	-2.54		
Cox6c			1.91	-2.47		
mt-Co3			1.32	-2.35		
Cox5b			2.39	-2.29		
mt-Nd1			2.10	-2.21		
Ndufa9			1.59	-2.19		
Ndufa6			2.69	-2.03		
Uqcrc2			2.01	-1.83		
Ndufs5			1.41	-1.80		
Uqcrc1			2.78	-1.77		
Ndufa8			1.66	-1.71		
Uqcrfs1			1.56	-1.70		
Cox5a			2.58	-1.66		
Uqcrb			1.93	-1.65		
Ndufs6			2.05	-1.56		
Ndufa3			2.90	-1.32		
Ndufb5			3.44	-1.30		
Ndufab1			1.53	-1.20		
Ndufs7			1.78	-1.15		
Ndufb11			1.52	-0.97		
Oxct1			1.43	0.60		
Cycs			1.68	0.74		
Hspd1			1.72	0.74		
Ogdh			1.91	0.82		
Mrpl38			1.50	2.17		
Mrpl20			1.34	2.67		
Ptcd3			1.33	2.71		
Mrpl11			1.48	2.76		
Mrpl22			1.40	2.98		
Acad8					1.41	-2.50
Ndufa4					1.71	-2.03
Tmlhe					1.97	-1.62
Bsg					1.43	-0.75
Phb					1.80	0.66
Phb2					1.79	0.77
Slc25a22					2.23	0.90
Cisd1					1.34	1.11
Pdk2					2.07	1.24
Ndufaf1					1.77	1.38
Ech1					3.05	1.56
Atpif1					1.67	2.09
Mrpl4					1.43	2.12
Fdx1					1.70	2.33
Cox15					1.44	2.70
Mrpl1					1.43	3.13
Mrpl44					1.80	3.20
Dnaja3					1.92	3.37

Gene Name	ClpP KO p-Value	ClpP KO log2 fold change	Dars2 KO p-Value	Dars2 KO log2 fold change	DKO p-Value	DKO log2 fold change
Glud1	1.99	-2.57			1.34	-1.64
Cpt2	1.92	-0.81			2.17	-1.09
Oat	2.24	2.33			1.53	2.03
Trap1	2.26	2.33			2.53	2.62
Poldip2	1.37	3.36			1.73	4.69
Clpx	1.30	4.17			1.52	4.91
mt-Co1			1.41	-3.44	1.44	-2.02
mt-Nd4			2.17	-3.43	1.49	-1.63
Ndufb4			1.37	-3.14	1.56	-0.97
mt-Co2			3.24	-3.04	1.64	-1.66
mt-Nd5			2.96	-2.95	2.02	-1.54
Cox7a1			2.06	-2.95	1.95	-1.43
Cox6b1			1.73	-2.92	1.85	-1.88
Ndufb7			1.84	-2.72	2.67	-1.77
Ndufb9			3.42	-2.44	2.14	-1.99
Ndufa13			3.76	-2.40	2.04	-0.86
Ndufs1			2.44	-2.25	2.12	-1.53
Cox7a2			3.35	-2.24	2.97	-1.29
Ndufv1			3.03	-2.23	2.44	-1.55
Ndufa10			3.09	-2.22	2.72	-1.45
Ndufa5			1.98	-2.16	1.69	-1.45
Cox4i1			2.64	-2.06	1.64	-1.07
Ndufb6			2.02	-2.04	1.96	-1.51
Ndufa12			2.63	-1.97	2.52	-1.29
Ndufa2			3.28	-1.96	1.56	-0.96
Ndufv2			2.85	-1.94	2.13	-1.49
Ndufs4			1.41	-1.93	2.54	-1.55
Ndufs3			3.14	-1.92	1.91	-1.55
Ndufb3			2.37	-1.84	1.90	-1.18
Ndufs2			2.27	-1.82	2.03	-1.40
Ndufs8			1.46	-1.76	1.44	-1.76
Ndufb10			2.40	-1.74	1.96	-1.35
Endog			1.36	-1.55	1.78	-1.94
Ndufc2			3.10	-1.47	2.47	-1.07
Ivd			1.84	-1.12	2.43	-1.36
Rmdn1			2.94	1.16	2.32	1.24
Timm9			1.60	1.20	1.79	1.06
Acot			2.59	1.36	2.26	1.15
Hspe1			2.74	1.38	3.09	1.56
Slirp			1.86	1.59	1.50	1.89
Mrpl49			2.56	1.73	1.65	0.85
Mrps34			2.47	2.07	1.79	1.42
Mrpl16			2.95	2.21	1.92	1.32
Mrpl41			2.19	2.25	1.93	2.03
Ghitm			1.85	2.32	1.59	2.39
Mrpl15			2.40	2.39	2.21	1.97
Cyb5r1			1.59	2.61	2.23	3.11
Mrpl46			1.70	2.94	1.65	2.77
Lonp1			1.87	3.11	1.72	2.89
Shmt2			2.45	3.30	2.15	3.11
Ndufb8	1.48	-0.60	2.48	-2.54	2.30	-2.25
Hspa9	1.37	1.16	1.73	1.26	2.79	2.18
Lrpprc	1.78	1.36	1.58	1.01	2.29	1.73
Grpel1	3.24	1.58	2.27	1.19	2.45	2.18
Nfu1	2.59	1.59	1.81	1.53	2.26	2.08

log$_2$ fold change

- mt-encoded subunits
- nuc-encoded subunits
- Translation
- Protein handling

log$_2$ fold change
< -2.2
-1.5 to -2.2
-1 to -1.5
-0.58 to -1
+ 1 to +0.58
+1.5 to +1
+2.2 to +1.5
> +2.2

Table 3.3: Proteins rescued in Dars2 KO mitochondria due to the lack of CLPP.
Proteins that changed significantly in DKO compared to Dars2 KO (left table), in contrast to proteins that are normalized in DKO that were changed before in Dars2 KO (right table). Fold change and cut-off see table 3.2.

	DKO/Dars2 KO	
	p-Value	log2 fold change
Glud1	1.91	-2.20
Cbr4	1.50	-1.47
Suclg2	1.35	-1.36
Cpt2	2.31	-1.21
Aldh5a1	1.88	-1.13
Mrpl16	1.43	-0.89
Mrpl49	1.32	-0.87
Mrpl22	1.35	-0.78
Mrps34	1.84	-0.64
Lrpprc	1.66	0.73
Ndufa10	1.37	0.77
Hspa9	1.76	0.91
Cox7a2	1.57	0.96
Ndufa3	1.32	0.96
Ndufa2	1.50	1.00
Uqcrc1	1.63	1.21
Uqcrb	1.40	1.23
Pdk2	1.73	1.35
mt-Co2	1.49	1.38
Ndufab1	1.53	1.40
mt-Nd5	2.13	1.42
Fdx1	1.45	1.48
Ndufa6	1.98	1.50
Uqcrc2	1.77	1.50
Ndufa13	3.48	1.54
Trap1	2.12	1.66
mt-Nd4	1.42	1.80
Ech1	3.03	1.88
Uqcr10	1.41	2.19
Clpx	2.93	2.69
Poldip2	1.64	3.85

	Dars2 KO/WT		DKO/Dars 2 KO		DKO/WT	
	p-Value	log2 fold change	p-Value	log2 fold change	p-Value	log2 fold change
Ndufa6	2.69	-2.03	1.98	1.50	0.94	-0.54
Uqcrc2	2.01	-1.83	1.77	1.50	0.30	-0.33
Uqcrc1	2.78	-1.77	1.63	1.21	0.81	-0.56
Uqcrb	1.93	-1.65	1.40	1.23	1.18	-0.42
Ndufa3	2.90	-1.32	1.32	0.96	0.44	-0.36
Ndufab1	1.53	-1.20	1.53	1.40	0.19	0.20
Mrpl22	1.40	2.98	1.35	-0.78	1.06	2.21

	log2 fold change
mt-encoded subunits	< -2.2
	-1.5 to -2.2
	-1 to -1.5
nuc-encoded subunits	-0.58 to -1
	+ 1 to +0.58
Translation	+1.5 to +1
	+2.2 to +1.5
Protein handling	> +2.2

Figure 3.22: Quantitative assessment of proteomes of purified mitochondria (3).
Proteins are ranked in a volcano plot according to their statistical ρ-value (y-axis) and their relative abundance ratio ($\log_2$ fold change) between DKO and Dars2 KO. Highlighted dots are represented as in Figure 3.21.

3.2.6 Dysregulation of mitochondrial protein synthesis is partially rescued by the loss of CLPP

Since the mitochondrial respiratory capacity was improved in DKOs compared to Dars2 KO mice, it was examined how the loss of CLPP could actually increase the levels of functionally active OXPHOS complexes. Based on the fact that loss of DARS2 first of all disrupts mitochondrial translation, the rates of protein synthesis and degradation in isolated cardiac mitochondria were analysed. Therefore, an *in organello* translation assay was performed using radioactive methionine (^{35}S-met) to label newly produced OXPHOS polypeptides (pulse) as well as to be able to follow their degradation over time (chase). The analysis displayed that the overall protein synthesis is strongly reduced when CLPP is absent, which is further supported by a clear reduction in the protein synthesis rate in CLPP deficient animals as determined by a time course pulse labeling (Figures 3.23 and 3.24A). Quantification of the whole range of proteins (overall rate) relative to WT showed that CLPP deficiency leads to a 25% decrease in mitochondrial translation both in DARS2-deficient as well as in WT background (Figures 3.23A, 3.23B and 3.24A). This effect was not caused by a general reduction in the levels of mitochondrial transcripts, since CLPP deficiency mainly elevates steady state levels of mitochondrial mRNAs (Figure 3.24B). Moreover, it was found that newly produced polypeptides are faster degraded in Dars2 KO and DKO mitochondria (Figures 3.23A-B), which is presumably caused by the higher levels of mitochondrial proteases available upon proteotoxic stress (Figure 3.16A-B). Remarkably, an overall increase in the amounts of individual OXPHOS subunits synthetized in DKO mitochondria was observed compared to Dars2 KO, although protein synthesis rate was reduced upon loss of CLPP (Figure 3.24C). Here, a profound upregulation was detected in the generation of cytochrome c oxidase I (COX1), NADH dehydrogenase subunit 6 (ND6), cytochrome b (CYTB) and ATP synthase F0 subunit 6 (ATP6) (Figure 3.24C). It could further be demonstrated that this effect was not caused by any residual DARS2 presence, since no protein was detected in either Dars2 KO or DKO heart extracts (Figure 3.24D). Instead, it became evident that loss of CLPP in in DARS2-deficient mitochondria leads to a substantial increase in the proficient versus abortive protein synthesis (Figures 3.23A and 3.24E). As DARS2 deficiency leads to abortion of mitochondrial protein synthesis, nearly 50 % of all newly synthetized OXPHOS subunits

exhibit low molecular mass, whereas in DKOs, the abortive translation is significantly decreased and accompanied by a raise in the synthesis rate of full-length OXPHOS subunits (Figures 3.23A and 3.24E). In contrast, ClpP KO mitochondria show no signs of aborted protein synthesis, since only ATP8/ND4L polypeptides were found in the low molecular weight fraction, suggesting that CLPP deficiency itself does not dysregulate mitochondrial protein synthesis, despite the reduction of the overall rate of translation (Figures 3.23A and 3.24E). Interestingly, full-length polypeptides generated in DKO mitochondria exhibit increased turnover rates, implicating that these OXPHOS subunits are more prone to degradation, although synthesized in higher amounts compared to Dars2 KOs (Figure 3.24F). Taken together, lack of CLPP in DARS2-deficients hearts leads to a partial rescue of translation, by increasing proficient protein synthesis and reducing abortive protein synthesis.
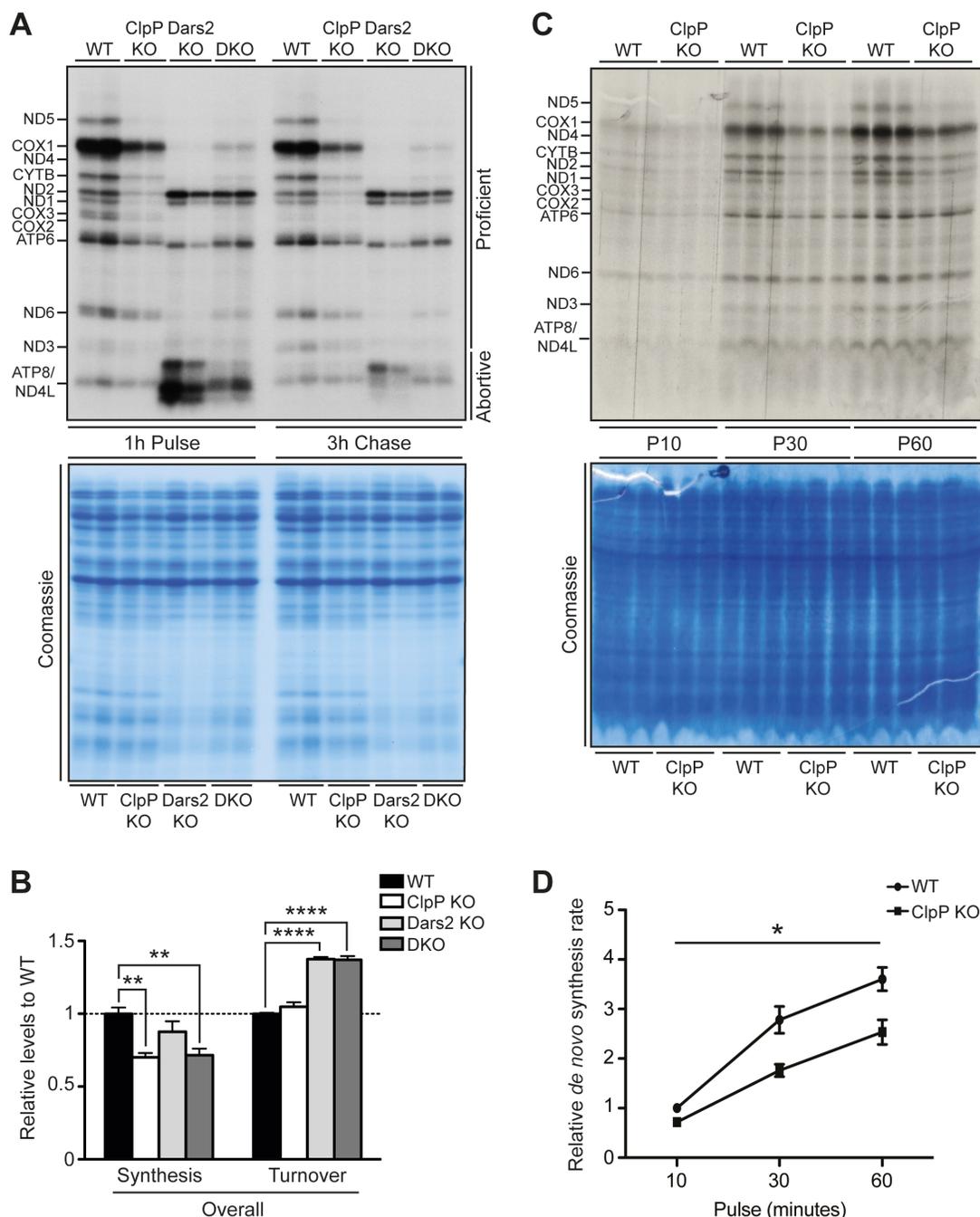
Figure 3.23: Dysregulation of mitochondrial translation can be partially rescued be the loss of CLPP (1).
(A-B) Representative gel of the *in organello* translation analysis of heart mitochondria (A) and corresponding relative overall protein synthesis and turnover rate (B). *De novo* synthetized proteins are isolated after labelling with ^{35}S-met (1 hour Pulse) or after cold chase (3h Chase). Positions of individual proteins are indicated on the left. Position of full-length proteins (Proficient) and low molecular weight polypeptides (Abortive) are indicated on the right. Note that in WT and ClpP KO low molecular weight polypeptides include ATP8/ND4L proteins. (C-D) Mitochondrial translation rate assessed by *in organello* ^{35}S-met pulse labelling for 10, 30 and 60 minutes in isolated heart mitochondria of WT and ClpP KO (C) and corresponding overall protein synthesis rate curves (D). Bars represent mean ± S.E.M. (Student's t test, *p < 0.05, **p < 0.01, ****p < 0.0001), (n=3-4). *In organello* translation was performed with Dr. Alexandra Kukat.
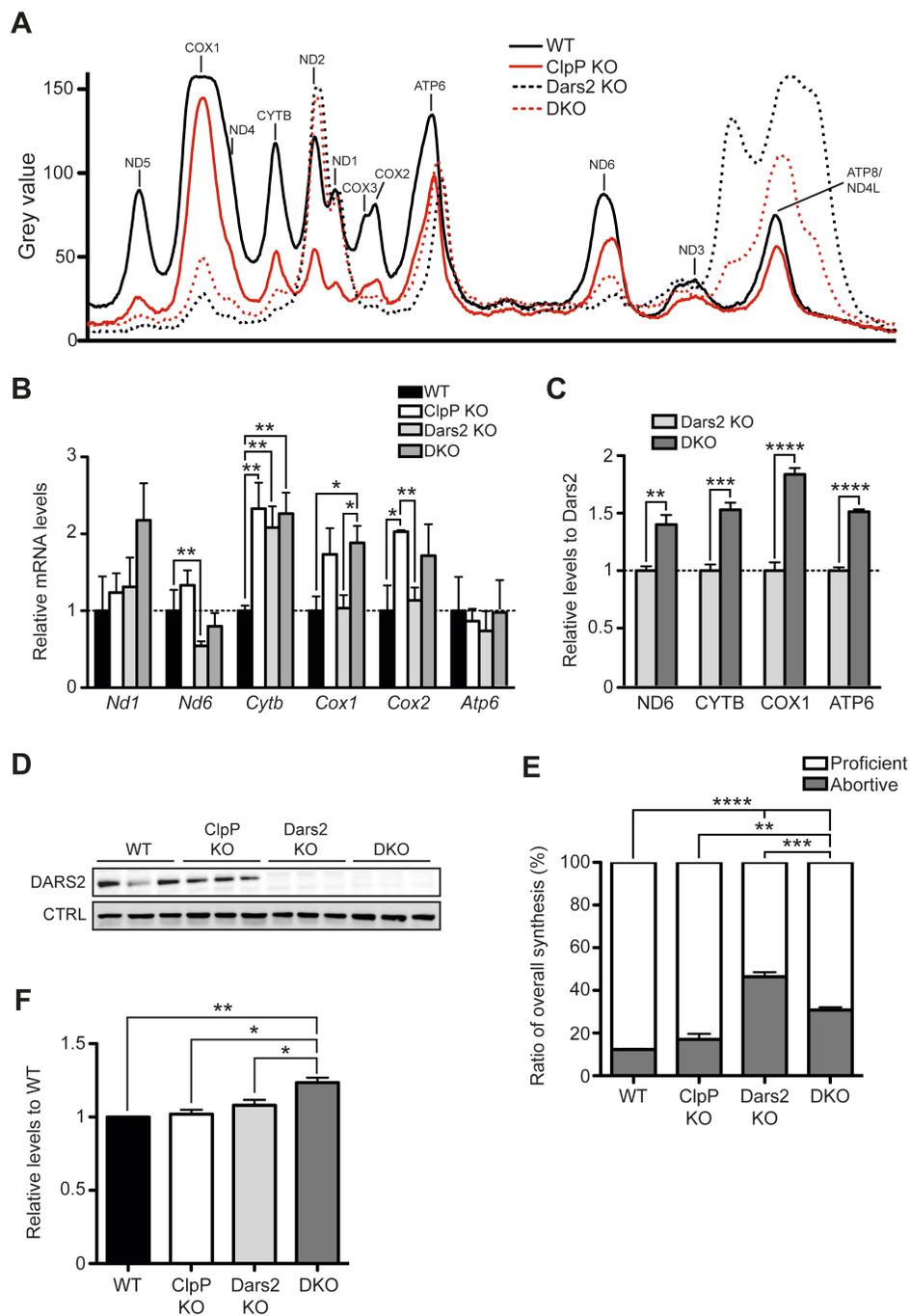
Figure 3.24: Dysregulation of mitochondrial translation can be partially rescued be the loss of CLPP (2).
(A) Representative densitometric analysis of *de novo* synthesized proteins in WT, ClpP KO, Dars2 KO and DKO heart mitochondria after labelling as in Figure 3.19A. (B) Relative expression levels of mtDNA-encoded OXPHOS subunits in ClpP KO, Dars2 KO and DKO hearts normalized to WT (n=5). (C) Relative levels of the individual *de novo* synthesized OXPHOS subunits in DKO mitochondria normalized to the corresponding Dars2 KO polypeptide level, (n=3-4). (D) Western blot analysis of DARS2 levels. HSC70 is used as a loading control (CTRL). (E) Relative levels of protein synthesis of Proficient and Abortive polypeptides, (n=3-4). (F) Quantification of the turnover rate of full-length (Proficient) *de novo* synthesized proteins, (n=3-4). Bars represent mean ± S.E.M. (Student's t test, *p < 0.05, **p < 0.01, ***p < 0.001, ****p < 0.0001).

4 Discussion

Mitochondria received a broad interest from the scientific community in recent years, since mitochondrial dysfunction contributes to the ageing process, as well as to diseases such as cancer, diabetes and various neurological disorders (Nunnari and Suomalainen, 2012). Organelle dysfunction, caused by mtDNA depletion, oxidative stress, alterations in morphology and dynamics or by aggregation of misfolded proteins, triggers a mitochondrial-to-nucleus response that orchestrates the expression of nuclear genes aimed at restoring homeostasis (Cagin and Enriquez, 2015). Understanding these so called "retrograde signalling" responses is key to develop new therapeutic approaches against a wide range of pathologies caused by mitochondrial dysfunction. A mitochondrial quality control machinery, which constantly monitors and supports protein folding and degradation, is essential to maintain a functional protein homeostasis. An early response here is the so-called mitochondrial unfolded protein response (UPR^{mt}) that is an emerging quality control pathway, ensuring the functionality of the mitochondrial proteome (Pellegrino et al., 2013). Even though the UPR^{mt} has been investigated to some extent by now, this stress response is still poorly studied in mammals. So far, the UPR^{mt} signalling is mainly defined in *C. elegans* models and has not been translated into the mammalian system yet.

This study aimed at deciphering the regulation of the mammalian UPR^{mt} signalling. For this purpose, *in vitro* studies were performed using the proposed UPR^{mt} markers HSP60 as well as mtHSP70 and their potential for stress induction was assessed. Second, it was investigated whether the regulation of potential UPR^{mt} mediators or mitochondrial chaperones and proteases *in vitro* could shed some light on this fundamental process. Finally, it was evaluated whether CLPP, a mitochondrial matrix protease shown to be essential for UPR^{mt} signalling in worms (Haynes et al., 2007), is required for the mammalian UPR^{mt} *in vivo*. Mouse models lacking the CLPP protease in a basal and a condition of high mitochondrial proteostatic stress were developed to answer this question. To fuel mitochondrial proteostatic stress, heart and skeletal muscle-specific DARS2-deficient mice were used, which lack the mitochondrial aspartyl aminoacyl-tRNA synthetase, essential for mitochondrial translation (Dogan et al., 2014).

4.1 UPR^{mt} signalling is constitutively active under regular cell culture conditions

4.1.1 HSP60 and mtHSP70 levels cannot be further elevated through stress induction *in vitro*

This study demonstrates that the mitochondrial chaperones HSP60 and mtHSP70 are highly abundant in 6 different cell types under regular cell culture conditions (Section 3.1.1). It also shows that expression of mutant mitochondrial proteins such as a defective ornithine decarboxylase (ΔOTC) as well as a mutant inner membrane import protein (TIM14ΔH3) did not further increase the levels of HSP60 and mtHSP70 (Section 3.1.1). Moreover, it was found that inhibition of mitochondrial translation or the generation of ROS by small molecules also did not elevate the levels of the UPR^{mt} markers *in vitro*. Finally, it was shown conclusively that *Hspd1* (HSP60) and *Hspa9* (mtHSP70) transcriptional reporters are constitutively active under regular cell culture conditions, proving that both proteins are highly expressed in various cell lines *in vitro* (Section 3.1.1). The high levels of HSP60 and mtHSP70 are consistent with the fact that both are reported

to be among the top 5-10% of the most abundant proteins in both human and mice tissues and cell lines (Wang et al., 2012).

These findings add weight to the notion that HSP60 is highly expressed in various human tumours, orchestrating a broad cell survival response (Lianos et al., 2015). It was shown that HSP60 is associated with survivin, one of the most "cancer-specific" genes, as well as it inhibits p53 tumour suppression (Ghosh et al., 2008). The cytoprotective role of HSP60 observed in cancer might also be true for proliferating cells in general, however, the cell lines used in this study were also of tumour origin or had been immortalized, which could be key for the constant elevation in HSP60 levels. Similarly, mtHSP70 (GRP75/Mortalin) was found elevated in many human tumours, tumour-derived cell lines and *in vitro* immortalized cells (Wadhwa et al., 2006). These authors also reported that upon immortalization of human embryonic fibroblasts subclones spontaneously increased mtHSP70 expression levels, which was shown to be the key change for increased tumourigenesis. Vice versa, reduction of mtHSP70 levels in human immortalized cells lead to a senescence-like growth arrest (Wadhwa et al., 2004). These observations further support the hypothesis that upregulation of HSP60 and mtHSP70 is inevitable in proliferating cells in order to keep their mitotic integrity.

Unlike the study of Zhao et al., the current study found no upregulation of HSP60 levels by the use of ΔOTC (Section 3.1.1). However, one possible explanation is that the basal levels of HSP60 shown by other studies were rather below the ones found in this investigation, showing that cells did not yet elevate HSP60 levels to the maximum and therefore were still capable of an upregulation (Martinus et al., 1996; Zhao et al., 2002). Also the fact that HSP60 is highly abundant in our cells without further stress application could explain why a possible increase is masked on the protein level (Section 3.1.1). Strikingly, upregulation of mtHSP70 was not observed in mammalian cell culture upon mitochondrial protein perturbations (Martinus et al., 1996; Zhao et al., 2002). However, *mtHSP70* mRNA levels were found to be slightly elevated upon ΔOTC treatment that was not further translated into higher protein levels, showing that increase in expression not necessarily translates into more proteins (Section 3.1.1).

Some evidence also suggests that interfering with the mitochondrial import machinery resulted in increased *HSP60* mRNA levels in HEK cells (Rainbolt et al., 2013). In contrast, similar changes could neither be observed on *HSP60* mRNA nor for protein levels upon transfection of a mutant TIM14ΔH3 isoform using the same cell line in this study (Section 3.1.1). However, it can again be suspected that the general upregulation of HSP60 *in vitro* makes it difficult to assess whether these markers do respond to mitochondrial import perturbations. It seems likely that these cultured cells experienced another degree of stress already or that the passage number strongly influenced the HSP60 as well as mtHSP70 levels.

Another way to measure *Hsp60* induction upon mitochondrial stress was achieved by the use of transcriptional reporters in both mammalian cells and in *C. elegans* (Houtkooper et al., 2013; Yoneda et al., 2004; Zhao et al., 2002). In addition, a transcriptional reporter for *hsp-6* (homologue of mammalian mtHSP70) was extensively used in *C. elegans* to study UPR^mt induction, which displayed a greater sensitivity to mitochondrial stress then the *hsp-60* transcriptional reporter (Yoneda et al., 2004). Various studies in *C. elegans* exploited the use of chemical compounds to induce reporter expression of either *hsp-6* or *hsp-60*. Inhibition of mitochondrial translation, by doxycyline or chloramphenicol, or the ROS-inducing agents such as paraquat, rotenone or antimycin A highly increased UPR^mt reporter expression (Houtkooper et al., 2013; Runkel et al., 2013; Yoneda et al., 2004). In contrast, no changes on the protein levels of HSP60 and mtHSP70 could be observed in the current study using the same set of chemical compounds (Section 3.1.1). The results are in line with those of other studies, which show that endogenous expression of UPR^mt markers is not influenced by these small molecules in Hep3B cells as well as in primary hepatocytes (Ishikawa et al., 2009; Michel et al., 2015). Interestingly, these authors found that rather the integrated stress response (ISR) reacts to the mitochondrial specific stresses, showing that mitochondrial dysfunction translates earlier into cellular stresses instead mitochondrial specific stress responses, such as the UPR^mt. Despite the number of *C. elegans* reports suggesting that translational inhibitors or ROS generating agents induce UPR^mt, there is still no evidence that this reflects the current endogenous situation because transcriptional reporters in worms do not necessarily correlate with the endogenous expression of the gene of interest, since promoter fragments

are rather short and possibly miss important *cis*-regulating elements. Moreover, it has not yet been proven that *hsp-6* and *hsp-60* expression initiates with direct recognition of unfolded proteins induced by small molecules.

Finally, the current study shows that GFP transcriptional reporters harbouring 2 kb upstream of the respective ORF of either *Hspd1* or *Hspa9* were constitutively active in cell culture, which is consistent with the observation that both proteins are highly abundant under regular cell culture conditions (Section 3.1.1). However, it can be suspected that rather short transcriptional reporters used by others could exclude some important up- or downstream regulatory elements (Yoneda et al., 2004; Zhao et al., 2002). In cell culture, *Hspd1* and *Hspa9* miss the key features of an ideal reporter gene, which would be a gene that is not or only mildly endogenously expressed in the cell of interest and is susceptible to assays that are sensitive, quantitative and reproducible. In contrast *C. elegans* GFP reporters fulfil these criteria, however, it is not clear whether the strong induction also reflects the changes on the protein levels.

Collectively, these findings demonstrate that HSP60 and mtHSP70 are not suitable to study the UPR^{mt} induction in cell culture, since they are highly endogenously expressed and not amenable to further upregulation.

4.1.2 Low oxygen conditions cannot reduce the levels of HSP60 and mtHSP70

This study shows that prolonged exposure of cells to low oxygen conditions does not reduce the high expression of HSP60 and mtHSP70 (Section 3.1.2.1). It has been demonstrated that reduction from 21% atmospheric oxygen conditions to 5% low oxygen conditions in 6 different cell lines does not decrease UPR^{mt} marker levels. Several reports have suggested that on the one hand high oxygen levels increase antioxidant defence mechanisms such as upregulation of mtHSP70 and on the other hand that hypoxic conditions (approx. 0,5% O_2) do not influence constitutive active proteins such as HSP60, which is in line with the observations of this study (Papandreou et al., 2006; Williamson et al., 2008).

107

This finding further supports the hypothesis that HSP60 and mtHSP70 are stably expressed proteins since they do not react to changes introduced by reduced oxygen levels. Both high oxygen levels as well as very low oxygen levels, also known as hypoxia, can lead to increased ROS levels, therefore leading to mitochondrial perturbations (Solaini et al., 2010; Tiede et al., 2011). Despite the number of reports suggesting that oxygen levels affect ROS production, hence the activation of adaptive stress responses, no changes in the UPR^{mt} markers HSP60 and mtHSP70 could be detected upon low oxygen conditions (Section 3.1.2.1). There are three possible explanations for these findings. First, oxygen levels and therefore the amount of ROS do not influence the levels of unfolded proteins. Second, the time exposed to low oxygen levels was too short in order to alleviate the stress inside mitochondria. Finally, cells have been kept for too long already under high oxygen conditions, which permanently changed expression levels of UPR^{mt} markers. Similarly, it was reported that cell cultivation in general induces adaptations not only in antioxidant defence enzymes such as the superoxide dismutase or catalase, but also in the levels of heat shock proteins, such as HSP60 (Halliwell, 2014; Khassaf et al., 2003; Tiede et al., 2011). Therefore, it seems likely that changes due to variation of the oxygen levels only mildly affect the general stress that cell have to cope with in cell culture.

Thus, these findings suggest that inferring with oxygen level for a short term does not influence mitochondrial chaperone abundance *in vitro*.

4.2 ATF5 is implicated into mitochondrial stress signalling

The current study provides a more comprehensive understanding of ATF5 within mitochondrial as well as cellular stress responses. It shows that downregulation of ATF5 causes a decrease of known UPR^{mt} markers *in vitro* (Section 3.1.2.2). Moreover, ATF5 has been shown to be located in the nucleus under regular cell culture conditions, whereas *in vivo* ATF5 is found in mitochondria (Section 3.1.3 and 3.2.3). Finally, it has been demonstrated that ATF5 is elevated upon mitochondrial perturbations both *in vitro* and *in vivo* (Section 3.1.4 and 3.2.3). It was suggested that ATF5 is the mammalian homologue of ATFS-1, the central mediator of the UPR^{mt} in *C. elegans* (Haynes et al., 2010).

The transcription factor ATF5 plays a major role in the development of the nervous system and in the survival of neural tumours (Greene et al., 2009). Similarly, a general pro-survival function as well as a role in cell cycle control was reported (Madarampalli et al., 2015; Persengiev et al., 2002; Persengiev and Green, 2003). The results of this study lend further credence to an earlier suggestion that ATF5 is induced in response to various cellular stresses such as ER stress, mitochondrial stress, arsenite exposure and proteasome inhibition (Dogan et al., 2014; Zhou et al., 2008). However, no role has been defined so far for ATF5 during UPR^{mt} signalling. Proceeding from the assumption that ATF5 is indeed corresponding to ATFS-1, ATF5 has been found to be localized to the nucleus under regular cell culture conditions, adding weight to the observation that UPR^{mt} signalling is active in these cells, as determined by high levels of both HSP60 and mtHSP70 (Section 3.1.1). In addition, ATF5 localizes to mitochondria in wild type mouse hearts, showing that ATF5, a transcription factor by nature, is able to translocate into mitochondria under endogenous conditions (Section 3.2.3). This is further supported by the observation that increasing levels of mitochondrial dysfunction in mutant hearts correlate with decreasing levels of ATF5 found in heart mitochondria (Section 3.2.3). These results further support the hypothesis that ATF5 may act as the *C. elegans* homologue ATFS-1 that is regularly imported into mitochondria and only translocated to the nucleus under mitochondrial stress conditions (Nargund et al., 2012). It should be noted that ATF5, in contrast to ATFS-1, was shown to be subject to translational control through phosphorylation of eIF2α in response to cellular stress (Zhou et al., 2008). This feature is shared with another transcription factor ATF4 that is the key activator of the integrated stress response (ISR) (Dey et al., 2010). It seems likely that a general programme is activated under various stress conditions, such as ER or mitochondrial stress, which results in a common cellular stress response. In accordance, the GCN2 kinase was found to be the upstream activator of eIF2α inducing ATF4/5 and a global attenuation of cytosolic translation (Michel et al., 2015). Interestingly, it was shown in *C. elegans* that the GCN2-eIF2α axis acts in parallel to the UPR^{mt} in order to sustain mitochondrial proteostasis and function (Baker et al., 2012). However, it is not clear by now, whether in the mammalian system both pathways are merged or if there is also another response branch leading to more organelle specific changes, as well. Evidence for another parallel signalling arises from the finding that UPR^{mt} markers directly correlate with ATF5 levels (Section 3.1.2.2 and 3.23). Nevertheless, a common feature of both the

UPR^{mt} and the ISR concentrates on the multifunctional transcription factor CHOP, which gets activates downstream of ATF4 and ATF5 (Oyadomari and Mori, 2004; Yamazaki et al., 2010). The UPR^{mt} markers HSP60 and ClpP harbour a CHOP-responsive element, but do not contain any ATF5 binding site (Section 3.1.1) (Zhao et al., 2002). Therefore, it is not clear whether the changes observed during ATF5 knockdown are direct or indirect via CHOP. Interestingly, it was shown recently that disruption of mtDNA expression leads to activation of CHOP that only triggers activation of the ISR but not the UPR^{mt} markers HSP60 and CLPP (Cortopassi et al., 2006; Michel et al., 2015). Nevertheless, there is some evidence that HSP60 and CLPP are not or only mildly changed upon mitochondrial perturbations, which raises the question if these markers are at all suitable to study UPR^{mt} induction (Cortopassi et al., 2006; Dogan et al., 2014; Moisoi et al., 2009; Piechota et al., 2006). In line with this evidence only slight changes of HSP60 could be observed in the experiments performed in this study (Section 3.1 and 3.23). However, mtHSP70 and LONP1 were found highly responsive to mitochondrial dysfunction *in vivo,* corresponding very well to levels of ATF4, ATF5 and CHOP (Section 3.2.3). Thus, the basic assumption in the current model is that ATF5 is induced upon mitochondrial stress activating cellular stress responses and subsequently mitochondrial quality control pathways. However, future studies will be important to discover a detailed mechanism.

Taking into account the data presented so far, it is recommended to re-evaluate how actually mitochondrial dysfunction, especially due to unfolded proteins, triggers general cellular or rather organelle-specific responses. For that reason, it is very important to unravel the upstream events of a mitochondria-induced ISR as well as how cap-dependent translational attenuation by eIF2α, a common feature of the UPR^{er}, UPR^{mt} and the ISR, affects distinct cellular pathways. Moreover, CHOP, the linking key transcription factor of all these responses, needs to be further assessed regarding post-transcriptional modifications as well as other potential transcriptional co-activators that ultimately determine the specificity of the response.

4.3   LONP1 displays and regulates UPR^mt signalling

In this study, it is shown for the first time that the matrix protease LONP1 not only responds to mitochondrial unfolded protein stress, but also regulates the mammalian UPR^mt signalling. The upregulation of LONP1 during unfolded protein stress has been demonstrated in three ways: (i) knockdown of the mitochondrial chaperones HSP60 and mtHSP70 elevated LONP1 expression (Section 3.1.4) (ii) knockdown of ATF5 also resulted in a vast increase of LONP1 levels (Section 3.1.5); and (iii) dysregulation of mitochondrial translation *in vivo*, resulting in the accumulation of unfolded/unassembled respiratory chain subunits, strongly induced LONP1 on both protein and mRNA level (Section 3.2.3). It is also shown that knockdown of LONP1 is accompanied by a reduction in the levels of mitochondrial chaperones, ATF5 as well as CHOP (Section 3.1.5). Here the study provides the first evidence that LONP1 is an upstream component of the UPR^mt signaling cascade in mammals.

To date numerous studies reported that LONP1 degrades denatured or oxidized proteins (Bota and Davies, 2002; Suzuki et al., 1994). However, LONP1 has not been directly linked to the UPR^mt signalling so far, although it was reported to degrade the UPR^mt mediator ATFS-1 upon import into mitochondria in *C. elegans* (Nargund et al., 2012). Instead, CLPP another mitochondrial matrix protease, was shown to be indispensable for UPR^mt signaling in *C. elegans* (Haynes et al., 2007). Interestingly, a recent study revealed that it is not CLPP which alleviates unfolded protein induced PINK1-accumulation in HeLa cells, but LONP1 (Jin and Youle, 2013). Moreover, the same authors demonstrate that downregulation of LONP1 strongly increases the load of overexpressed ΔOTC, showing that LONP1 degrades excess of unfolded or misfolded proteins. Consistent with these results, an increased LONP1 expression could be observed upon reduced chaperone capacity or by increased unfolded OXPHOS subunits in the current study (Section 3.1.4 and 3.2.3). These findings further support the hypothesis that the abundance of LONP1 reflects the levels of unfolded proteins in the mitochondrial matrix. Remarkably, it has been shown that the relative contribution of yeast Pim1 (homolog of mammalian LONP1) to the prevention of protein aggregates under high stress conditions was by far greater compared to the mitochondrial chaperones Hsp60 and mtHsp70, although less abundant (Bender et

al., 2011). These observations add weight to the notion that LONP1 is the central factor in clearing unfolded proteins and preventing stress, rather than the mitochondrial chaperones HSP60 and mtHSP70. Very recently it has been demonstrated that loss of LONP1 leads to a reduction of HSP60 and mtHSP70 protein levels under oxidative stress (Kao et al., 2015). Moreover, it was shown that LONP1 directly interacts with the HSP60-mtHSP70 complex regulating their levels under cellular stress. Consistent with the study of Kao et al., the current study also demonstrated the dependency of HSP60 and mtHSP70 expression on LONP1 (Section 3.1.5). Strikingly, LONP1 overexpression is associated with cancer, whereas its decline is connected with age, senescence and apoptosis (Bota et al., 2005; Cheng et al., 2013; Ngo and Davies, 2007). These features are shared with HSP60 and mtHSP70 (Section 4.1.1), showing that mitochondrial quality control pathways are intimately linked to cell health.

The current study shows that the expression of the mitochondrial chaperone TRAP1 as well as the previously described transcription factors ATF5 and CHOP also correlates with LONP1 levels, suggesting that LONP1 ultimately determines the response (Section 3.15). These observations add weight to the notion that LONP1 regulates the levels of UPR^{mt} markers, hence UPR^{mt} signalling. Since loss of ATF5 triggers a strong LONP1 induction, it can be suspected that LONP1 expression is induced independent of ATF5 (Section 3.1.5). These results gave rise to the hypothesis that loss of ATF5 increases the load of unfolded/misfolded proteins in mitochondria that are probably the cause for LONP1 induction. It seems likely that an alternative feedback loop triggers LONP1 expression upon unfolded protein stress that is separated from ATF5-CHOP-induced UPR^{mt} signalling. It can be suspected that loss of ATF5 influences other cellular stress pathways, such as the ISR or the UPR^{er} via ATF4/CHOP, that challenge the load of unfolded proteins in mitochondria (Section 4.2). In line with that it was reported that LONP1 as well as mtHSP70 were strongly induced upon ER stress that further indicates the existence of a connection between ER and mitochondrial function (Hori et al., 2002). Interestingly, the ER-stress induced upregulation of LONP1 and mtHSP70 could be inhibited by loss of PERK, an ER stress-dependent kinase that also phosphorylates eIF2α (Hori et al., 2002). This observation further supports the hypothesis that ER and mitochondrial homeostasis are interconnected and stress response pathways are shared.

Although the regulatory mechanisms governing LONP1 expression are still unclear, this study suggests that LONP1 is upregulated during unfolded protein stress. Moreover, first evidence is provided that the levels of UPR[mt] markers are dependent on LONP1. However, future studies need to unravel the specific mechanisms by which the mitochondrial quality control network integrates into the cellular stress pathways. Based on the observation that UPR[mt] is difficult to model in cell culture, the generation of mouse models that either lack or overexpress potential factors implicated in UPR[mt] signalling, such as ATF5 or LONP1, is recommended.

4.4 Mammalian CLPP regulates mitochondrial translation, but not the mitochondrial unfolded protein response *in vivo*

At the current stage, this is the first study that demonstrates that the mitochondrial matrix protease CLPP is not part of the mammalian UPR[mt] signalling using an *in vivo* model (Section 3.2.3). The role of CLPP in the regulation of the UPR[mt] has attracted much interest in the past years using *C. elegans* or mammalian cell culture models (Haynes et al., 2007; Rath et al., 2012; Zhao et al., 2002). These studies suggest CLPP either as a read out for UPR[mt] activation or as factor that indirectly regulates UPR[mt] markers.

The cutting-edge study on the UPR[mt] in mammalian cells showed that CLPP is induced upon overexpression of a mutant, aggregation-prone protein (ΔOTC) in the mitochondrial matrix (Zhao et al., 2002). Moreover, it was shown that a stoichiometric mismatch of nDNA and mtDNA-encoded proteins, termed mitonuclear imbalance, triggered UPR[mt] activation, amongst others *Clpp* expression (Houtkooper et al., 2013). In contrast, it was recently found that loss of DARS2 in heart causes strong dysregulation of mitochondrial protein synthesis leading to high UPR[mt] upregulation, without any effect on CLPP expression (Dogan et al., 2014). In line with this finding it was reported that other types of mitochondrial stresses, such as inhibition of mitochondrial translation or depletion of mtDNA, MELAS and NARP mtDNA point mutations, OXPHOS inhibition, or loss of HTRA2 expression do not trigger CLPP expression (Fujita et al., 2007; Ishikawa et al., 2009; Michel et al., 2015; Moisoi et al., 2009). It should be noted that the *C. elegans*

homologue CLPP-1 is required for *hsp-6* and *hsp-60* induction (Haynes et al., 2007). Furthermore, it was proposed that CLPP-1 function is required because it generates peptides that are exported through HAF-1 that inhibit the mitochondrial import of ATFS-1 by a yet unknown mechanism (Haynes et al., 2010; Nargund et al., 2012). However, a detailed mechanism by which CLPP signals this response in mammals was not found.

The current study provides the first direct evidence that CLPP is dispensable for the UPR^{mt} activation in a DARS2-deficient background, as an unaffected increase of both protein and transcript levels of mitochondrial chaperones and proteases could be detected in the absence of CLPP (Section 3.2.3). Recent studies have shown that a CLPP-deficient mouse model displays ubiquitous induction of mitochondrial chaperones and inflammatory factors (Gispert et al., 2013). In line with that, the current study showed that loss of CLPP induced also a mild stress that upregulates chaperones exclusively (Section 3.2.3). It should be noted that activation of mitochondrial proteases serves as second defence system, which was not only induced in Dars2 KO but also in DKOs (Section 3.2.3). Moreover, loss of CLPP did not diminish the high expression of two transcription factors (CHOP and ATF5) that were proposed to play central roles in the UPR^{mt} (Haynes et al., 2010; Zhao et al., 2002). As described before (Section 4.2), both CHOP and ATF5 are also implicated in the ISR (Teske et al., 2013; Zhou et al., 2008). In line with the current observations, the ISR was found activated upon mitochondrial dysfunction in mammals (Dogan et al., 2014; Silva et al., 2009). In addition, phosphorylation of eIF2α as well as upregulation of ATF4 caused by mitochondrial dysfunction were not compromised by the lack of CLPP, showing that the ISR is activated independent of CLPP (Section 3.2.3). Conversely, it was reported that eIF2α phosphorylation is dependent on CLPP in murine cells (Rath et al., 2012). However, this study made use of a of a bacterial CLPP inhibitor Z-LY-CMK that was shown to be functional in worms (Haynes et al., 2007), but not further assessed in mammalian cells. Nevertheless, the results mentioned in section 3.2.3 demonstrate that eIF2α can be phosphorylated *in vivo* independent of CLPP under unfolded protein stress. Moreover, the activation of systemic stress signalling measured by the "mitokine" FGF21 (Tyynismaa et al., 2010) remains also unchanged upon CLPP deletion (Section 3.2.3). Interestingly, ClpP KO hearts already display signs of cellular stress responses as indicated by elevated ATF4 and FGF21 expression levels (Section 3.2.3). Intrigued by the observation that either

mitochondrial stress or ER stress induce the ISR, it can be postulated that both responses are intrinsically tied to each other (Section 4.2). This is consistent with the fact that the "mitokine" FGF21 is induced not only during mitochondrial stress, but also during ER stress (Dogan et al., 2014; Jiang et al., 2014). Finally, the impairment of autophagy characterized by accumulation of P62 that was induced upon loss of DARS2 (Dogan et al., 2014), was also not affected by the loss of CLPP (Section 3.2.3). Thus, all stress response pathways investigated do not involve a CLPP-mediated response.

This study has not only shown that CLPP is not required for UPR^{mt} signaling, but has also provided a way how to investigate this rather complex signaling *in vivo* by using a heart-specific short lived mouse model of mitochondrial dysfunction such as Dars2 KO mice. This straightforward approach can be used in future to study other potential factors that have been shown to be implicated in the UPR^{mt} in other organisms. Taken together these results suggest that mammalian UPR^{mt} might be intimately linked with ISR leading to cell non-autonomous changes in metabolism, yet the current study refutes any role of CLPP in this process.

Another key finding of this study is that loss of CLPP, a major mitochondrial matrix protease, in an environment of disrupted mitochondrial translation is actually beneficial for the animal. Lifespan increased significantly by roughly 30%, which was due to a milder phenotype in the heart as shown by decrease in heart weight, regain of normal body weight, less signs of hypertrophy and less fibrosis (Section 3.2.2). Altogether, it was demonstrated that double-deficient mice are healthier for longer period of time and clearly reduce the signs of cardiomyopathy. Most importantly COX/SDH staining revealed a profound rescue of COX negative cells (Section 3.2.2). Sequential analysis of OXPHOS complex levels and *in gel* activity showed that complex I and complex IV exhibit higher activities in DKO compared to Dars2 KO (Section 3.2.4). In agreement with these findings, respiration through complex I and combined complex I and II significantly improved as well (Section 3.2.4). The analysis of individual OXPHOS subunits by SDS-PAGE revealed that mitochondrial-encoded and also nuclear-encoded subunits not only of complex I and IV, but also complex III strongly increased their levels (Section 3.2.4). A plausible explanation is that the levels of nuclear-encoded subunits depend on the availability of mitochondrial-encoded subunits in order to be assembled in correct stoichiometry. Unassembled subunits

overload mitochondria and are more prone to degradation (Leonhard et al., 2000). Interestingly, complex V subunits are not affect in their levels, even though complex V also contains mitochondrial-encoded subunits (Section 3.2.4). In addition, the improved phenotype of DKO compared to DARS2 KO mitochondria could be confirmed by the use of a label-free mass spectrometric analysis (Section 3.2.5). Not only mitochondrial encoded subunits, but also nuclear encoded subunits could be rescued by loss of CLPP in DARS2-deficient mitochondrial, which is in line with steady-state level obtained by Western blot analysis (Section 3.2.4). Taken together, mitochondrial respiration can be partially rescued in DARS2-deficient mice, when CLPP is lost.

These results were clearly not expected since CLPP deficiency on its own accounts for Perrault syndrome that gives rise to sensorineural hearing loss and premature ovarian failure in humans (Jenkinson et al., 2013). In accordance with the situation in humans, a similar phenotype was observed in CLPP deficient mice (Gispert et al., 2013); however, the molecular basis leading to the specific phenotypes has not been defined so far. The current study provides the first evidence that loss of CLPP leads to a moderate defect in mitochondrial protein synthesis that could be the primary cause of the disease (Section 3.26). Likewise, mutations in HARS2 (Pierce et al., 2011), LARS2 (Pierce et al., 2013) and TWINKLE (Morino et al., 2014), three out of four other genes causing Perrault syndrome, also have a straight impact on mitochondrial translation. In line with these observations, a recent study demonstrated that loss of CLPP impairs mitoribosome assembly that might be the cause for the translational defect (Priyanka Maiti, PhD Thesis). Strikingly, inhibition of CLPP as well as inhibition of mitochondrial translation could be used as therapeutic strategy for human acute leukemia, suggesting also that CLPP might be intimately linked to mitochondrial translation (Cole et al., 2015; Skrtic et al., 2011).

High rates of translation in cells were shown to be disadvantageous for protein folding (Sherman and Qian, 2013). Moreover, inhibition of translation by roughly 15-20% highly reduced the formation of protein aggregates resulting from mutant folding impaired proteins (Meriin et al., 2012a; Meriin et al., 2012b). In line with these observations in the current study it could be found that reduction of mitochondrial translation of approx. 25% due to loss of CLPP was also beneficial for a switch from aborted to proficient protein synthesis in DARS2-deficient mice, preventing the generation of toxic protein

intermediates, hence a possible aggregation of aborted proteins (Section 3.2.6). This would explain the reduction of proteotoxic stress in DKO mitochondria, although it does not add weight to the notion that proficient protein synthesis is improved in these animals.

Based on these observations, it can be argued that a reduced rate of mitochondrial translation inflicted by the loss of CLPP allows an augmented generation of full-length OXPHOS subunits to occur inside DARS2-deficient mitochondria, thus partially correcting the respiratory defect. This effect was not due to an increased stability of OXPHOS subunits, as they are subject to higher degradation in DKO hearts (Section 3.2.6). There are two possible scenarios of how the loss of CLPP enhances the level of proficient mitochondrial protein synthesis (Figure 4.1). Firstly, tRNAs are generally less consumed during slowed down translation in CLPP-deficient mitochondria, hence the aspartate-tRNA pool lasts longer, enabling a prolonged proficient protein synthesis. The second explanation would be that slow mitochondrial translation caused by the absence of CLPP allows other tRNAs to replace aspartate-tRNA in the nascent polypeptides. Probably anticodons similar to the one of aspartate-tRNA get incorporated generating "pseudo" mitochondrial-encoded OXPHOS subunits that exhibit some residual activity. Moreover, overrepresentation of uncharged tRNAs can also lead to wrong charging (Raina and Ibba, 2014). Given the fact that uncharged tRNAs cognate for aspartate are overrepresented in DARS2-deficient mitochondria and loss of CLPP causes slowed down translation, possibly enabling misincorporation, it can be speculated that this could be the reason for enhanced proficient protein synthesis. These suboptimal OXPHOS subunits would be more prone to misfolding and degradation. An indirect proof for this scenario would be the fact that full-length mtDNA-encoded subunits generated in DKO mitochondria are more rapidly turned over (Section 3.2.6). Similar observations were made in mtDNA mutator mice that accumulate high levels of mtDNA mutations, leading to the expression of OXPHOS subunits with amino acid substitutions that are more rapidly degraded (Edgar et al., 2009). Apart from the obvious effect on the proficient protein synthesis, a tremendous decrease in the level of aborted peptides produced in DKOs compared to Dars2 KO mitochondria could also be found (Section 3.2.6). High amounts of these peptides could cause proteotoxic stress independent of the effect on the levels of OXPHOS complexes and put an additional burden to already troubled mitochondria. Most probably, the improved phenotype in DKO

mitochondria arises from a combination of both, the enhanced mitochondrial respiratory capacity and the strong decline in the amount of potentially toxic aberrant polypeptides.

This study has not only shown that CLPP is not implicated in the UPR^{mt} signalling, but has also provided evidence that it is actually involved in the regulation of mitochondrial translation. Another key finding was that CLPP is not involved in the degradation of unassembled or misfolded mitochondrial-encoded subunits in mammals. At the current stage there was no clear role defined for CLPP in mammalian mitochondria, only observations made in other organisms mainly bacteria and *C. elegans* that implicate CLPP in the degradation of misfolded or damaged proteins (Baker and Sauer, 2012; Haynes et al., 2007). In summary, the results of the current study provide the first evidence for a role of CLPP in mammalian mitochondrial translation, while refuting its role in the UPR^{mt} signalling. They also open a possibility for exploration of therapeutic intervention targeting CLPP activity in the large group of mitochondrial diseases that directly affect mitochondrial protein synthesis.
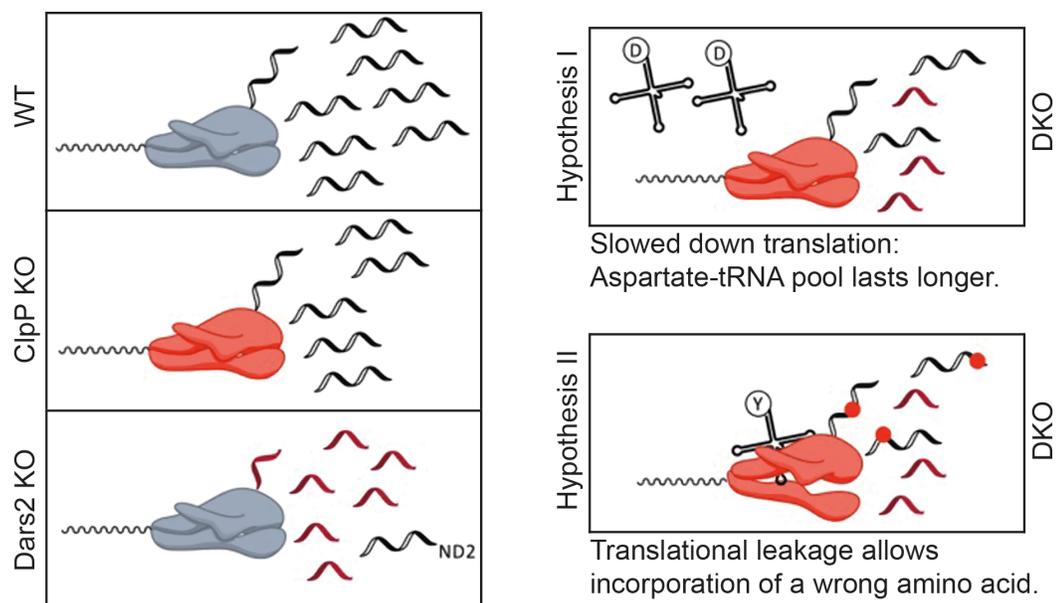
Figure 4.1: Proposed model of mitochondrial translation in DKO compared to WT or single mutant phenotype. CLPP deficiency leads to a slowed down mitochondrial translation, whereas DARS2 deficiency causes aborted protein synthesis. However, translational rate is not affected by the loss of DARS2. DKO mitochondrial translation shifts aborted protein synthesis to proficient protein synthesis by a slowed down translation. This improvement in DKO mitochondrial translation is either achieved by hypothesis I or II.

Bibliography

Abe, Y., Shodai, T., Muto, T., Mihara, K., Torii, H., Nishikawa, S., Endo, T., and Kohda, D. (2000). Structural basis of presequence recognition by the mitochondrial protein import receptor Tom20. Cell *100*, 551-560.

Al Rawi, S., Louvet-Vallee, S., Djeddi, A., Sachse, M., Culetto, E., Hajjar, C., Boyd, L., Legouis, R., and Galy, V. (2011). Postfertilization autophagy of sperm organelles prevents paternal mitochondrial DNA transmission. Science *334*, 1144-1147.

Alberts, B., Bray, D., Lewis, J., Raff, M., Roberts, K., and Watson, J.D. (1983). Molecular biology of the cell. (New York & London: Garland Publishing Inc.).

Aldridge, J.E., Horibe, T., and Hoogenraad, N.J. (2007). Discovery of genes activated by the mitochondrial unfolded protein response (mtUPR) and cognate promoter elements. PloS one *2*, e874.

Amunts, A., Brown, A., Toots, J., Scheres, S.H., and Ramakrishnan, V. (2015). Ribosome. The structure of the human mitochondrial ribosome. Science *348*, 95-98.

Anand, R., Langer, T., and Baker, M.J. (2013). Proteolytic control of mitochondrial function and morphogenesis. Biochimica et biophysica acta *1833*, 195-204.

Andersson, S.G., Zomorodipour, A., Andersson, J.O., Sicheritz-Ponten, T., Alsmark, U.C., Podowski, R.M., Naslund, A.K., Eriksson, A.S., Winkler, H.H., and Kurland, C.G. (1998). The genome sequence of Rickettsia prowazekii and the origin of mitochondria. Nature *396*, 133-140.

Andrews, B., Carroll, J., Ding, S., Fearnley, I.M., and Walker, J.E. (2013). Assembly factors for the membrane arm of human complex I. Proceedings of the National Academy of Sciences of the United States of America *110*, 18934-18939.

Antonellis, A., and Green, E.D. (2008). The role of aminoacyl-tRNA synthetases in genetic diseases. Annual review of genomics and human genetics *9*, 87-107.

Arlt, H., Steglich, G., Perryman, R., Guiard, B., Neupert, W., and Langer, T. (1998). The formation of respiratory chain complexes in mitochondria is under the proteolytic control of the m-AAA protease. The EMBO journal *17*, 4837-4847.

Augustin, S., Nolden, M., Muller, S., Hardt, O., Arnold, I., and Langer, T. (2005). Characterization of peptides released from mitochondria: evidence for constant proteolysis and peptide efflux. The Journal of biological chemistry *280*, 2691-2699.

Baker, B.M., Nargund, A.M., Sun, T., and Haynes, C.M. (2012). Protective coupling of mitochondrial function and protein synthesis via the eIF2alpha kinase GCN-2. PLoS genetics *8*, e1002760.

Baker, M.J., Tatsuta, T., and Langer, T. (2011). Quality control of mitochondrial proteostasis. Cold Spring Harbor perspectives in biology *3*.

Baker, T.A., and Sauer, R.T. (2012). ClpXP, an ATP-powered unfolding and protein-degradation machine. Biochimica et biophysica acta *1823*, 15-28.

Banci, L., Bertini, I., Cefaro, C., Ciofi-Baffoni, S., Gallo, A., Martinelli, M., Sideris, D.P., Katrakili, N., and Tokatlidis, K. (2009). MIA40 is an oxidoreductase that catalyzes oxidative protein folding in mitochondria. Nature structural & molecular biology *16*, 198-206.

Baqri, R.M., Pietron, A.V., Gokhale, R.H., Turner, B.A., Kaguni, L.S., Shingleton, A.W., Kunes, S., and Miller, K.E. (2014). Mitochondrial chaperone TRAP1 activates the mitochondrial UPR and extends healthspan in Drosophila. Mechanisms of ageing and development *141-142*, 35-45.

Barrell, B.G., Anderson, S., Bankier, A.T., de Bruijn, M.H., Chen, E., Coulson, A.R., Drouin, J., Eperon, I.C., Nierlich, D.P., Roe, B.A., et al. (1980). Different pattern of codon recognition by mammalian mitochondrial tRNAs. Proceedings of the National Academy of Sciences of the United States of America *77*, 3164-3166.

Bayat, V., Thiffault, I., Jaiswal, M., Tetreault, M., Donti, T., Sasarman, F., Bernard, G., Demers-Lamarche, J., Dicaire, M.J., Mathieu, J., et al. (2012). Mutations in the mitochondrial methionyl-tRNA synthetase cause a neurodegenerative phenotype in flies and a recessive ataxia (ARSAL) in humans. PLoS biology *10*, e1001288.

Becker, T., Wenz, L.S., Kruger, V., Lehmann, W., Muller, J.M., Goroncy, L., Zufall, N., Lithgow, T., Guiard, B., Chacinska, A., et al. (2011). The mitochondrial import protein Mim1 promotes biogenesis of multispanning outer membrane proteins. The Journal of cell biology *194*, 387-395.

Beckman, K.B., and Ames, B.N. (1998). The free radical theory of aging matures. Physiological reviews *78*, 547-581.

Beebe, K., Mock, M., Merriman, E., and Schimmel, P. (2008). Distinct domains of tRNA synthetase recognize the same base pair. Nature *451*, 90-93.

Belostotsky, R., Ben-Shalom, E., Rinat, C., Becker-Cohen, R., Feinstein, S., Zeligson, S., Segel, R., Elpeleg, O., Nassar, S., and Frishberg, Y. (2011). Mutations in the mitochondrial seryl-tRNA synthetase cause hyperuricemia, pulmonary hypertension,

renal failure in infancy and alkalosis, HUPRA syndrome. American journal of human genetics *88*, 193-200.

Bender, T., Lewrenz, I., Franken, S., Baitzel, C., and Voos, W. (2011). Mitochondrial enzymes are protected from stress-induced aggregation by mitochondrial chaperones and the Pim1/LON protease. Molecular biology of the cell *22*, 541-554.

Benedetti, C., Haynes, C.M., Yang, Y., Harding, H.P., and Ron, D. (2006). Ubiquitin-like protein 5 positively regulates chaperone gene expression in the mitochondrial unfolded protein response. Genetics *174*, 229-239.

Bertram, G., Innes, S., Minella, O., Richardson, J., and Stansfield, I. (2001). Endless possibilities: translation termination and stop codon recognition. Microbiology *147*, 255-269.

Bogenhagen, D., and Clayton, D.A. (1977). Mouse L cell mitochondrial DNA molecules are selected randomly for replication throughout the cell cycle. Cell *11*, 719-727.

Bogenhagen, D.F., Rousseau, D., and Burke, S. (2008). The layered structure of human mitochondrial DNA nucleoids. The Journal of biological chemistry *283*, 3665-3675.

Bonnefond, L., Fender, A., Rudinger-Thirion, J., Giege, R., Florentz, C., and Sissler, M. (2005). Toward the full set of human mitochondrial aminoacyl-tRNA synthetases: characterization of AspRS and TyrRS. Biochemistry *44*, 4805-4816.

Bota, D.A., and Davies, K.J. (2002). Lon protease preferentially degrades oxidized mitochondrial aconitase by an ATP-stimulated mechanism. Nature cell biology *4*, 674-680.

Bota, D.A., Ngo, J.K., and Davies, K.J. (2005). Downregulation of the human Lon protease impairs mitochondrial structure and function and causes cell death. Free radical biology & medicine *38*, 665-677.

Bota, D.A., Van Remmen, H., and Davies, K.J. (2002). Modulation of Lon protease activity and aconitase turnover during aging and oxidative stress. FEBS letters *532*, 103-106.

Brix, J., Rudiger, S., Bukau, B., Schneider-Mergener, J., and Pfanner, N. (1999). Distribution of binding sequences for the mitochondrial import receptors Tom20, Tom22, and Tom70 in a presequence-carrying preprotein and a non-cleavable preprotein. The Journal of biological chemistry *274*, 16522-16530.

Bross, P., Andresen, B.S., Knudsen, I., Kruse, T.A., and Gregersen, N. (1995). Human ClpP protease: cDNA sequence, tissue-specific expression and chromosomal assignment of the gene. FEBS letters *377*, 249-252.

Bross, P., Li, Z., Hansen, J., Hansen, J.J., Nielsen, M.N., Corydon, T.J., Georgopoulos, C., Ang, D., Lundemose, J.B., Niezen-Koning, K., et al. (2007). Single-nucleotide variations in the genes encoding the mitochondrial Hsp60/Hsp10 chaperone system and their disease-causing potential. J Hum Genet *52*, 56-65.

Bross, P., Naundrup, S., Hansen, J., Nielsen, M.N., Christensen, J.H., Kruhoffer, M., Palmfeldt, J., Corydon, T.J., Gregersen, N., Ang, D., et al. (2008). The Hsp60-(p.V98I) mutation associated with hereditary spastic paraplegia SPG13 compromises chaperonin function both in vitro and in vivo. The Journal of biological chemistry *283*, 15694-15700.

Brown, A., Amunts, A., Bai, X.C., Sugimoto, Y., Edwards, P.C., Murshudov, G., Scheres, S.H., and Ramakrishnan, V. (2014). Structure of the large ribosomal subunit from human mitochondria. Science *346*, 718-722.

Buchberger, A., Bukau, B., and Sommer, T. (2010). Protein quality control in the cytosol and the endoplasmic reticulum: brothers in arms. Molecular cell *40*, 238-252.

Bukau, B., Weissman, J., and Horwich, A. (2006). Molecular chaperones and protein quality control. Cell *125*, 443-451.

Bullard, J.M., Cai, Y.C., and Spremulli, L.L. (2000). Expression and characterization of the human mitochondrial leucyl-tRNA synthetase. Biochimica et biophysica acta *1490*, 245-258.

Burbulla, L.F., Fitzgerald, J.C., Stegen, K., Westermeier, J., Thost, A.K., Kato, H., Mokranjac, D., Sauerwald, J., Martins, L.M., Woitalla, D., et al. (2014). Mitochondrial proteolytic stress induced by loss of mortalin function is rescued by Parkin and PINK1. Cell death & disease *5*, e1180.

Cagin, U., and Enriquez, J.A. (2015). The complex crosstalk between mitochondria and the nucleus: What goes in between? The international journal of biochemistry & cell biology *63*, 10-15.

Cagnoli, C., Stevanin, G., Brussino, A., Barberis, M., Mancini, C., Margolis, R.L., Holmes, S.E., Nobili, M., Forlani, S., Padovan, S., et al. (2010). Missense mutations in the AFG3L2 proteolytic domain account for approximately 1.5% of European autosomal dominant cerebellar ataxias. Human mutation *31*, 1117-1124.

Cha, S.S., An, Y.J., Lee, C.R., Lee, H.S., Kim, Y.G., Kim, S.J., Kwon, K.K., De Donatis, G.M., Lee, J.H., Maurizi, M.R., et al. (2010). Crystal structure of Lon protease: molecular architecture of gated entry to a sequestered degradation chamber. The EMBO journal *29*, 3520-3530.

Chacinska, A., Koehler, C.M., Milenkovic, D., Lithgow, T., and Pfanner, N. (2009). Importing mitochondrial proteins: machineries and mechanisms. Cell *138*, 628-644.

Chacinska, A., Lind, M., Frazier, A.E., Dudek, J., Meisinger, C., Geissler, A., Sickmann, A., Meyer, H.E., Truscott, K.N., Guiard, B., et al. (2005). Mitochondrial presequence translocase: switching between TOM tethering and motor recruitment involves Tim21 and Tim17. Cell *120*, 817-829.

Chacinska, A., Pfannschmidt, S., Wiedemann, N., Kozjak, V., Sanjuan Szklarz, L.K., Schulze-Specking, A., Truscott, K.N., Guiard, B., Meisinger, C., and Pfanner, N. (2004). Essential role of Mia40 in import and assembly of mitochondrial intermembrane space proteins. The EMBO journal *23*, 3735-3746.

Cheng, C.W., Kuo, C.Y., Fan, C.C., Fang, W.C., Jiang, S.S., Lo, Y.K., Wang, T.Y., Kao, M.C., and Lee, A.Y. (2013). Overexpression of Lon contributes to survival and aggressive phenotype of cancer cells through mitochondrial complex I-mediated generation of reactive oxygen species. Cell death & disease *4*, e681.

Cheng, M.Y., Hartl, F.U., Martin, J., Pollock, R.A., Kalousek, F., Neupert, W., Hallberg, E.M., Hallberg, R.L., and Horwich, A.L. (1989). Mitochondrial heat-shock protein hsp60 is essential for assembly of proteins imported into yeast mitochondria. Nature *337*, 620-625.

Christian, B.E., and Spremulli, L.L. (2009). Evidence for an active role of IF3mt in the initiation of translation in mammalian mitochondria. Biochemistry *48*, 3269-3278.

Christian, B.E., and Spremulli, L.L. (2012). Mechanism of protein biosynthesis in mammalian mitochondria. Biochimica et biophysica acta *1819*, 1035-1054.

Chrzanowska-Lightowlers, Z.M., Pajak, A., and Lightowlers, R.N. (2011). Termination of protein synthesis in mammalian mitochondria. The Journal of biological chemistry *286*, 34479-34485.

Chung, C.T., and Miller, R.H. (1988). A rapid and convenient method for the preparation and storage of competent bacterial cells. Nucleic acids research *16*, 3580.

Claros, M.G., and Vincens, P. (1996). Computational method to predict mitochondrially imported proteins and their targeting sequences. European journal of biochemistry / FEBS *241*, 779-786.

Clay Montier, L.L., Deng, J.J., and Bai, Y. (2009). Number matters: control of mammalian mitochondrial DNA copy number. Journal of genetics and genomics = Yi chuan xue bao *36*, 125-131.

Clayton, D.A. (2003). Mitochondrial DNA replication: what we know. IUBMB life *55*, 213-217.

Cole, A., Wang, Z., Coyaud, E., Voisin, V., Gronda, M., Jitkova, Y., Mattson, R., Hurren, R., Babovic, S., Maclean, N., et al. (2015). Inhibition of the Mitochondrial Protease ClpP as a Therapeutic Strategy for Human Acute Myeloid Leukemia. Cancer cell *27*, 864-876.

Cora, D., Di Cunto, F., Provero, P., Silengo, L., and Caselle, M. (2004). Computational identification of transcription factor binding sites by functional analysis of sets of genes sharing overrepresented upstream motifs. BMC bioinformatics *5*, 57.

Cortopassi, G., Danielson, S., Alemi, M., Zhan, S.S., Tong, W., Carelli, V., Martinuzzi, A., Marzuki, S., Majamaa, K., and Wong, A. (2006). Mitochondrial disease activates transcripts of the unfolded protein response and cell cycle and inhibits vesicular secretion and oligodendrocyte-specific transcripts. Mitochondrion *6*, 161-175.

Cox, J., and Mann, M. (2008). MaxQuant enables high peptide identification rates, individualized p.p.b.-range mass accuracies and proteome-wide protein quantification. Nature biotechnology *26*, 1367-1372.

Cox, J., and Mann, M. (2012). 1D and 2D annotation enrichment: a statistical method integrating quantitative proteomics with complementary high-throughput data. BMC bioinformatics *13 Suppl 16*, S12.

Cox, J., Neuhauser, N., Michalski, A., Scheltema, R.A., Olsen, J.V., and Mann, M. (2011). Andromeda: a peptide search engine integrated into the MaxQuant environment. Journal of proteome research *10*, 1794-1805.

Craig, E.A., Kramer, J., and Kosic-Smithers, J. (1987). SSC1, a member of the 70-kDa heat shock protein multigene family of Saccharomyces cerevisiae, is essential for growth. Proceedings of the National Academy of Sciences of the United States of America *84*, 4156-4160.

Curran, S.P., Leuenberger, D., Oppliger, W., and Koehler, C.M. (2002). The Tim9p-Tim10p complex binds to the transmembrane domains of the ADP/ATP carrier. The EMBO journal *21*, 942-953.

Darlington, G.J., Bernhard, H.P., Miller, R.A., and Ruddle, F.H. (1980). Expression of liver phenotypes in cultured mouse hepatoma cells. Journal of the National Cancer Institute *64*, 809-819.

DeLuca, S.Z., and O'Farrell, P.H. (2012). Barriers to male transmission of mitochondrial DNA in sperm development. Developmental cell *22*, 660-668.

Deocaris, C.C., Kaul, S.C., and Wadhwa, R. (2006). On the brotherhood of the mitochondrial chaperones mortalin and heat shock protein 60. Cell stress & chaperones *11*, 116-128.

Desautels, M., and Goldberg, A.L. (1982). Demonstration of an ATP-dependent, vanadate-sensitive endoprotease in the matrix of rat liver mitochondria. The Journal of biological chemistry *257*, 11673-11679.

Dey, S., Baird, T.D., Zhou, D., Palam, L.R., Spandau, D.F., and Wek, R.C. (2010). Both transcriptional regulation and translational control of ATF4 are central to the integrated stress response. The Journal of biological chemistry *285*, 33165-33174.

Di Bella, D., Lazzaro, F., Brusco, A., Plumari, M., Battaglia, G., Pastore, A., Finardi, A., Cagnoli, C., Tempia, F., Frontali, M., et al. (2010). Mutations in the mitochondrial protease gene AFG3L2 cause dominant hereditary ataxia SCA28. Nature genetics *42*, 313-321.

Dimmer, K.S., Papic, D., Schumann, B., Sperl, D., Krumpe, K., Walther, D.M., and Rapaport, D. (2012). A crucial role for Mim2 in the biogenesis of mitochondrial outer membrane proteins. Journal of cell science *125*, 3464-3473.

Dogan, S.A., Pujol, C., Maiti, P., Kukat, A., Wang, S., Hermans, S., Senft, K., Wibom, R., Rugarli, E.I., and Trifunovic, A. (2014). Tissue-specific loss of DARS2 activates stress responses independently of respiratory chain deficiency in the heart. Cell metabolism *19*, 458-469.

Dubaquie, Y., Looser, R., Funfschilling, U., Jeno, P., and Rospert, S. (1998). Identification of in vivo substrates of the yeast mitochondrial chaperonins reveals overlapping but non-identical requirement for hsp60 and hsp10. The EMBO journal *17*, 5868-5876.

Edgar, D., Shabalina, I., Camara, Y., Wredenberg, A., Calvaruso, M.A., Nijtmans, L., Nedergaard, J., Cannon, B., Larsson, N.G., and Trifunovic, A. (2009). Random point mutations with major effects on protein-coding genes are the driving force behind premature aging in mtDNA mutator mice. Cell metabolism *10*, 131-138.

Edvardson, S., Shaag, A., Kolesnikova, O., Gomori, J.M., Tarassov, I., Einbinder, T., Saada, A., and Elpeleg, O. (2007). Deleterious mutation in the mitochondrial arginyl-transfer RNA synthetase gene is associated with pontocerebellar hypoplasia. American journal of human genetics *81*, 857-862.

Elo, J.M., Yadavalli, S.S., Euro, L., Isohanni, P., Gotz, A., Carroll, C.J., Valanne, L., Alkuraya, F.S., Uusimaa, J., Paetau, A., et al. (2012). Mitochondrial phenylalanyl-tRNA synthetase mutations underlie fatal infantile Alpers encephalopathy. Human molecular genetics *21*, 4521-4529.

Endres, M., Neupert, W., and Brunner, M. (1999). Transport of the ADP/ATP carrier of mitochondria from the TOM complex to the TIM22.54 complex. The EMBO journal *18*, 3214-3221.

Ernster, L., and Schatz, G. (1981). Mitochondria: A historical review. J. Cell Biol. *91*, 227s-255s.

Evstafieva, A.G., Garaeva, A.A., Khutornenko, A.A., Klepikova, A.V., Logacheva, M.D., Penin, A.A., Novakovsky, G.E., Kovaleva, I.E., and Chumakov, P.M. (2014). A sustained deficiency of mitochondrial respiratory complex III induces an apoptotic cell death through the p53-mediated inhibition of pro-survival activities of the activating transcription factor 4. Cell death & disease *5*, e1511.

Fender, A., Gaudry, A., Juhling, F., Sissler, M., and Florentz, C. (2012). Adaptation of aminoacylation identity rules to mammalian mitochondria. Biochimie *94*, 1090-1097.

Fender, A., Sauter, C., Messmer, M., Putz, J., Giege, R., Florentz, C., and Sissler, M. (2006). Loss of a primordial identity element for a mammalian mitochondrial aminoacylation system. The Journal of biological chemistry *281*, 15980-15986.

Feng, J., Bussiere, F., and Hekimi, S. (2001). Mitochondrial electron transport is a key determinant of life span in Caenorhabditis elegans. Developmental cell *1*, 633-644.

Fenton, W.A., Weissman, J.S., and Horwich, A.L. (1996). Putting a lid on protein folding: structure and function of the co-chaperonin, GroES. Chemistry & biology *3*, 157-161.

Fischer, F., Hamann, A., and Osiewacz, H.D. (2012). Mitochondrial quality control: an integrated network of pathways. Trends in biochemical sciences *37*, 284-292.

Fujita, Y., Ito, M., Nozawa, Y., Yoneda, M., Oshida, Y., and Tanaka, M. (2007). CHOP (C/EBP homologous protein) and ASNS (asparagine synthetase) induction in cybrid cells harboring MELAS and NARP mitochondrial DNA mutations. Mitochondrion *7*, 80-88.

Fukuda, R., Zhang, H., Kim, J.W., Shimoda, L., Dang, C.V., and Semenza, G.L. (2007). HIF-1 regulates cytochrome oxidase subunits to optimize efficiency of respiration in hypoxic cells. Cell *129*, 111-122.

Galluzzi, L., Kepp, O., and Kroemer, G. (2012). Mitochondria: master regulators of danger signalling. Nature reviews. Molecular cell biology *13*, 780-788.

Gambill, B.D., Voos, W., Kang, P.J., Miao, B., Langer, T., Craig, E.A., and Pfanner, N. (1993). A dual role for mitochondrial heat shock protein 70 in membrane translocation of preproteins. The Journal of cell biology *123*, 109-117.

Gerdes, F., Tatsuta, T., and Langer, T. (2012). Mitochondrial AAA proteases--towards a molecular understanding of membrane-bound proteolytic machines. Biochimica et biophysica acta *1823*, 49-55.

Ghosh, J.C., Dohi, T., Kang, B.H., and Altieri, D.C. (2008). Hsp60 regulation of tumor cell apoptosis. The Journal of biological chemistry *283*, 5188-5194.

Gispert, S., Parganlija, D., Klinkenberg, M., Drose, S., Wittig, I., Mittelbronn, M., Grzmil, P., Koob, S., Hamann, A., Walter, M., et al. (2013). Loss of mitochondrial peptidase Clpp leads to infertility, hearing loss plus growth retardation via accumulation of CLPX, mtDNA and inflammatory factors. Human molecular genetics *22*, 4871-4887.

Glick, B.S., Brandt, A., Cunningham, K., Muller, S., Hallberg, R.L., and Schatz, G. (1992). Cytochromes c1 and b2 are sorted to the intermembrane space of yeast mitochondria by a stop-transfer mechanism. Cell *69*, 809-822.

Gluzman, Y. (1981). SV40-transformed simian cells support the replication of early SV40 mutants. Cell *23*, 175-182.

Goldberg, A.L., and Waxman, L. (1985). The role of ATP hydrolysis in the breakdown of proteins and peptides by protease La from Escherichia coli. The Journal of biological chemistry *260*, 12029-12034.

Gottesman, S. (1996). Proteases and their targets in Escherichia coli. Annual review of genetics *30*, 465-506.

Gottesman, S., Roche, E., Zhou, Y., and Sauer, R.T. (1998). The ClpXP and ClpAP proteases degrade proteins with carboxy-terminal peptide tails added by the SsrA-tagging system. Genes & development *12*, 1338-1347.

Gotz, A., Tyynismaa, H., Euro, L., Ellonen, P., Hyotylainen, T., Ojala, T., Hamalainen, R.H., Tommiska, J., Raivio, T., Oresic, M., et al. (2011). Exome sequencing identifies mitochondrial alanyl-tRNA synthetase mutations in infantile mitochondrial cardiomyopathy. American journal of human genetics *88*, 635-642.

Granot, Z., Kobiler, O., Melamed-Book, N., Eimerl, S., Bahat, A., Lu, B., Braun, S., Maurizi, M.R., Suzuki, C.K., Oppenheim, A.B., et al. (2007). Turnover of mitochondrial steroidogenic acute regulatory (StAR) protein by Lon protease: the unexpected effect of proteasome inhibitors. Molecular endocrinology *21*, 2164-2177.

Gray, M.W., Burger, G., and Lang, B.F. (1999). Mitochondrial evolution. Science *283*, 1476-1481.

Greber, B.J., Bieri, P., Leibundgut, M., Leitner, A., Aebersold, R., Boehringer, D., and Ban, N. (2015). Ribosome. The complete structure of the 55S mammalian mitochondrial ribosome. Science *348*, 303-308.

Greber, B.J., Boehringer, D., Leibundgut, M., Bieri, P., Leitner, A., Schmitz, N., Aebersold, R., and Ban, N. (2014). The complete structure of the large subunit of the mammalian mitochondrial ribosome. Nature *515*, 283-286.

Greene, L.A., Lee, H.Y., and Angelastro, J.M. (2009). The transcription factor ATF5: role in neurodevelopment and neural tumors. Journal of neurochemistry *108*, 11-22.

Griparic, L., Kanazawa, T., and van der Bliek, A.M. (2007). Regulation of the mitochondrial dynamin-like protein Opa1 by proteolytic cleavage. The Journal of cell biology *178*, 757-764.

Grohmann, K., Amairic, F., Crews, S., and Attardi, G. (1978). Failure to detect "cap" structures in mitochondrial DNA-coded poly(A)-containing RNA from HeLa cells. Nucleic acids research *5*, 637-651.

Guo, M., and Schimmel, P. (2013). Essential nontranslational functions of tRNA synthetases. Nature chemical biology *9*, 145-153.

Halliwell, B. (2014). Cell culture, oxidative stress, and antioxidants: avoiding pitfalls. Biomedical journal *37*, 99-105.

Hansen, J., Corydon, T.J., Palmfeldt, J., Durr, A., Fontaine, B., Nielsen, M.N., Christensen, J.H., Gregersen, N., and Bross, P. (2008). Decreased expression of the mitochondrial matrix proteases Lon and ClpP in cells from a patient with hereditary spastic paraplegia (SPG13). Neuroscience *153*, 474-482.

Hansen, J., Svenstrup, K., Ang, D., Nielsen, M.N., Christensen, J.H., Gregersen, N., Nielsen, J.E., Georgopoulos, C., and Bross, P. (2007). A novel mutation in the HSPD1 gene in a patient with hereditary spastic paraplegia. J Neurol *254*, 897-900.

Hansen, J.J., Bross, P., Westergaard, M., Nielsen, M.N., Eiberg, H., Borglum, A.D., Mogensen, J., Kristiansen, K., Bolund, L., and Gregersen, N. (2003). Genomic structure of the human mitochondrial chaperonin genes: HSP60 and HSP10 are localised head to head on chromosome 2 separated by a bidirectional promoter. Human genetics *112*, 71-77.

Hansen, J.J., Durr, A., Cournu-Rebeix, I., Georgopoulos, C., Ang, D., Nielsen, M.N., Davoine, C.S., Brice, A., Fontaine, B., Gregersen, N., et al. (2002). Hereditary spastic paraplegia SPG13 is associated with a mutation in the gene encoding the mitochondrial chaperonin Hsp60. American journal of human genetics *70*, 1328-1332.

Haque, M.E., Grasso, D., and Spremulli, L.L. (2008). The interaction of mammalian mitochondrial translational initiation factor 3 with ribosomes: evolution of terminal extensions in IF3mt. Nucleic acids research *36*, 589-597.

Harbauer, A.B., Zahedi, R.P., Sickmann, A., Pfanner, N., and Meisinger, C. (2014). The protein import machinery of mitochondria-a regulatory hub in metabolism, stress, and disease. Cell metabolism *19*, 357-372.

Harding, H.P., Zhang, Y., and Ron, D. (1999). Protein translation and folding are coupled by an endoplasmic-reticulum-resident kinase. Nature *397*, 271-274.

Harding, H.P., Zhang, Y., Zeng, H., Novoa, I., Lu, P.D., Calfon, M., Sadri, N., Yun, C., Popko, B., Paules, R., et al. (2003). An integrated stress response regulates amino acid metabolism and resistance to oxidative stress. Molecular cell *11*, 619-633.

Harman, D. (1956). Aging: a theory based on free radical and radiation chemistry. J Gerontol *11*, 298-300.

Hartl, F.U., Bracher, A., and Hayer-Hartl, M. (2011). Molecular chaperones in protein folding and proteostasis. Nature *475*, 324-332.

Hatefi, Y. (1985). The mitochondrial electron transport and oxidative phosphorylation system. Ann. Rev. Biochem. *54*, 1015-1069.

Haynes, C.M., Petrova, K., Benedetti, C., Yang, Y., and Ron, D. (2007). ClpP mediates activation of a mitochondrial unfolded protein response in C. elegans. Developmental cell *13*, 467-480.

Haynes, C.M., Yang, Y., Blais, S.P., Neubert, T.A., and Ron, D. (2010). The matrix peptide exporter HAF-1 signals a mitochondrial UPR by activating the transcription factor ZC376.7 in C. elegans. Molecular cell *37*, 529-540.

He, S., and Fox, T.D. (1997). Membrane translocation of mitochondrially coded Cox2p: distinct requirements for export of N and C termini and dependence on the conserved protein Oxa1p. Molecular biology of the cell *8*, 1449-1460.

Hell, K., Herrmann, J.M., Pratje, E., Neupert, W., and Stuart, R.A. (1998). Oxa1p, an essential component of the N-tail protein export machinery in mitochondria. Proceedings of the National Academy of Sciences of the United States of America *95*, 2250-2255.

Helm, M., Giege, R., and Florentz, C. (1999). A Watson-Crick base-pair-disrupting methyl group (m1A9) is sufficient for cloverleaf folding of human mitochondrial tRNALys. Biochemistry *38*, 13338-13346.

Herrmann, J.M., Stuart, R.A., Craig, E.A., and Neupert, W. (1994). Mitochondrial heat shock protein 70, a molecular chaperone for proteins encoded by mitochondrial DNA. The Journal of cell biology *127*, 893-902.

Hetz, C., Chevet, E., and Oakes, S.A. (2015). Proteostasis control by the unfolded protein response. Nature cell biology *17*, 829-838.

Holmes, K., Williams, C.M., Chapman, E.A., and Cross, M.J. (2010). Detection of siRNA induced mRNA silencing by RT-qPCR: considerations for experimental design. BMC research notes *3*, 53.

Holt, I.J., Harding, A.E., and Morgan-Hughes, J.A. (1988). Deletions of muscle mitochondrial DNA in patients with mitochondrial myopathies. Nature *331*, 717-719.

Hori, O., Ichinoda, F., Tamatani, T., Yamaguchi, A., Sato, N., Ozawa, K., Kitao, Y., Miyazaki, M., Harding, H.P., Ron, D., et al. (2002). Transmission of cell stress from endoplasmic reticulum to mitochondria: enhanced expression of Lon protease. The Journal of cell biology *157*, 1151-1160.

Horibe, T., and Hoogenraad, N.J. (2007). The chop gene contains an element for the positive regulation of the mitochondrial unfolded protein response. PloS one *2*, e835.

Horst, M., Oppliger, W., Rospert, S., Schonfeld, H.J., Schatz, G., and Azem, A. (1997). Sequential action of two hsp70 complexes during protein import into mitochondria. The EMBO journal *16*, 1842-1849.

Houtkooper, R.H., Mouchiroud, L., Ryu, D., Moullan, N., Katsyuba, E., Knott, G., Williams, R.W., and Auwerx, J. (2013). Mitonuclear protein imbalance as a conserved longevity mechanism. Nature *497*, 451-457.

Ibba, M., and Soll, D. (2000). Aminoacyl-tRNA synthesis. Annual review of biochemistry *69*, 617-650.

Ishikawa, F., Akimoto, T., Yamamoto, H., Araki, Y., Yoshie, T., Mori, K., Hayashi, H., Nose, K., and Shibanuma, M. (2009). Gene expression profiling identifies a role for CHOP during inhibition of the mitochondrial respiratory chain. Journal of biochemistry *146*, 123-132.

Ito, K., and Akiyama, Y. (2005). Cellular functions, mechanism of action, and regulation of FtsH protease. Annual review of microbiology *59*, 211-231.

Jacobs, H.T., and Turnbull, D.M. (2005). Nuclear genes and mitochondrial translation: a new class of genetic disease. Trends in genetics : TIG *21*, 312-314.

Jaeschke, A., Karasarides, M., Ventura, J.J., Ehrhardt, A., Zhang, C., Flavell, R.A., Shokat, K.M., and Davis, R.J. (2006). JNK2 is a positive regulator of the cJun transcription factor. Molecular cell *23*, 899-911.

Jenkinson, E.M., Rehman, A.U., Walsh, T., Clayton-Smith, J., Lee, K., Morell, R.J., Drummond, M.C., Khan, S.N., Naeem, M.A., Rauf, B., et al. (2013). Perrault syndrome is caused by recessive mutations in CLPP, encoding a mitochondrial ATP-dependent chambered protease. American journal of human genetics *92*, 605-613.

Jensen, M.B., and Jasper, H. (2014). Mitochondrial proteostasis in the control of aging and longevity. Cell metabolism *20*, 214-225.

Jiang, S., Yan, C., Fang, Q.C., Shao, M.L., Zhang, Y.L., Liu, Y., Deng, Y.P., Shan, B., Liu, J.Q., Li, H.T., et al. (2014). Fibroblast growth factor 21 is regulated by the IRE1alpha-XBP1 branch of the unfolded protein response and counteracts endoplasmic reticulum stress-induced hepatic steatosis. The Journal of biological chemistry *289*, 29751-29765.

Jin, J., Hulette, C., Wang, Y., Zhang, T., Pan, C., Wadhwa, R., and Zhang, J. (2006). Proteomic identification of a stress protein, mortalin/mthsp70/GRP75: relevance to Parkinson disease. Molecular & cellular proteomics : MCP *5*, 1193-1204.

Jin, S.M., and Youle, R.J. (2013). The accumulation of misfolded proteins in the mitochondrial matrix is sensed by PINK1 to induce PARK2/Parkin-mediated mitophagy of polarized mitochondria. Autophagy *9*, 1750-1757.

Jones, C.N., Wilkinson, K.A., Hung, K.T., Weeks, K.M., and Spremulli, L.L. (2008). Lack of secondary structure characterizes the 5' ends of mammalian mitochondrial mRNAs. Rna *14*, 862-871.

Jovaisaite, V., and Auwerx, J. (2015). The mitochondrial unfolded protein response-synchronizing genomes. Current opinion in cell biology *33*, 74-81.

Kang, S.G., Dimitrova, M.N., Ortega, J., Ginsburg, A., and Maurizi, M.R. (2005). Human mitochondrial ClpP is a stable heptamer that assembles into a tetradecamer in the presence of ClpX. The Journal of biological chemistry *280*, 35424-35432.

Kang, S.G., Maurizi, M.R., Thompson, M., Mueser, T., and Ahvazi, B. (2004). Crystallography and mutagenesis point to an essential role for the N-terminus of human mitochondrial ClpP. Journal of structural biology *148*, 338-352.

Kang, S.G., Ortega, J., Singh, S.K., Wang, N., Huang, N.N., Steven, A.C., and Maurizi, M.R. (2002). Functional proteolytic complexes of the human mitochondrial ATP-dependent protease, hClpXP. The Journal of biological chemistry *277*, 21095-21102.

Kao, T.Y., Chiu, Y.C., Fang, W.C., Cheng, C.W., Kuo, C.Y., Juan, H.F., Wu, S.H., and Lee, A.Y. (2015). Mitochondrial Lon regulates apoptosis through the association with Hsp60-mtHsp70 complex. Cell death & disease *6*, e1642.

Khassaf, M., McArdle, A., Esanu, C., Vasilaki, A., McArdle, F., Griffiths, R.D., Brodie, D.A., and Jackson, M.J. (2003). Effect of vitamin C supplements on antioxidant defence and stress proteins in human lymphocytes and skeletal muscle. The Journal of physiology *549*, 645-652.

Kimura, K., Tanaka, N., Nakamura, N., Takano, S., and Ohkuma, S. (2007). Knockdown of mitochondrial heat shock protein 70 promotes progeria-like phenotypes in caenorhabditis elegans. The Journal of biological chemistry *282*, 5910-5918.

Kincaid, B., and Bossy-Wetzel, E. (2013). Forever young: SIRT3 a shield against mitochondrial meltdown, aging, and neurodegeneration. Frontiers in aging neuroscience *5*, 48.

King, M.P., and Attardi, G. (1989). Human cells lacking mtDNA: repopulation with exogenous mitochondria by complementation. Science *246*, 500-503.

Koc, E.C., and Spremulli, L.L. (2002). Identification of mammalian mitochondrial translational initiation factor 3 and examination of its role in initiation complex formation with natural mRNAs. The Journal of biological chemistry *277*, 35541-35549.

Konovalova, S., and Tyynismaa, H. (2013). Mitochondrial aminoacyl-tRNA synthetases in human disease. Molecular genetics and metabolism *108*, 206-211.

Koppen, M., Metodiev, M.D., Casari, G., Rugarli, E.I., and Langer, T. (2007). Variable and tissue-specific subunit composition of mitochondrial m-AAA protease complexes linked to hereditary spastic paraplegia. Molecular and cellular biology *27*, 758-767.

Kronidou, N.G., Oppliger, W., Bolliger, L., Hannavy, K., Glick, B.S., Schatz, G., and Horst, M. (1994). Dynamic interaction between Isp45 and mitochondrial hsp70 in the protein import system of the yeast mitochondrial inner membrane. Proceedings of the National Academy of Sciences of the United States of America *91*, 12818-12822.

Krumpe, K., Frumkin, I., Herzig, Y., Rimon, N., Ozbalci, C., Brugger, B., Rapaport, D., and Schuldiner, M. (2012). Ergosterol content specifies targeting of tail-anchored proteins to mitochondrial outer membranes. Molecular biology of the cell *23*, 3927-3935.

Kukat, C., Wurm, C.A., Spahr, H., Falkenberg, M., Larsson, N.G., and Jakobs, S. (2011). Super-resolution microscopy reveals that mammalian mitochondrial nucleoids have a uniform size and frequently contain a single copy of mtDNA. Proceedings of the National Academy of Sciences of the United States of America *108*, 13534-13539.

Kumazawa, Y., Himeno, H., Miura, K., and Watanabe, K. (1991). Unilateral aminoacylation specificity between bovine mitochondria and eubacteria. Journal of biochemistry *109*, 421-427.

Kurland, C.G., and Andersson, S.G. (2000). Origin and evolution of the mitochondrial proteome. Microbiology and molecular biology reviews : MMBR *64*, 786-820.

Kutik, S., Stojanovski, D., Becker, L., Becker, T., Meinecke, M., Kruger, V., Prinz, C., Meisinger, C., Guiard, B., Wagner, R., et al. (2008). Dissecting membrane insertion of mitochondrial beta-barrel proteins. Cell *132*, 1011-1024.

Laemmli, U.K. (1970). Cleavage of structural proteins during the assembly of the head of bacteriophage T4. Nature *227*, 680-685.

Langer, T., and Neupert, W. (1991). Heat shock proteins hsp60 and hsp70: their roles in folding, assembly and membrane translocation of proteins. Current topics in microbiology and immunology *167*, 3-30.

Larsson, N.G. (2010). Somatic mitochondrial DNA mutations in mammalian aging. Annual review of biochemistry *79*, 683-706.

Larsson, N.G., Wang, J., Wilhelmsson, H., Oldfors, A., Rustin, P., Lewandoski, M., Barsh, G.S., and Clayton, D.A. (1998). Mitochondrial transcription factor A is necessary for mtDNA maintenance and embryogenesis in mice. Nat. Genet. *18*, 231-236.

Lazarou, M., Jin, S.M., Kane, L.A., and Youle, R.J. (2012). Role of PINK1 binding to the TOM complex and alternate intracellular membranes in recruitment and activation of the E3 ligase Parkin. Developmental cell *22*, 320-333.

Lemieux, H., Semsroth, S., Antretter, H., Hofer, D., and Gnaiger, E. (2011). Mitochondrial respiratory control and early defects of oxidative phosphorylation in the failing human heart. The international journal of biochemistry & cell biology *43*, 1729-1738.

Leonhard, K., Guiard, B., Pellecchia, G., Tzagoloff, A., Neupert, W., and Langer, T. (2000). Membrane protein degradation by AAA proteases in mitochondria: extraction of substrates from either membrane surface. Molecular cell *5*, 629-638.

Leonhard, K., Herrmann, J.M., Stuart, R.A., Mannhaupt, G., Neupert, W., and Langer, T. (1996). AAA proteases with catalytic sites on opposite membrane surfaces comprise a proteolytic system for the ATP-dependent degradation of inner membrane proteins in mitochondria. The EMBO journal *15*, 4218-4229.

Leonhard, K., Stiegler, A., Neupert, W., and Langer, T. (1999). Chaperone-like activity of the AAA domain of the yeast Yme1 AAA protease. Nature *398*, 348-351.

Li, Y., Dudek, J., Guiard, B., Pfanner, N., Rehling, P., and Voos, W. (2004). The presequence translocase-associated protein import motor of mitochondria. Pam16 functions in an antagonistic manner to Pam18. The Journal of biological chemistry *279*, 38047-38054.

Lianos, G.D., Alexiou, G.A., Mangano, A., Mangano, A., Rausei, S., Boni, L., Dionigi, G., and Roukos, D.H. (2015). The role of heat shock proteins in cancer. Cancer letters *360*, 114-118.

Liao, H.X., and Spremulli, L.L. (1990). Identification and initial characterization of translational initiation factor 2 from bovine mitochondria. The Journal of biological chemistry *265*, 13618-13622.

Lill, R., and Muhlenhoff, U. (2008). Maturation of iron-sulfur proteins in eukaryotes: mechanisms, connected processes, and diseases. Annual review of biochemistry *77*, 669-700.

Lim, J.H., Martin, F., Guiard, B., Pfanner, N., and Voos, W. (2001). The mitochondrial Hsp70-dependent import system actively unfolds preproteins and shortens the lag phase of translocation. The EMBO journal *20*, 941-950.

Lindquist, S. (1986). The heat-shock response. Annual review of biochemistry *55*, 1151-1191.

Liu, Q., Krzewska, J., Liberek, K., and Craig, E.A. (2001). Mitochondrial Hsp70 Ssc1: role in protein folding. The Journal of biological chemistry *276*, 6112-6118.

Lowth, B.R., Kirstein-Miles, J., Saiyed, T., Brotz-Oesterhelt, H., Morimoto, R.I., Truscott, K.N., and Dougan, D.A. (2012). Substrate recognition and processing by a Walker B mutant of the human mitochondrial AAA+ protein CLPX. Journal of structural biology *179*, 193-201.

Luce, K., and Osiewacz, H.D. (2009). Increasing organismal healthspan by enhancing mitochondrial protein quality control. Nature cell biology *11*, 852-858.

Lyons, G.E., Muhlebach, S., Moser, A., Masood, R., Paterson, B.M., Buckingham, M.E., and Perriard, J.C. (1991). Developmental regulation of creatine kinase gene expression by myogenic factors in embryonic mouse and chick skeletal muscle. Development *113*, 1017-1029.

Ma, J., and Spremulli, L.L. (1996). Expression, purification, and mechanistic studies of bovine mitochondrial translational initiation factor 2. The Journal of biological chemistry *271*, 5805-5811.

Madarampalli, B., Yuan, Y., Liu, D., Lengel, K., Xu, Y., Li, G., Yang, J., Liu, X., Lu, Z., and Liu, D.X. (2015). ATF5 Connects the Pericentriolar Materials to the Proximal End of the Mother Centriole. Cell *162*, 580-592.

Magen, D., Georgopoulos, C., Bross, P., Ang, D., Segev, Y., Goldsher, D., Nemirovski, A., Shahar, E., Ravid, S., Luder, A., et al. (2008). Mitochondrial hsp60 chaperonopathy causes an autosomal-recessive neurodegenerative disorder linked to brain hypomyelination and leukodystrophy. American journal of human genetics *83*, 30-42.

Mapa, K., Sikor, M., Kudryavtsev, V., Waegemann, K., Kalinin, S., Seidel, C.A., Neupert, W., Lamb, D.C., and Mokranjac, D. (2010). The conformational dynamics of the mitochondrial Hsp70 chaperone. Molecular cell *38*, 89-100.

Margulis, L. (1970). Origin of eukaryotic cells. Yale University Press, New Haven, Conn.

Marintchev, A., and Wagner, G. (2004). Translation initiation: structures, mechanisms and evolution. Quarterly reviews of biophysics *37*, 197-284.

Martin, J. (1997). Molecular chaperones and mitochondrial protein folding. Journal of bioenergetics and biomembranes *29*, 35-43.

Martin, J., Mahlke, K., and Pfanner, N. (1991). Role of an energized inner membrane in mitochondrial protein import. Delta psi drives the movement of presequences. The Journal of biological chemistry *266*, 18051-18057.

Martin, J., Mayhew, M., Langer, T., and Hartl, F.U. (1993). The reaction cycle of GroEL and GroES in chaperonin-assisted protein folding. Nature *366*, 228-233.

Martindale, J.L., and Holbrook, N.J. (2002). Cellular response to oxidative stress: signaling for suicide and survival. Journal of cellular physiology *192*, 1-15.

Martinelli, P., La Mattina, V., Bernacchia, A., Magnoni, R., Cerri, F., Cox, G., Quattrini, A., Casari, G., and Rugarli, E.I. (2009). Genetic interaction between the m-AAA protease isoenzymes reveals novel roles in cerebellar degeneration. Human molecular genetics *18*, 2001-2013.

Martinelli, P., and Rugarli, E.I. (2010). Emerging roles of mitochondrial proteases in neurodegeneration. Biochimica et biophysica acta *1797*, 1-10.

Martinus, R.D., Garth, G.P., Webster, T.L., Cartwright, P., Naylor, D.J., Hoj, P.B., and Hoogenraad, N.J. (1996). Selective induction of mitochondrial chaperones in response to loss of the mitochondrial genome. European journal of biochemistry / FEBS *240*, 98-103.

Marzetti, E., Csiszar, A., Dutta, D., Balagopal, G., Calvani, R., and Leeuwenburgh, C. (2013). Role of mitochondrial dysfunction and altered autophagy in cardiovascular aging

and disease: from mechanisms to therapeutics. American journal of physiology. Heart and circulatory physiology *305*, H459-476.

Matsushima, Y., Goto, Y., and Kaguni, L.S. (2010). Mitochondrial Lon protease regulates mitochondrial DNA copy number and transcription by selective degradation of mitochondrial transcription factor A (TFAM). Proceedings of the National Academy of Sciences of the United States of America *107*, 18410-18415.

McBride, H.M., Neuspiel, M., and Wasiak, S. (2006). Mitochondria: more than just a powerhouse. Current biology : CB *16*, R551-560.

McCullough, K.D., Martindale, J.L., Klotz, L.O., Aw, T.Y., and Holbrook, N.J. (2001). Gadd153 sensitizes cells to endoplasmic reticulum stress by down-regulating Bcl2 and perturbing the cellular redox state. Molecular and cellular biology *21*, 1249-1259.

McFarland, R., Kirby, D.M., Fowler, K.J., Ohtake, A., Ryan, M.T., Amor, D.J., Fletcher, J.M., Dixon, J.W., Collins, F.A., Turnbull, D.M., et al. (2004). De novo mutations in the mitochondrial ND3 gene as a cause of infantile mitochondrial encephalopathy and complex I deficiency. Annals of neurology *55*, 58-64.

McLean, J.R., Cohn, G.L., Brandt, I.K., and Simpson, M.V. (1958). Incorporation of labeled amino acids into the protein of muscle and liver mitochondria. The Journal of biological chemistry *233*, 657-663.

Mears, J.A., Cannone, J.J., Stagg, S.M., Gutell, R.R., Agrawal, R.K., and Harvey, S.C. (2002). Modeling a minimal ribosome based on comparative sequence analysis. Journal of molecular biology *321*, 215-234.

Mears, J.A., Sharma, M.R., Gutell, R.R., McCook, A.S., Richardson, P.E., Caulfield, T.R., Agrawal, R.K., and Harvey, S.C. (2006). A structural model for the large subunit of the mammalian mitochondrial ribosome. Journal of molecular biology *358*, 193-212.

Meier, S., Neupert, W., and Herrmann, J.M. (2005). Proline residues of transmembrane domains determine the sorting of inner membrane proteins in mitochondria. The Journal of cell biology *170*, 881-888.

Meineke, B., Engl, G., Kemper, C., Vasiljev-Neumeyer, A., Paulitschke, H., and Rapaport, D. (2008). The outer membrane form of the mitochondrial protein Mcr1 follows a TOM-independent membrane insertion pathway. FEBS letters *582*, 855-860.

Meriin, A.B., Mense, M., Colbert, J.D., Liang, F., Bihler, H., Zaarur, N., Rock, K.L., and Sherman, M.Y. (2012a). A novel approach to recovery of function of mutant proteins by slowing down translation. The Journal of biological chemistry *287*, 34264-34272.

Meriin, A.B., Zaarur, N., and Sherman, M.Y. (2012b). Association of translation factor eEF1A with defective ribosomal products generates a signal for aggresome formation. Journal of cell science *125*, 2665-2674.

Mi, H., Dong, Q., Muruganujan, A., Gaudet, P., Lewis, S., and Thomas, P.D. (2010). PANTHER version 7: improved phylogenetic trees, orthologs and collaboration with the Gene Ontology Consortium. Nucleic acids research *38*, D204-210.

Michel, S., Canonne, M., Arnould, T., and Renard, P. (2015). Inhibition of mitochondrial genome expression triggers the activation of CHOP-10 by a cell signaling dependent on the integrated stress response but not the mitochondrial unfolded protein response. Mitochondrion *21*, 58-68.

Mikelsaar, R. (1983). Human mitochondrial genome and the evolution of methionine transfer ribonucleic acids. Journal of theoretical biology *105*, 221-232.

Miller, W.L. (2013). Steroid hormone synthesis in mitochondria. Molecular and cellular endocrinology *379*, 62-73.

Mitsumoto, A., Takeuchi, A., Okawa, K., and Nakagawa, Y. (2002). A subset of newly synthesized polypeptides in mitochondria from human endothelial cells exposed to hydroperoxide stress. Free radical biology & medicine *32*, 22-37.

Moisoi, N., Klupsch, K., Fedele, V., East, P., Sharma, S., Renton, A., Plun-Favreau, H., Edwards, R.E., Teismann, P., Esposti, M.D., et al. (2009). Mitochondrial dysfunction triggered by loss of HtrA2 results in the activation of a brain-specific transcriptional stress response. Cell death and differentiation *16*, 449-464.

Mokranjac, D., Sichting, M., Neupert, W., and Hell, K. (2003). Tim14, a novel key component of the import motor of the TIM23 protein translocase of mitochondria. The EMBO journal *22*, 4945-4956.

Montoya, J., Ojala, D., and Attardi, G. (1981). Distinctive features of the 5´-terminal sequences of the human mitochondrial mRNAs. Nature *290*, 465-470.

Mori, K. (2009). Signalling pathways in the unfolded protein response: development from yeast to mammals. Journal of biochemistry *146*, 743-750.

Morino, H., Pierce, S.B., Matsuda, Y., Walsh, T., Ohsawa, R., Newby, M., Hiraki-Kamon, K., Kuramochi, M., Lee, M.K., Klevit, R.E., et al. (2014). Mutations in Twinkle primase-helicase cause Perrault syndrome with neurologic features. Neurology *83*, 2054-2061.

Moro, F., Okamoto, K., Donzeau, M., Neupert, W., and Brunner, M. (2002). Mitochondrial protein import: molecular basis of the ATP-dependent interaction of MtHsp70 with Tim44. The Journal of biological chemistry *277*, 6874-6880.

Mouchiroud, L., Houtkooper, R.H., Moullan, N., Katsyuba, E., Ryu, D., Canto, C., Mottis, A., Jo, Y.S., Viswanathan, M., Schoonjans, K., et al. (2013). The NAD(+)/Sirtuin Pathway Modulates Longevity through Activation of Mitochondrial UPR and FOXO Signaling. Cell *154*, 430-441.

Munkacsy, E., and Rea, S.L. (2014). The paradox of mitochondrial dysfunction and extended longevity. Exp Gerontol *56*, 221-233.

Nagao, A., Suzuki, T., Katoh, T., Sakaguchi, Y., and Suzuki, T. (2009). Biogenesis of glutaminyl-mt tRNAGln in human mitochondria. Proceedings of the National Academy of Sciences of the United States of America *106*, 16209-16214.

Narendra, D., Tanaka, A., Suen, D.F., and Youle, R.J. (2008). Parkin is recruited selectively to impaired mitochondria and promotes their autophagy. The Journal of cell biology *183*, 795-803.

Narendra, D.P., Jin, S.M., Tanaka, A., Suen, D.F., Gautier, C.A., Shen, J., Cookson, M.R., and Youle, R.J. (2010). PINK1 is selectively stabilized on impaired mitochondria to activate Parkin. PLoS biology *8*, e1000298.

Nargund, A.M., Fiorese, C.J., Pellegrino, M.W., Deng, P., and Haynes, C.M. (2015). Mitochondrial and nuclear accumulation of the transcription factor ATFS-1 promotes OXPHOS recovery during the UPR(mt). Molecular cell *58*, 123-133.

Nargund, A.M., Pellegrino, M.W., Fiorese, C.J., Baker, B.M., and Haynes, C.M. (2012). Mitochondrial import efficiency of ATFS-1 regulates mitochondrial UPR activation. Science *337*, 587-590.

Neupert, W., and Brunner, M. (2002). The protein import motor of mitochondria. Nature reviews. Molecular cell biology *3*, 555-565.

Neupert, W., and Herrmann, J.M. (2007). Translocation of proteins into mitochondria. Annual review of biochemistry *76*, 723-749.

Ngo, J.K., and Davies, K.J. (2007). Importance of the lon protease in mitochondrial maintenance and the significance of declining lon in aging. Annals of the New York Academy of Sciences *1119*, 78-87.

Ngo, J.K., and Davies, K.J. (2009). Mitochondrial Lon protease is a human stress protein. Free radical biology & medicine *46*, 1042-1048.

Nishitoh, H. (2012). CHOP is a multifunctional transcription factor in the ER stress response. Journal of biochemistry *151*, 217-219.

Nolden, M., Ehses, S., Koppen, M., Bernacchia, A., Rugarli, E.I., and Langer, T. (2005). The m-AAA protease defective in hereditary spastic paraplegia controls ribosome assembly in mitochondria. Cell *123*, 277-289.

Nunnari, J., and Suomalainen, A. (2012). Mitochondria: in sickness and in health. Cell *148*, 1145-1159.

Osawa, S., Jukes, T.H., Watanabe, K., and Muto, A. (1992). Recent evidence for evolution of the genetic code. Microbiological reviews *56*, 229-264.

Ostermann, J., Horwich, A.L., Neupert, W., and Hartl, F.U. (1989). Protein folding in mitochondria requires complex formation with hsp60 and ATP hydrolysis. Nature *341*, 125-130.

Otera, H., Taira, Y., Horie, C., Suzuki, Y., Suzuki, H., Setoguchi, K., Kato, H., Oka, T., and Mihara, K. (2007). A novel insertion pathway of mitochondrial outer membrane proteins with multiple transmembrane segments. The Journal of cell biology *179*, 1355-1363.

Ott, M., and Herrmann, J.M. (2010). Co-translational membrane insertion of mitochondrially encoded proteins. Biochimica et biophysica acta *1803*, 767-775.

Oyadomari, S., and Mori, M. (2004). Roles of CHOP/GADD153 in endoplasmic reticulum stress. Cell death and differentiation *11*, 381-389.

Papa, L., and Germain, D. (2011). Estrogen receptor mediates a distinct mitochondrial unfolded protein response. Journal of cell science *124*, 1396-1402.

Papa, L., and Germain, D. (2014). SirT3 regulates the mitochondrial unfolded protein response. Molecular and cellular biology *34*, 699-710.

Papandreou, I., Cairns, R.A., Fontana, L., Lim, A.L., and Denko, N.C. (2006). HIF-1 mediates adaptation to hypoxia by actively downregulating mitochondrial oxygen consumption. Cell metabolism *3*, 187-197.

Paschen, S.A., Neupert, W., and Rapaport, D. (2005). Biogenesis of beta-barrel membrane proteins of mitochondria. Trends in biochemical sciences *30*, 575-582.

Pedersen, C.B., Bross, P., Winter, V.S., Corydon, T.J., Bolund, L., Bartlett, K., Vockley, J., and Gregersen, N. (2003). Misfolding, degradation, and aggregation of variant proteins. The molecular pathogenesis of short chain acyl-CoA dehydrogenase (SCAD) deficiency. The Journal of biological chemistry *278*, 47449-47458.

Peisker, K., Chiabudini, M., and Rospert, S. (2010). The ribosome-bound Hsp70 homolog Ssb of Saccharomyces cerevisiae. Biochimica et biophysica acta *1803*, 662-672.

Pellegrino, M.W., Nargund, A.M., and Haynes, C.M. (2013). Signaling the mitochondrial unfolded protein response. Biochimica et biophysica acta *1833*, 410-416.

Persengiev, S.P., Devireddy, L.R., and Green, M.R. (2002). Inhibition of apoptosis by ATFx: a novel role for a member of the ATF/CREB family of mammalian bZIP transcription factors. Genes & development *16*, 1806-1814.

Persengiev, S.P., and Green, M.R. (2003). The role of ATF/CREB family members in cell growth, survival and apoptosis. Apoptosis : an international journal on programmed cell death *8*, 225-228.

Piechota, J., Szczesny, R., Wolanin, K., Chlebowski, A., and Bartnik, E. (2006). Nuclear and mitochondrial genome responses in HeLa cells treated with inhibitors of mitochondrial DNA expression. Acta biochimica Polonica *53*, 485-495.

Pierce, S.B., Chisholm, K.M., Lynch, E.D., Lee, M.K., Walsh, T., Opitz, J.M., Li, W., Klevit, R.E., and King, M.C. (2011). Mutations in mitochondrial histidyl tRNA synthetase HARS2 cause ovarian dysgenesis and sensorineural hearing loss of Perrault syndrome. Proceedings of the National Academy of Sciences of the United States of America *108*, 6543-6548.

Pierce, S.B., Gersak, K., Michaelson-Cohen, R., Walsh, T., Lee, M.K., Malach, D., Klevit, R.E., King, M.C., and Levy-Lahad, E. (2013). Mutations in LARS2, encoding mitochondrial leucyl-tRNA synthetase, lead to premature ovarian failure and hearing loss in Perrault syndrome. American journal of human genetics *92*, 614-620.

Pinti, M., Gibellini, L., De Biasi, S., Nasi, M., Roat, E., O'Connor, J.E., and Cossarizza, A. (2011). Functional characterization of the promoter of the human Lon protease gene. Mitochondrion *11*, 200-206.

Pirinen, E., Canto, C., Jo, Y.S., Morato, L., Zhang, H., Menzies, K.J., Williams, E.G., Mouchiroud, L., Moullan, N., Hagberg, C., et al. (2014). Pharmacological Inhibition of poly(ADP-ribose) polymerases improves fitness and mitochondrial function in skeletal muscle. Cell metabolism *19*, 1034-1041.

Potting, C., Wilmes, C., Engmann, T., Osman, C., and Langer, T. (2010). Regulation of mitochondrial phospholipids by Ups1/PRELI-like proteins depends on proteolysis and Mdm35. The EMBO journal *29*, 2888-2898.

Radke, S., Chander, H., Schafer, P., Meiss, G., Kruger, R., Schulz, J.B., and Germain, D. (2008). Mitochondrial protein quality control by the proteasome involves ubiquitination and the protease Omi. The Journal of biological chemistry *283*, 12681-12685.

Raina, M., and Ibba, M. (2014). tRNAs as regulators of biological processes. Frontiers in genetics *5*, 171.

Rainbolt, T.K., Atanassova, N., Genereux, J.C., and Wiseman, R.L. (2013). Stress-regulated translational attenuation adapts mitochondrial protein import through Tim17A degradation. Cell metabolism *18*, 908-919.

Rainey, R.N., Glavin, J.D., Chen, H.W., French, S.W., Teitell, M.A., and Koehler, C.M. (2006). A new function in translocation for the mitochondrial i-AAA protease Yme1: import of polynucleotide phosphorylase into the intermembrane space. Molecular and cellular biology *26*, 8488-8497.

Rappsilber, J., Ishihama, Y., and Mann, M. (2003). Stop and go extraction tips for matrix-assisted laser desorption/ionization, nanoelectrospray, and LC/MS sample pretreatment in proteomics. Analytical chemistry *75*, 663-670.

Rassow, J., Maarse, A.C., Krainer, E., Kubrich, M., Muller, H., Meijer, M., Craig, E.A., and Pfanner, N. (1994). Mitochondrial protein import: biochemical and genetic evidence for interaction of matrix hsp70 and the inner membrane protein MIM44. The Journal of cell biology *127*, 1547-1556.

Rath, E., Berger, E., Messlik, A., Nunes, T., Liu, B., Kim, S.C., Hoogenraad, N., Sans, M., Sartor, R.B., and Haller, D. (2012). Induction of dsRNA-activated protein kinase links mitochondrial unfolded protein response to the pathogenesis of intestinal inflammation. Gut *61*, 1269-1278.

Reading, D.S., Hallberg, R.L., and Myers, A.M. (1989). Characterization of the yeast HSP60 gene coding for a mitochondrial assembly factor. Nature *337*, 655-659.

Rehling, P., Model, K., Brandner, K., Kovermann, P., Sickmann, A., Meyer, H.E., Kuhlbrandt, W., Wagner, R., Truscott, K.N., and Pfanner, N. (2003). Protein insertion into the mitochondrial inner membrane by a twin-pore translocase. Science *299*, 1747-1751.

Richter, K., Haslbeck, M., and Buchner, J. (2010). The heat shock response: life on the verge of death. Molecular cell *40*, 253-266.

Riley, L.G., Cooper, S., Hickey, P., Rudinger-Thirion, J., McKenzie, M., Compton, A., Lim, S.C., Thorburn, D., Ryan, M.T., Giege, R., et al. (2010). Mutation of the mitochondrial tyrosyl-tRNA synthetase gene, YARS2, causes myopathy, lactic acidosis, and sideroblastic anemia--MLASA syndrome. American journal of human genetics *87*, 52-59.

Ristow, M., and Schmeisser, K. (2014). Mitohormesis: Promoting Health and Lifespan by Increased Levels of Reactive Oxygen Species (ROS). Dose-response : a publication of International Hormesis Society *12*, 288-341.

Ron, D., and Walter, P. (2007). Signal integration in the endoplasmic reticulum unfolded protein response. Nature reviews. Molecular cell biology *8*, 519-529.

Rospert, S., Looser, R., Dubaquie, Y., Matouschek, A., Glick, B.S., and Schatz, G. (1996). Hsp60-independent protein folding in the matrix of yeast mitochondria. The EMBO journal *15*, 764-774.

Rowley, N., Prip-Buus, C., Westermann, B., Brown, C., Schwarz, E., Barrell, B., and Neupert, W. (1994). Mdj1p, a novel chaperone of the DnaJ family, is involved in mitochondrial biogenesis and protein folding. Cell *77*, 249-259.

Rugarli, E.I., and Langer, T. (2006). Translating m-AAA protease function in mitochondria to hereditary spastic paraplegia. Trends in molecular medicine *12*, 262-269.

Runkel, E.D., Liu, S., Baumeister, R., and Schulze, E. (2013). Surveillance-activated defenses block the ROS-induced mitochondrial unfolded protein response. PLoS genetics *9*, e1003346.

Ryan, M.T., Herd, S.M., Sberna, G., Samuel, M.M., Hoogenraad, N.J., and Hoj, P.B. (1997). The genes encoding mammalian chaperonin 60 and chaperonin 10 are linked head-to-head and share a bidirectional promoter. Gene *196*, 9-17.

Saiki, R.K., Scharf, S., Faloona, F., Mullis, K.B., Horn, G.T., Erlich, H.A., and Arnheim, N. (1985). Enzymatic amplification of beta-globin genomic sequences and restriction site analysis for diagnosis of sickle cell anemia. Science *230*, 1350-1354.

Sanni, A., Walter, P., Boulanger, Y., Ebel, J.P., and Fasiolo, F. (1991). Evolution of aminoacyl-tRNA synthetase quaternary structure and activity: Saccharomyces cerevisiae mitochondrial phenylalanyl-tRNA synthetase. Proceedings of the National Academy of Sciences of the United States of America *88*, 8387-8391.

Santagata, S., Bhattacharyya, D., Wang, F.H., Singha, N., Hodtsev, A., and Spanopoulou, E. (1999). Molecular cloning and characterization of a mouse homolog of bacterial ClpX, a novel mammalian class II member of the Hsp100/Clp chaperone family. The Journal of biological chemistry *274*, 16311-16319.

Santos-Cortez, R.L., Lee, K., Azeem, Z., Antonellis, P.J., Pollock, L.M., Khan, S., Irfanullah, Andrade-Elizondo, P.B., Chiu, I., Adams, M.D., et al. (2013). Mutations in KARS, encoding lysyl-tRNA synthetase, cause autosomal-recessive nonsyndromic hearing impairment DFNB89. American journal of human genetics *93*, 132-140.

Sauer, R.T., and Baker, T.A. (2011). AAA+ proteases: ATP-fueled machines of protein destruction. Annual review of biochemistry *80*, 587-612.

Scheper, G.C., van der Klok, T., van Andel, R.J., van Berkel, C.G., Sissler, M., Smet, J., Muravina, T.I., Serkov, S.V., Uziel, G., Bugiani, M., et al. (2007). Mitochondrial aspartyl-tRNA synthetase deficiency causes leukoencephalopathy with brain stem and spinal cord involvement and lactate elevation. Nature genetics *39*, 534-539.

Scherer, W.F., Syverton, J.T., and Gey, G.O. (1953). Studies on the propagation in vitro of poliomyelitis viruses. IV. Viral multiplication in a stable strain of human malignant epithelial cells (strain HeLa) derived from an epidermoid carcinoma of the cervix. The Journal of experimental medicine *97*, 695-710.

Schmidt, O., Pfanner, N., and Meisinger, C. (2010). Mitochondrial protein import: from proteomics to functional mechanisms. Nature reviews. Molecular cell biology *11*, 655-667.

Schneider, H.C., Westermann, B., Neupert, W., and Brunner, M. (1996). The nucleotide exchange factor MGE exerts a key function in the ATP-dependent cycle of mt-Hsp70-Tim44 interaction driving mitochondrial protein import. The EMBO journal *15*, 5796-5803.

Schroder, M. (2006). The unfolded protein response. Molecular biotechnology *34*, 279-290.

Seburn, K.L., Nangle, L.A., Cox, G.A., Schimmel, P., and Burgess, R.W. (2006). An active dominant mutation of glycyl-tRNA synthetase causes neuropathy in a Charcot-Marie-Tooth 2D mouse model. Neuron *51*, 715-726.

Sharma, M.R., Booth, T.M., Simpson, L., Maslov, D.A., and Agrawal, R.K. (2009). Structure of a mitochondrial ribosome with minimal RNA. Proceedings of the National Academy of Sciences of the United States of America *106*, 9637-9642.

Sharma, M.R., Koc, E.C., Datta, P.P., Booth, T.M., Spremulli, L.L., and Agrawal, R.K. (2003). Structure of the mammalian mitochondrial ribosome reveals an expanded functional role for its component proteins. Cell *115*, 97-108.

Shen, X., Ellis, R.E., Lee, K., Liu, C.Y., Yang, K., Solomon, A., Yoshida, H., Morimoto, R., Kurnit, D.M., Mori, K., et al. (2001). Complementary signaling pathways regulate the unfolded protein response and are required for C. elegans development. Cell *107*, 893-903.

Sherman, M.Y., and Qian, S.B. (2013). Less is more: improving proteostasis by translation slow down. Trends in biochemical sciences *38*, 585-591.

Shevchenko, A., Tomas, H., Havlis, J., Olsen, J.V., and Mann, M. (2006). In-gel digestion for mass spectrometric characterization of proteins and proteomes. Nature protocols *1*, 2856-2860.

Sigler, P.B., Xu, Z., Rye, H.S., Burston, S.G., Fenton, W.A., and Horwich, A.L. (1998). Structure and function in GroEL-mediated protein folding. Annual review of biochemistry *67*, 581-608.

Silva, J.M., Wong, A., Carelli, V., and Cortopassi, G.A. (2009). Inhibition of mitochondrial function induces an integrated stress response in oligodendroglia. Neurobiology of disease *34*, 357-365.

Silver, L.M. (1995). Mouse Genetics Concepts and Application. (New York: Oxford University Press).

Skrtic, M., Sriskanthadevan, S., Jhas, B., Gebbia, M., Wang, X., Wang, Z., Hurren, R., Jitkova, Y., Gronda, M., Maclean, N., et al. (2011). Inhibition of mitochondrial translation as a therapeutic strategy for human acute myeloid leukemia. Cancer cell *20*, 674-688.

Smale, S.T., and Kadonaga, J.T. (2003). The RNA polymerase II core promoter. Annual review of biochemistry *72*, 449-479.

Smirnova, E.V., Lakunina, V.A., Tarassov, I., Krasheninnikov, I.A., and Kamenski, P.A. (2012). Noncanonical functions of aminoacyl-tRNA synthetases. Biochemistry. Biokhimiia *77*, 15-25.

Smits, P., Smeitink, J., and van den Heuvel, L. (2010). Mitochondrial translation and beyond: processes implicated in combined oxidative phosphorylation deficiencies. Journal of biomedicine & biotechnology *2010*, 737385.

Solaini, G., Baracca, A., Lenaz, G., and Sgarbi, G. (2010). Hypoxia and mitochondrial oxidative metabolism. Biochimica et biophysica acta *1797*, 1171-1177.

Song, Z., Chen, H., Fiket, M., Alexander, C., and Chan, D.C. (2007). OPA1 processing controls mitochondrial fusion and is regulated by mRNA splicing, membrane potential, and Yme1L. The Journal of cell biology *178*, 749-755.

Stadtman, E.R., and Berlett, B.S. (1998). Reactive oxygen-mediated protein oxidation in aging and disease. Drug metabolism reviews *30*, 225-243.

Steenweg, M.E., Ghezzi, D., Haack, T., Abbink, T.E., Martinelli, D., van Berkel, C.G., Bley, A., Diogo, L., Grillo, E., Te Water Naude, J., et al. (2012). Leukoencephalopathy with thalamus and brainstem involvement and high lactate 'LTBL' caused by EARS2 mutations. Brain : a journal of neurology *135*, 1387-1394.

Steinberg, S., Gautheret, D., and Cedergren, R. (1994). Fitting the structurally diverse animal mitochondrial tRNAs(Ser) to common three-dimensional constraints. Journal of molecular biology *236*, 982-989.

Stewart, J.B., and Chinnery, P.F. (2015). The dynamics of mitochondrial DNA heteroplasmy: implications for human health and disease. Nature reviews. Genetics *16*, 530-542.

Strub, A., Lim, J.H., Pfanner, N., and Voos, W. (2000). The mitochondrial protein import motor. Biological chemistry *381*, 943-949.

Suen, D.F., Narendra, D.P., Tanaka, A., Manfredi, G., and Youle, R.J. (2010). Parkin overexpression selects against a deleterious mtDNA mutation in heteroplasmic cybrid cells. Proceedings of the National Academy of Sciences of the United States of America *107*, 11835-11840.

Suzuki, C.K., Suda, K., Wang, N., and Schatz, G. (1994). Requirement for the yeast gene LON in intramitochondrial proteolysis and maintenance of respiration. Science *264*, 273-276.

Szegezdi, E., Logue, S.E., Gorman, A.M., and Samali, A. (2006). Mediators of endoplasmic reticulum stress-induced apoptosis. EMBO reports *7*, 880-885.

Temperley, R.J., Wydro, M., Lightowlers, R.N., and Chrzanowska-Lightowlers, Z.M. (2010). Human mitochondrial mRNAs--like members of all families, similar but different. Biochimica et biophysica acta *1797*, 1081-1085.

Teske, B.F., Fusakio, M.E., Zhou, D., Shan, J., McClintick, J.N., Kilberg, M.S., and Wek, R.C. (2013). CHOP induces activating transcription factor 5 (ATF5) to trigger apoptosis in response to perturbations in protein homeostasis. Molecular biology of the cell *24*, 2477-2490.

Tiede, L.M., Cook, E.A., Morsey, B., and Fox, H.S. (2011). Oxygen matters: tissue culture oxygen levels affect mitochondrial function and structure as well as responses to HIV viroproteins. Cell death & disease *2*, e246.

Timmis, J.N., Ayliffe, M.A., Huang, C.Y., and Martin, W. (2004). Endosymbiotic gene transfer: organelle genomes forge eukaryotic chromosomes. Nature reviews. Genetics *5*, 123-135.

Trifunovic, A., Wredenberg, A., Falkenberg, M., Spelbrink, J.N., Rovio, A.T., Bruder, C.E., Bohlooly, Y.M., Gidlof, S., Oldfors, A., Wibom, R., et al. (2004). Premature ageing in mice expressing defective mitochondrial DNA polymerase. Nature *429*, 417-423.

Truscott, K.N., Voos, W., Frazier, A.E., Lind, M., Li, Y., Geissler, A., Dudek, J., Muller, H., Sickmann, A., Meyer, H.E., et al. (2003). A J-protein is an essential subunit of the presequence translocase-associated protein import motor of mitochondria. The Journal of cell biology *163*, 707-713.

Tuppen, H.A., Blakely, E.L., Turnbull, D.M., and Taylor, R.W. (2010). Mitochondrial DNA mutations and human disease. Biochimica et biophysica acta *1797*, 113-128.

Tyynismaa, H., Carroll, C.J., Raimundo, N., Ahola-Erkkila, S., Wenz, T., Ruhanen, H., Guse, K., Hemminki, A., Peltola-Mjosund, K.E., Tulkki, V., et al. (2010). Mitochondrial myopathy induces a starvation-like response. Human molecular genetics *19*, 3948-3958.

Tyynismaa, H., Mjosund, K.P., Wanrooij, S., Lappalainen, I., Ylikallio, E., Jalanko, A., Spelbrink, J.N., Paetau, A., and Suomalainen, A. (2005). Mutant mitochondrial helicase Twinkle causes multiple mtDNA deletions and a late-onset mitochondrial disease in mice. Proceedings of the National Academy of Sciences of the United States of America *102*, 17687-17692.

Van Dyck, L., Pearce, D.A., and Sherman, F. (1994). PIM1 encodes a mitochondrial ATP-dependent protease that is required for mitochondrial function in the yeast Saccharomyces cerevisiae. The Journal of biological chemistry *269*, 238-242.

Virbasius, J.V., and Scarpulla, R.C. (1994). Activation of the human mitochondrial transcription factor A gene by nuclear respiratory factors: a potential regulatory link between nuclear and mitochondrial gene expression in organelle biogenesis. Proc. Natl. Acad. Sci. USA *91*, 1309-1313.

Voisine, C., Craig, E.A., Zufall, N., von Ahsen, O., Pfanner, N., and Voos, W. (1999). The protein import motor of mitochondria: unfolding and trapping of preproteins are distinct and separable functions of matrix Hsp70. Cell *97*, 565-574.

Voos, W. (2009). Mitochondrial protein homeostasis: the cooperative roles of chaperones and proteases. Research in microbiology *160*, 718-725.

Voos, W. (2013). Chaperone-protease networks in mitochondrial protein homeostasis. Biochimica et biophysica acta *1833*, 388-399.

Voos, W., and Rottgers, K. (2002). Molecular chaperones as essential mediators of mitochondrial biogenesis. Biochimica et biophysica acta *1592*, 51-62.

Wadhwa, R., Takano, S., Kaur, K., Deocaris, C.C., Pereira-Smith, O.M., Reddel, R.R., and Kaul, S.C. (2006). Upregulation of mortalin/mthsp70/Grp75 contributes to human carcinogenesis. International journal of cancer. Journal international du cancer *118*, 2973-2980.

Wadhwa, R., Takano, S., Taira, K., and Kaul, S.C. (2004). Reduction in mortalin level by its antisense expression causes senescence-like growth arrest in human immortalized cells. The journal of gene medicine *6*, 439-444.

Wagner, I., Arlt, H., van Dyck, L., Langer, T., and Neupert, W. (1994). Molecular chaperones cooperate with PIM1 protease in the degradation of misfolded proteins in mitochondria. The EMBO journal *13*, 5135-5145.

Wai, T., Ao, A., Zhang, X., Cyr, D., Dufort, D., and Shoubridge, E.A. (2010). The role of mitochondrial DNA copy number in mammalian fertility. Biology of reproduction *83*, 52-62.

Wallace, D.C. (2005). A mitochondrial paradigm of metabolic and degenerative diseases, aging, and cancer: a dawn for evolutionary medicine. Annual review of genetics *39*, 359-407.

Wallace, D.C. (2007). Why do we still have a maternally inherited mitochondrial DNA? Insights from evolutionary medicine. Annual review of biochemistry *76*, 781-821.

Wallace, D.C., Singh, G., Lott, M.T., Hodge, J.A., Schurr, T.G., Lezza, A.M.S., ElsasII, L.J., and Nikoskelainen, E. (1988). Mitochondrial DNA mutation associated with Leber's hereditary optic neuropathy. Science *242*, 1427-1430.

Walter, P., and Ron, D. (2011). The unfolded protein response: from stress pathway to homeostatic regulation. Science *334*, 1081-1086.

Walter, S. (2002). Structure and function of the GroE chaperone. Cellular and molecular life sciences : CMLS *59*, 1589-1597.

Wang, M., Weiss, M., Simonovic, M., Haertinger, G., Schrimpf, S.P., Hengartner, M.O., and von Mering, C. (2012). PaxDb, a database of protein abundance averages across all three domains of life. Molecular & cellular proteomics : MCP *11*, 492-500.

Weber, E.R., Hanekamp, T., and Thorsness, P.E. (1996). Biochemical and functional analysis of the YME1 gene product, an ATP and zinc-dependent mitochondrial protease from S. cerevisiae. Molecular biology of the cell *7*, 307-317.

Weiss, C., Schneider, S., Wagner, E.F., Zhang, X., Seto, E., and Bohmann, D. (2003). JNK phosphorylation relieves HDAC3-dependent suppression of the transcriptional activity of c-Jun. The EMBO journal *22*, 3686-3695.

Westermann, B., Prip-Buus, C., Neupert, W., and Schwarz, E. (1995). The role of the GrpE homologue, Mge1p, in mediating protein import and protein folding in mitochondria. The EMBO journal *14*, 3452-3460.

Williams, G.S., Boyman, L., Chikando, A.C., Khairallah, R.J., and Lederer, W.J. (2013). Mitochondrial calcium uptake. Proceedings of the National Academy of Sciences of the United States of America *110*, 10479-10486.

Williamson, C.L., Dabkowski, E.R., Dillmann, W.H., and Hollander, J.M. (2008). Mitochondria protection from hypoxia/reoxygenation injury with mitochondria heat shock protein 70 overexpression. American journal of physiology. Heart and circulatory physiology *294*, H249-256.

Xu, J. (2005). Preparation, culture, and immortalization of mouse embryonic fibroblasts. Current protocols in molecular biology / edited by Frederick M. Ausubel ... [et al.] *Chapter 28*, Unit 28 21.

Xu, Z., Horwich, A.L., and Sigler, P.B. (1997). The crystal structure of the asymmetric GroEL-GroES-(ADP)7 chaperonin complex. Nature *388*, 741-750.

Yaffe, D., and Saxel, O. (1977). Serial passaging and differentiation of myogenic cells isolated from dystrophic mouse muscle. Nature *270*, 725-727.

Yamazaki, T., Ohmi, A., Kurumaya, H., Kato, K., Abe, T., Yamamoto, H., Nakanishi, N., Okuyama, R., Umemura, M., Kaise, T., et al. (2010). Regulation of the human CHOP gene promoter by the stress response transcription factor ATF5 via the AARE1 site in human hepatoma HepG2 cells. Life sciences *87*, 294-301.

Yang, W., and Hekimi, S. (2010). Two modes of mitochondrial dysfunction lead independently to lifespan extension in Caenorhabditis elegans. Aging cell *9*, 433-447.

Yoneda, T., Benedetti, C., Urano, F., Clark, S.G., Harding, H.P., and Ron, D. (2004). Compartment-specific perturbation of protein handling activates genes encoding mitochondrial chaperones. Journal of cell science *117*, 4055-4066.

Youle, R.J., and Narendra, D.P. (2011). Mechanisms of mitophagy. Nature reviews. Molecular cell biology *12*, 9-14.

Yu, A.Y., and Houry, W.A. (2007). ClpP: a distinctive family of cylindrical energy-dependent serine proteases. FEBS letters *581*, 3749-3757.

Yun, J., and Finkel, T. (2014). Mitohormesis. Cell metabolism *19*, 757-766.

Yusupov, M.M., Yusupova, G.Z., Baucom, A., Lieberman, K., Earnest, T.N., Cate, J.H., and Noller, H.F. (2001). Crystal structure of the ribosome at 5.5 A resolution. Science *292*, 883-896.

Zagryadskaya, E.I., Kotlova, N., and Steinberg, S.V. (2004). Key elements in maintenance of the tRNA L-shape. Journal of molecular biology *340*, 435-444.

Zamzami, N., Marchetti, P., Castedo, M., Decaudin, D., Macho, A., Hirsch, T., Susin, S.A., Petit, P.X., Mignotte, B., and Kroemer, G. (1995). Sequential reduction of mitochondrial transmembrane potential and generation of reactive oxygen species in early programmed cell death. The Journal of experimental medicine *182*, 367-377.

Zhao, F., Xuan, Z., Liu, L., and Zhang, M.Q. (2005). TRED: a Transcriptional Regulatory Element Database and a platform for in silico gene regulation studies. Nucleic acids research *33*, D103-107.

Zhao, Q., Wang, J., Levichkin, I.V., Stasinopoulos, S., Ryan, M.T., and Hoogenraad, N.J. (2002). A mitochondrial specific stress response in mammalian cells. The EMBO journal *21*, 4411-4419.

Zhou, D., Palam, L.R., Jiang, L., Narasimhan, J., Staschke, K.A., and Wek, R.C. (2008). Phosphorylation of eIF2 directs ATF5 translational control in response to diverse stress conditions. The Journal of biological chemistry *283*, 7064-7073.

Acknowledgements

There it is, the end of my thesis. Crazy. If someone had told me in the beginning that I will finish after three years, I wouldn't have believed it. Being lucky enough to have found some kind of "needle in the haystack", I'm now very grateful to so many people, who accompanied me during this challenging, but very fulfilling time in my life.

At first, I really want to thank the members of my thesis committee Prof. Aleksandra Trifunovic, Prof. Elena Rugarli and Prof. Peter Kloppenburg for their time and consideration.

Special thanks goes to Sandra (Prof. Aleksandra Trifunovic) for the continuous support and understanding during this thesis! I'm very obliged to you for really pushing me to generate the 3rd double mutant mouse after two unsuccessful trials – that was really key for this thesis! Moreover, thank you for your trust and for the freedom that I needed to move forward personally and professionally during my PhD. Finally, thank you for the nice cigarette breaks, the best rum and the best roastbeef ever.

The work presented here would have been also not possible without the support of CECAD that provided me with a three-year excellence fellowship. Special thanks here go to Dr. Doris Birker and Jenny Ostermann from the Cologne Graduate School of Ageing Research for their continuous support (formerly CECAD Graduate School).

My sincere thanks also go to Dr. Alexandra Kukat for her understanding, encouragement and personal attention. Thank you for really taking time to guide me the past three years through all the ups and downs. Moreover, thank you for your time during my thesis-writing period, where you have provided me with great support, sound advice, good teaching, good company, and lots of good ideas. Thank you very much indeed!

Many thanks go also to Katharina Senft (Katha) who was there for me from the very beginning! You helped me a lot when I was new in the lab and you also supported me during the whole time, both personally and experimentally! Thank you!

Marijana Aradjanski ("Deutsche Marijana")! I'm very grateful that we both got lab buddies and close friends! Thank you for our nice talks, the great time in the States, the nice pictures you make and for introducing me to Rakija!

Estella Cepeda Corres! Estella! My fellow sufferer during the writing period! We made it! Thank you for being a great friend inside and outside the lab! Thank you also for your friendly and honest personality that was really uplifting me every day! So, I guess I'll see you at Spatz!

Many thanks to Linda Baumann, Tina Becker, Dr. Marija Herholz, Dr. Karolina Szczepanowska, Steffen Hermans, Eduard Hofsetz, Suvoshee Ghosh, Elke Mainz, Victor Pavlenko, Carlos Ruiz Puig, Dr. Priyanka Maiti, Dr. Anil Dogan, Dr. Claire Puyol and Dr. Rozina Kardakaris for the great working atmosphere, cakes, sweets, buffers, high-level talks, searching things, Mensa walks, laughing, ... Thank you guys!

Special thanks are addressed to all my friends and to my family for help and support and fun. I would have been lost without you all.

Last, but not least, I want to address my very special thanks from all my heart to Lisa, for her endless support, for being with me, for her love.

Erklärung

Ich versichere, dass ich die von mir vorgelegte Dissertation selbständig angefertigt, die benutzten Quellen und Hilfsmittel vollständig angegeben und die Stellen der Arbeit - einschließlich Tabellen, Karten und Abbildungen -, die anderen Werken im Wortlaut oder dem Sinn nach entnommen sind, in jedem Einzelfall als Entlehnung kenntlich gemacht habe; dass diese Dissertation noch keiner anderen Fakultät oder Universität zur Prüfung vorgelegen hat; dass sie - abgesehen von unten angegebenen Teilpublikationen - noch nicht veröffentlicht worden ist sowie, dass ich eine solche Veröffentlichung vor Abschluss des Promotionsverfahrens nicht vornehmen werde.

Die Bestimmungen der Promotionsordnung sind mir bekannt. Die von mir vorgelegte Dissertation ist von Prof. Dr. Aleksandra Trifunovic betreut worden.

Köln, den 24.10.2015

_____

(Dominic Seiferling)

Teilpublikationen

Seiferling, D., Szczepanowska K., Becker C., Senft K., Hermans S., Kukat A., and Trifunovic A. (2015) Loss of CLPP alleviates mitochondrial cardiomyopathy without affecting the mammalian mitochondrial unfolded protein response. EMBO reports, *in review*.

Curriculum Vitae

ZUR PERSON

Dominic Seiferling

Ehrenstraße 66

50672 Köln

dominic.seiferling@uni-koeln.de

* 28th January 1986, Heidelberg

HOCHSCHULBILDUNG

10/2012 –	**Doktorarbeit (PhD studies) in Genetik,** Universität zu Köln "Cluster of Excellence in Cellular Stress Responses and Aging-associated diseases (CECAD)" Graduate School
	Doktorarbeit: "Regulation of the mammalian mitochondrial unfolded protein response" am CECAD Forschungszentrum, Universität zu Köln
04/2010 – 07/2012	**Masterstudium in "Biological Sciences"**, Universität zu Köln Abschluss: "Master of Science in Biological Sciences"
	Masterthesis: "Generation of synthetic modified mRNA for targeted conversion of cell types" am Institut für rekonstruktive Neurobiologie, Universität Bonn
10/2006 – 08/2009	**Bachelorstudium in Biologie**, Universität zu Köln Abschluss: "Bachelor of Science in Biology"
	Bachelorthesis: "Physiologische und biochemische Charakterisierung der oxidativen Stressantwort in *Corynebacterium glutamicum*" am Institut für Biochemie, Universität zu Köln

SCHULBILDUNG

2003 – 2006	**Biotechnologisches Gymnasium,** Bruchsal Abschluss: allg. Hochschulreif

BERUFSERFAHRUNG

10/2012 –	**Wissenschaftlicher Mitarbeiter (CECAD Stipendium)** am CECAD Forschungszentrum (AG Trifunovic), Universität zu Köln
11/2011 – 07/2012	**Studentischer Mitarbeiter** am Institut für rekonstruktive Neurobiologie (AG Edenhofer), Universität Bonn
10/2009 – 12/2009	**Wissenschaftlicher Mitarbeiter** am Institut für Biochemie (AG Krämer), Universität zu Köln
05/2008 – 01/2009	**Studentischer Mitarbeiter** am Institut für Botanik (AG Flügge), Universität zu Köln

STIPENDIEN

10/2012 –	„Cluster of Excellence in Cellular Stress Responses and Aging-Associated Diseases" (CECAD) Doktorandenstipendium, Universität zu Köln

PUBLICATIONS

Thier M., Wörsdörfer P., Lakes Y.B., Gorris R., Herms S., Opitz T., <u>Seiferling D.</u>, Quandel T., Hoffmann P., Nöthen M., Brüstle O., Edenhofer F. (2012) Direct conversion of fibroblasts into stably expandable neural stem cells. *Cell Stem Cell,* **10**: 473-9.

Follmann M., Ochrombel I., Krämer R., Trötschel C., Poetsch A., Rückert C., Hüser A., Persicke M., <u>Seiferling D.</u>, Kalinowski J., Marin K. (2009) Functional genomics of pH homeostasis in *Corynebacterium glutamicum* revealed novel links between pH response, oxidative stress, iron homeostasis and methionine synthesis. *BMC Genomics*, **10**: 621.

SPRACHKENNTNISSE

Deutsch (Muttersprache), Englisch (fließend), Spanisch (Grundkenntnisse)

Köln, den 24.11.2015